UNIVERSIDADE DE BRASÍLIA

PROGRAMA DE PÓS-GRADUAÇÃO EM ZOOLOGIA

Delimitação de espécies de *Pimelodella* Eigenmann & Eigenmann, 1888 (Siluriformes: Heptapteridae) na bacia do Alto rio Paraguai

Veida Raquel Meireles Pierre

Brasília

Maio/2024

UNIVERSIDADE DE BRASÍLIA

PROGRAMA DE PÓS-GRADUAÇÃO EM ZOOLOGIA

-

Delimitação de espécies de *Pimelodella* Eigenmann & Eigenmann, 1888 (Siluriformes: Heptapteridae) na bacia do Alto rio Paraguai

Veida Raquel Meireles Pierre

Dissertação de Mestrado apresentada ao Programa de Pós-graduação em Zoologia, Instituto de Ciências Biológicas, da Universidade de Brasília, como parte dos requisitos necessários à obtenção do título de Mestre em Zoologia.

Orientadora: Veronica Slobodian

Brasília

Maio/2024

Delimitação de espécies de *Pimelodella* Eigenmann & Eigenmann, 1888 (Siluriformes: Heptapteridae) na bacia do Alto rio Paraguai

Veida Raquel Meireles Pierre

Orientadora: Profa. Dra. Veronica Slobodian

Dissertação de Mestrado apresentada ao Programa de Pós-graduação em Zoologia, Instituto de Ciências Biológicas, da Universidade de Brasília, como parte dos requisitos necessários à obtenção do título de Mestre em Zoologia.

Aprovada por

Veronica Slobodian, Presidente – UnB (PPG Zoo)

Maria Elina Bichuette – UFSCar

Flávio Alicino Bockmann – USP

Julia Klaczko – UnB (PPG Zoo)

Brasília

Maio/2024

Ficha catalográfica

Ficha catalográfica elaborada automaticamente,
com os dados fornecidos pelo(a) autor(a)

P623d

Pierre, Veida Raquel Meireles
Delimitação de espécies de Pimelodella Eigenmann & Eigenmann, 1888 (Siluriformes: Heptapteridae) na bacia do Alto rio Paraguai / Veida Raquel Meireles Pierre; orientador Veronica Slobodian. -- Brasília, 2024.
138 p.

Dissertação(Mestrado em Zoologia) -- Universidade de Brasília, 2024.

1. Ictiofauna de água doce. 2. Morfometria geométrica. 3. Taxonomia. 4. Bacia do Alto rio Paraguai. 5. Bagres. I. Slobodian, Veronica, orient. II. Título.

“Slow down, you're doing fine

You can't be everything you wanna be before your time

Although it's so romantic on the borderline tonight”

***Vienna*, Billy Joel**

Agradecimentos

Dois anos de mestrado constituem um período que, apesar de breve e frenético em termos de pesquisa, com as pessoas especiais pode se tornar uma jornada muito bem vivida. Neste espaço, expressarei minha gratidão por aqueles que fizeram parte dessa trajetória, compartilhando meus desafios e conquistas, e também por aqueles que deixaram uma marca em minha vida de alguma forma.

Gostaria de começar agradecendo a Deus, cuja luz tem sido meu caminho, provendo-me de esperança e serenidade nos momentos mais difíceis, e proporcionando-me momentos bons, de conquistas e gratidão. Agradeço também aos meus pais, Silvia e Vamildo Pierre, aos quais sou imensamente grata por terem me incentivado durante toda minha formação, sempre priorizando meu ensino e o de minha irmã, e me ensinando o valor da educação. Agradeço por serem meus maiores apoiadores em qualquer coisa que escolho fazer. Sem o suporte deles, certamente o caminho para trilhar seria mais árduo. À minha irmã, Vitória Pierre, agradeço pelo seu constante incentivo e animação, sempre demonstrando interesse no que eu estudo, mesmo sem entender nada, e, mesmo à distância, suavizar meus momentos difíceis com seu humor.

Sou imensamente grata à minha orientadora, Veronica Slobodian, por ter me possibilitado estudar aquilo que amo e por ser quem me apresentou os mundos da ictiologia e da taxonomia. Fazer ciência e estudar o que gosta torna-se mais gratificante quando se pode contar com uma orientadora tão inspiradora, didática e repleta de ideias. Agradeço por todas as aulas, conversas, e conselhos de vida. Seu entusiasmo e cuidado com a pesquisa enriqueceram e ajudaram a trilhar minha jornada acadêmica.

Sou grata também ao meu namorado, Lucas Ceccon, que sempre esteve comigo, sendo meu melhor amigo e grande apoiador, me fazendo rir mesmo em momentos de aflição e cansaço. Sua presença tornou esse percurso mais leve. Além disso, não posso deixar de mencionar sua contribuição direta à minha pesquisa, sendo minha companhia nos vários fins de semana no laboratório enquanto eu fotografava peixes; disponibilizando seus talentos artísticos para me ensinar e auxiliar na edição de imagens; ouvindo-me falar de peixe; e pela paciência e apoio, principalmente no período caótico do final da escrita desta dissertação.

Além disso, um agradecimento especial aos meus amigos integrantes e agregados do Laboratório de Ictiologia Sistemática (LIS) da UnB, Artur Firmino, Rayssa Nayara, Júlia Papalardo, Thaís Carvalho, Leonardo Ferreira-Sousa, Izabel Salvi, Tatiana Hanada, Isabelle Feijão, Brenda Oliveira, Guilherme Carvalho, Luiz Silva-Marques e todas as demais pessoas que integram ou já integraram o laboratório. O meu mestrado não teria sido tão proveitoso se não fosse a presença desses companheiros no meu dia a dia, que fazem do laboratório um ambiente caótico e incrivelmente acolhedor. Guardarei com carinho as memórias deste período, assim como todos os campos e viagens que fizemos.

E falando em memórias, não poderia deixar de mencionar minha gratidão à Rosana Tidon, minha primeira orientadora na graduação e quem me apresentou a morfometria geométrica. Agradeço por ter me ensinado tanto e por ter me incentivado a seguir meus sonhos. Agradeço também aos meus antigos companheiros do Laboratório de Biologia Evolutiva da UnB, Fábio Cavalcanti, Fred Horst, Keven Horoito, Angie Montoya, Gabriel Marins, e José Pedro Viana, e em especial a Lara H. P. Vieira e Laís Ribeiro (com nossas aulas de estatística e lanches da tarde). Inclusive, um agradecimento em particular à Lara, quem me mostrou que não preciso ter medo de estatística ou de fazer análises no R. Se hoje sou capaz de utilizar o R sem receio, é graças a ela.

Agradeço também aos meus amigos Ana Carolina Sartório, Mariana Higa, Luane Tomé, Pedro Paulo, Rayane Sarafim, Geovanna Marja, e Dennys Lucas por todos esses anos de amizade e por tantas vezes terem sido meu suporte emocional. Sou grata por termos mantido a amizade, mesmo com os diferentes caminhos que cada um seguiu.

Ademais, esse mestrado não teria possível sem o apoio das coleções científicas que disponibilizaram todo o material necessário para minha pesquisa. Assim, agradeço à: Coleção de Peixes da Universidade Federal de Mato Grosso (CPUFMT), Coleção de Peixes do Museu de Ciências e Tecnologia (MCP-Peixes), Coleção Ictiológica do Núcleo de Pesquisas em Limnologia, Ictiologia e Aquicultura (NUPELIA), Coleção Zoológica da Universidade Federal de Mato Grosso do Sul (ZUFMS-PIS), Laboratório de Ictiologia de Ribeirão Preto (LIRP), Museu de Zoologia da Universidade de São Paulo (MZUSP), e Museu de Zoologia da

Universidade Estadual de Londrina (MZUEL-Peixes).

Sou grata ao Laboratório de Anatomia Comparada dos Vertebrados (LACV) da UnB por ter disponibilizado seu espaço e equipamentos para todas as fotografias necessárias para a minha pesquisa. Também agradeço ao LIRP e ao Instituto de Biodiversidade e Sustentabilidade NUPEM/UFRJ por terem gentilmente cedido seus espaços e os equipamentos de raio-x. No Nupem, fui recebida calorosamente pelos professores Dr. Fabio Di Dario e Dra. Ana Cristina Petry, aos quais sou muito grata. Além disso, estendo meu agradecimento ao Prof. Dr. Marcelo Britto por ter me recebido cordialmente no Museu Nacional do Rio de Janeiro, onde realizei minha primeira visita técnica à coleção científica.

Por fim, o presente trabalho foi realizado com apoio da Coordenação de Aperfeiçoamento de Pessoal de Nível Superior – Brasil (CAPES) – Código de Financiamento 001. Agradeço a esta agência de fomento pela bolsa de mestrado concedida. Além disso, gostaria de agradecer à CAPES e ao Programa de Pós-graduação em Zoologia (PPGZoo) pelos auxílios financeiros recebidos por meio do Programa de Apoio à Pós-Graduação (PROAP-Capes, Edital 04/2021 PPGZoo), e do Programa de Desenvolvimento da Pós-Graduação (PDPG) (Edital 03/2023 PPGZoo).

Sumário

Lista de figuras

Introdução geral

Chapter 1

analyses, corresponding to the origin of adipose fin.

Figure 4. Dorsal view of *Pimelodella mucosa*, ZUFMS-PIS 3256, 75.3 mm SL, with the positions of the 12 landmarks (red dots): (1) snout tip; (2) anterior limit of the right posterior nostril; (3) anterior limit of the left posterior nostril; (4) anterior limit of the right eye; (5) posterior limit of the right eye; (6) anterior limit of the left eye; (7) posterior limit of the left eye; (8) anterior limit of the supraoccipital process; (9) posterior limit of the supraoccipital process; (10) origin of dorsal fin at the spinelet; (11) posterior limit of the right branchiostegal membrane; (12) posterior limit of the left branchiostegal membrane. The white circumferences, designated by the letters “a” and “b”, show the landmarks excluded from the analyses, corresponding to the origins of pectoral-fin spines.

Figure 5. Lateral view of species of *Pimelodella* found in the Upper rio Paraguai basin. **A.** *P. avanhandavae*, MCP-Peixes 36119, 89.4 mm SL; **B.** *P. gracilis*, MZUEL-Peixes 14001, 93.7 mm SL; **C.** *P. griffini*, ZUFMS-PIS 1607, 69.4 mm SL; **D.** *P. guato*, holotype, ZUFMS-PIS 8515, 78.5 mm SL; **E.** *P. megalura*, MCP-Peixes 15708, 74.3 mm SL; **F.** *P. mucosa*, ZUFMS-PIS 3256, 76.3 mm SL; **G.** *P. notomelas*, MZUEL-Peixes 7743, 52.6 mm SL; and **H.** *P. taeniophora*, MCP-Peixes 15708, 74.33 mm SL.

Figure 6. Boxplot of centroid size for each species of *Pimelodella* in external lateral view. The circles represent the outliers.

Figure 7. Scatterplot of Principal Components one (PC1) and two (PC2) from the residuals of the allometric regression in external lateral view. The variance percentage for each PC is provided in parentheses.

Figure 8. Scatterplot of Principal Components **A.** One (PC1) and two (PC2); and **B.** One and three (PC3), from the Principal Components Analysis (PCA) in external lateral view, with frequency ellipses of 90%. The variance percentage for each PC is provided in parentheses.

Figure 9. Wireframe visualizations of shape variation between the extremes of **A.** Principal Component 1 (PC1) axis; **B.** Principal Component 2 (PC2) axis and **C.** Principal Component 3 (PC3) axis in lateral photographic view. Black wireframe illustrates the shape configuration at the negative extreme of each PC axis. Gray

wireframe represents the shape configuration at the positive extreme of each PC axis. Variance percentages of each PC are provided in parentheses.

Figure 10. Boxplot of centroid size for each species of *Pimelodella* in osteological lateral view. The circles represent the outliers.

Figure 11. Scatterplot of Principal Components one (PC1) and two (PC2) from the residuals of the allometric regression in osteological lateral view. The variance percentage for each PC is provided in parentheses.

Figure 12. Scatterplot of Principal Components **A.** One (PC1) and two (PC2) and **B.** One and three (PC3) from the Principal Components Analysis (PCA) in osteological lateral view, with frequency ellipses of 90%. The variance percentage for each PC is provided in parentheses.

Figure 13. Wireframe visualizations of shape variation between the extremes of **A.** Principal Component 1 (PC1) axis; **B.** Principal Component 2 (PC2) axis; and **C.** Principal Component 3 (PC3) axis in osteological lateral view. Black wireframe illustrates the shape configuration at the negative extreme of each PC axis. Gray wireframe represents the shape configuration at the positive extreme of each PC axis. Variance percentages of each PC are provided in parentheses.

Figure 14. Boxplot of centroid size for each species of *Pimelodella* in external dorsal view. The circles represent the outliers.

Figure 15. Scatterplot of Principal Components **A.** One (PC1) and two (PC2) and **B.** One and three (PC3) from the Principal Components Analysis (PCA) based on the regression residuals in external dorsal view, with equal frequency ellipses of 90%. The variance percentage for each PC is provided in parentheses.

Figure 16. Wireframe visualizations of shape variation between the extremes of **A.** Principal Component 1 (PC1) axis; **B.** Principal Component 2 (PC2) axis and **C.** Principal Component 3 (PC3) axis in external dorsal view. Black wireframe illustrates the shape configuration at the negative extreme of each PC axis. Gray wireframe represents the shape configuration at the positive extreme of each PC axis. Variance percentages of each PC are provided in parentheses.

Figure 17. Scatterplot of Principal Components one (PC1) and two (PC2) with frequency ellipses of 90% of **A.** External lateral view; **B.** Osteological lateral view and

C. External dorsal view. The variance percentage for each PC is provided in parentheses.

Chapter 2.

FIGURE 1. *Pimelodella guato*, holotype, ZUFMS-PIS 8515, 78.5 mm SL, Brazil, Mato Grosso do Sul, Corumbá municipality, rio Paraguai basin, rio Miranda, sandy beaches at Passo do Lontra region, 19°34'37"S 57°00'42"W. A. Dorsal; B. Left lateral; and C. Ventral views. Scale bar = 1 cm.

FIGURE 2. Left lateral view of radiographs of *Pimelodella* species, illustrating the dorsal lamina of Weberian complex vertebrae of A. *Pimelodella guato*, paratype, ZUFMS-PIS 647, 90.1 mm SL; B. *P. taeniophora*, ZUFMS-PIS 6320, 68.9 mm SL; C. *P. mucosa*, holotype, CAS 63720, 97.4 mm SL; and D. *P. serrata*, LIRP 10022, 83.6 mm SL.

FIGURE 3. Pectoral-fin spine of A. *Pimelodella guato*, paratype, CIUnB 1772, 91.2 mm SL, length of spine 16.7 mm; B. *P. taeniophora*, ZUFMS-PIS 6320, 68.9 mm SL, length of spine 11.4 mm; C. *P. mucosa*, holotype, CAS 63720, 97.4 mm SL, length of spine 22.8 mm; D. *P. serrata*, holotype, FMNH 57979, 55.7 mm SL, length of spine 18.3 mm; and E. *P. howesi*, holotype, ANSP 69036, 79.3 mm SL, length of spine 17.8 mm.

FIGURE 4. Geographic distribution of *Pimelodella guato* in the rio Paraguai basin (red star, type-locality; red dots, paratype localities). The symbols might represent more than one voucher specimen each.

FIGURE 5. Sexually dimorphic traits in an adult male specimen of *Pimelodella guato* (paratype, CIUnB 1772, 93.8 mm SL). A. Filament on the non-spinous portion of dorsal-fin second (unbranched) ray, indicated by a white arrow; and B. Enlarged urogenital papilla, indicated by a white arrow. Scale bars = 1 cm.

Lista de tabelas

Chapter 1.

Chapter 2.

TABLE 1. Morphometric data for the holotype and 42 paratypes of *Pimelodella guato*. N = number of specimens; SD = Standard deviation.

Resumo

Delimitação de espécies de *Pimelodella* Eigenmann & Eigenmann, 1888 (Siluriformes: Heptapteridae) na bacia do Alto rio Paraguai

Veida Raquel Meireles Pierre

Veronica Slobodian

Resumo da Dissertação de Mestrado apresentada ao Programa de Pós-graduação em Zoologia, Instituto de Ciências Biológicas, da Universidade de Brasília, como parte dos requisitos necessários à obtenção do título de Mestre em Zoologia.

O gênero *Pimelodella* é o mais diverso dentro de sua família, Heptapteridae, e é delimitado por uma combinação exclusiva de caracteres. Com uma distribuição extensa na região Neotropical, as espécies de *Pimelodella* são dulcícolas, sendo encontradas nas principais bacias neotropicais, incluindo a bacia do Alto rio Paraguai, que compreende um mosaico de paisagens e uma rede hidrográfica bastante heterogênea. A bacia do Alto Paraguai apresenta uma elevada diversidade biológica e altas taxas de endemismo, principalmente em terras altas. Devido à morfologia externa semelhante compartilhada entre as espécies de *Pimelodella*, o processo de delimitação e identificação é desafiador, resultando em um gargalo no conhecimento taxonômico do grupo. Assim, o presente estudo visa contribuir para o conhecimento acerca da delimitação das espécies de *Pimelodella* que ocorrem na bacia do Alto rio Paraguai, investigando diferenças de forma entre essas espécies a partir da morfometria geométrica. No geral, as espécies variaram significativamente na forma, apesar da sobreposição parcial de grupos no morfoespaço. As variações na forma do corpo foram principalmente associadas à posição relativa das nadadeiras dorsal e adiposa e à profundidade do corpo. A morfometria geométrica mostrou-se eficiente para recuperar a variação de forma e delimitar algumas espécies de *Pimelodella*, como *P. mucosa* e *P. gracilis*. Enquanto a morfometria linear (clássica) e os dados merísticos podem ser utilizados para delimitar espécies de *Pimelodella*, os dados obtidos a partir da morfometria

geométrica complementam essas delimitações, assim como ajudam a explicar e discutir as diferenças na forma do corpo. Além disso, este trabalho traz a descrição de uma nova espécie de *Pimelodella* com ocorrência também na bacia do rio Paraguai, apresentando uma chave de identificação para as espécies do gênero que ocorrem nessa bacia, e trazendo uma discussão biogeográfica acerca de sua distribuição.

Palavras-chave: Bagres, Chave de identificação, Ictiofauna de água doce, Morfometria geométrica, Pantanal, Taxonomia.

Brasília

Maio/2024

ABSTRACT

Delimitation of species of *Pimelodella* Eigenmann & Eigenmann, 1888 (Siluriformes: Heptapteridae) in Upper rio Paraguai basin

Veida Raquel Meireles Pierre

Veronica Slobodian

Abstract da Dissertação de Mestrado apresentada ao Programa de Pós-graduação em Zoologia, Instituto de Ciências Biológicas, da Universidade de Brasília, como parte dos requisitos necessários à obtenção do título de Mestre em Zoologia.

The genus *Pimelodella* is the most diverse within its family, Heptapteridae, and is delimited by an unique combination of characters. Having a large distribution in the Neotropical region, *Pimelodella* species are freshwater fishes found in the major neotropical basins, including the Upper rio Paraguai basin. This basin comprises a mosaic of landscapes and a highly heterogeneous hydrographic network, exhibiting high biological diversity and high rates of endemism, especially in upland areas. Due to the similarities in external morphology of *Pimelodella* species, the process of delimitation and identification is challenging, resulting in a taxonomic bottleneck for their comprehension. Thus, this study aims to contribute to the delimitation of *Pimelodella* species occurring in the Upper rio Paraguai basin, investigating shape differences between these species using geometric morphometrics. Overall, the species varied significantly in shape, despite the partial overlap of groups in morphospace. Body shape variations were mainly associated with the relative position of the dorsal and adipose fins and body depth. Geometric morphometrics proved to be efficient for recovering shape variation and delimit some *Pimelodella* species, such as *P. mucosa* and *P. gracilis*. While linear morphometrics (classic) and meristic data can be used to delimit *Pimelodella* species, data obtained from geometric morphometrics complement these delimitations, and allow discussions regarding differences in body shape. Additionally, this work describes a new species of *Pimelodella* also occurring

in the rio Paraguai basin, presenting an identification key for the species of this genus occurring in this basin, and providing a biogeographical discussion regarding its distribution.

Key-words: Catfishes, Freshwater ichthyofauna, Geometric morphometrics, Identification key, Pantanal, Taxonomy.

Brasília

Maio/2024

Introdução geral

1. O gênero *Pimelodella* Eigenmann & Eigenmann, 1888

O gênero *Pimelodella* Eigenmann & Eigenmann, 1888, compreende espécies dulcícolas geralmente encontradas em riachos, associadas a bancos arenosos, próximas à vegetação marginal, ou em fendas de rochas (Bockmann, Guazzelli, 2003; Slobodian *et al.*, 2017; Slobodian, Pastana, 2018). São peixes de hábitos geralmente noturnos e são considerados peixes ornamentais, com sua captura geralmente se restringindo ao âmbito do aquarismo, apesar de espécimes maiores serem eventualmente pescados para alimentação (Bockmann, Guazzelli, 2003; Bockmann, Slobodian, 2013).

Esse gênero destaca-se como o mais diverso dentro de Heptapteridae, compreendendo 84 espécies válidas (Fricke *et al.*, 2024). O táxon foi descrito em 1888 por Eigenmann e Eigenmann, indicando *Pimelodus cristatus* Müller & Troschel, 1849, como espécie-tipo, que então foi realocada a *Pimelodella cristata*. Nessa descrição, foram incorporadas 10 espécies previamente alocadas no gênero *Pimelodus* Lacepède, 1803, e foi descrita uma nova espécie, *Pimelodella pectinifer* Eigenmann, Eigenmann, 1888. Assim, *Pimelodella* foi inicialmente descrita a partir das seguintes características: “cabeça inteiramente coberta de pele; processo occipital estreito, de mesma largura em toda a extensão, encontrando-se com a placa dorsal; fontanela prolongada para trás até o processo occipital com uma ponte através dela atrás do olho” (Eigenmann, Eigenmann, 1888: 131) (Fig. 1).

Em 1917, Eigenmann realizou a primeira revisão taxonômica do gênero, fornecendo informações de distribuição geográfica e descrição das espécies. Nesse trabalho, foram reconhecidas 33 espécies e uma subespécie de *Pimelodella*, das quais 10 eram táxons novos (Eigenmann, 1917). Com essa publicação, a diagnose de *Pimelodella* passou a compreender as seguintes características: “narinas remotas; dentes viliformes, em faixas; membranas branquiais livres do istmo; dorsal curta, com um espinho pungente; anal curta, com 11–15 raios; peitoral com um espinho forte e pungente armado de diversas formas com dentes espinhosos em sua borda posterior (interna); uma nadadeira longa e adiposa; nadadeira caudal profundamente bifurcada, um ou outro lóbulo frequentemente mais largo ou mais longo; barbilhões maxilares bem desenvolvidos alcançando a extremidade da peitoral ou além da caudal; dois

pares de barbilhões mentonianos, algumas vezes em uma linha quase reta; uma fontanela frontal e uma parietal, esta última atingindo a base do processo occipital, que é estreito e alcança, ou quase alcança, a placa anterior à dorsal; processo umeral semelhante a um espinho; teto da boca sem dentes; cabeça coberta com pele fina" (Eigenmann, 1917: 229) (Fig. 1).

Figura 1. *Pimelodella guato* Pierre & Slobodian, 2024, ZUFMS-PIS 6370, 127,9 mm CP, Mato Grosso do Sul, Município de Coxim, rio Taquari, 18°31'32"S, 54°44'30"W, coletado por H. Gimenes-Jr, M. B. Mendonça, P. Camelier, M. Kaluza, F. Severo-Neto, R. Rech, F. Vasconcelos e R. Mochi em 16 de Dezembro de 2019.

Apesar de sua abrangente revisão taxonômica, Eigenmann (1917) reconheceu a complexidade em delimitar as espécies de *Pimelodella*. O autor observou que muitas

características de morfologia externa das espécies descritas eram influenciadas por outros fatores, como idade e localidade, e salientou assim a provisoriedade de tais descrições (Eigenmann, 1917). De fato, os caracteres diagnósticos propostos para o gênero e para suas respectivas espécies na época não foram suficientes para delimitar as espécies de *Pimelodella* ao longo do tempo, à medida que novas espécies foram sendo descritas ou realocadas no gênero (Ferraris, 2007).

Além disso, o gênero carece de estudos filogenéticos publicados, de forma que trabalhos concernindo a taxonomia e sistemática do gênero, de maneira abrangente, estão disponíveis apenas em teses e dissertações (*e.g.,* Guazzelli, 1997, 2003; Bockmann, 1998; Slobodian, 2013; Conde-Saldaña, 2016; Peixoto, 2011), assim como a última revisão taxonômica do gênero (Slobodian, 2017). Na ausência de um estudo filogenético compreensivo publicado para o gênero, *Pimelodella* é atualmente delimitada por uma combinação exclusiva de caracteres: “corpo moderadamente alongado, geralmente entre 12 e 30 cm de comprimento padrão (apesar de alguns indivíduos de *Pimelodella cristata* poderem exceder 30 cm de comprimento padrão); processo supraoccipital longo, geralmente alcançando a placa nucal anterior; fontanelas anterior e posterior abertas, longas e separadas pela barra epifisária; limites dos olhos bem definidos pela borda orbital livre, bem acentuados anteriormente e dorsalmente; nadadeiras peitorais com um raio não ramificado forte e pungente (espinho), geralmente com dentações nas suas porções anterior e posterior, e 7–9 (geralmente 8) raios ramificados; geralmente seis raios branquiostégios; nadadeira caudal profundamente bifurcada; raios medianos da nadadeira caudal não articulados à placa hipural; hipural 5 como uma estrutura livre da placa hipural; corpo geralmente com uma faixa média-lateral escura se estendendo do focinho ou simplesmente posterior ao opérculo até a inserção, ou sobre os raios medianos da nadadeira caudal” (Slobodian, Pastana, 2018: 1) (Fig. 1).

Devido à morfologia externa muito semelhante compartilhada entre as espécies de *Pimelodella*, o processo de delimitação e identificação ao nível de espécie é desafiador (Slobodian *et al.*, 2017). Essa complexidade resulta em um gargalo no conhecimento taxonômico acerca do gênero, que vem sendo cada vez mais estudado a partir de revisões taxonômicas (Guazzelli, 1997, 2003; Slobodian, 2017), descrições de novas espécies (*e.g.*, Trajano *et al.*, 2004; Slobodian *et al.*, 2017; Slobodian, Pastana, 2018; Conde-Saldaña *et al.*, 2019; Cortés-Hernández *et al.*, 2020) e

redescrições (Slobodian *et al.*, 2021; Cortés-Hernández *et al.*, 2023). Com uma distribuição extensa que se estende desde o Panamá até a Argentina, as espécies pertencentes a esse gênero compõem ambientes dulcícolas, sendo encontradas nas principais bacias neotropicais (Bockmann, Guazzelli, 2003; Ferraris, 2007; Bockmann, Slobodian, 2013, 2018; Koerber *et al.*, 2017; Mirande, Koerber, 2020; Slobodian *et al.*, 2022; Fricke *et al.*, 2024).

2. Bacia do rio Paraguai

A bacia do rio Paraguai figura como uma das mais importantes na região Neotropical, integrando a bacia do rio da Prata, juntamente com as bacias do Paraná e do Uruguai. A bacia do rio da Prata, como um todo, corresponde à segunda maior rede hidrográfica da América do Sul, abrangendo áreas no Brasil (nas regiões Sul, Sudeste e Centro-Oeste), Bolívia, Paraguai, Uruguai, e Argentina (Tucci, Clarke, 1998). Dentre as três bacias componentes, a do rio Paraguai é a segunda maior, compreendendo mais de 35% da extensão total da bacia do rio da Prata (Tucci, Clarke, 1998).

Apresentando o rio Paraguai como seu principal corpo d'água, a bacia do rio Paraguai engloba rios e riachos distribuídos pelo Brasil (nos Estados do Mato Grosso e Mato Grosso do Sul), Bolívia, Paraguai e Argentina. Neste último território, a bacia conecta-se à bacia do rio Paraná, próximo à cidade de Corrientes (Tucci *et al.*, 1995). A bacia é subdivida, de forma que a porção brasileira, denominada bacia do Alto Paraguai, ocupa uma área superior a 361 mil quilômetros quadrados nos Estados do Mato Grosso e Mato Grosso do Sul (Fig. 2), apresentando também uma pequena proporção em territórios boliviano e paraguaio (Carvalho, 1986; Tucci *et al.*, 1995).

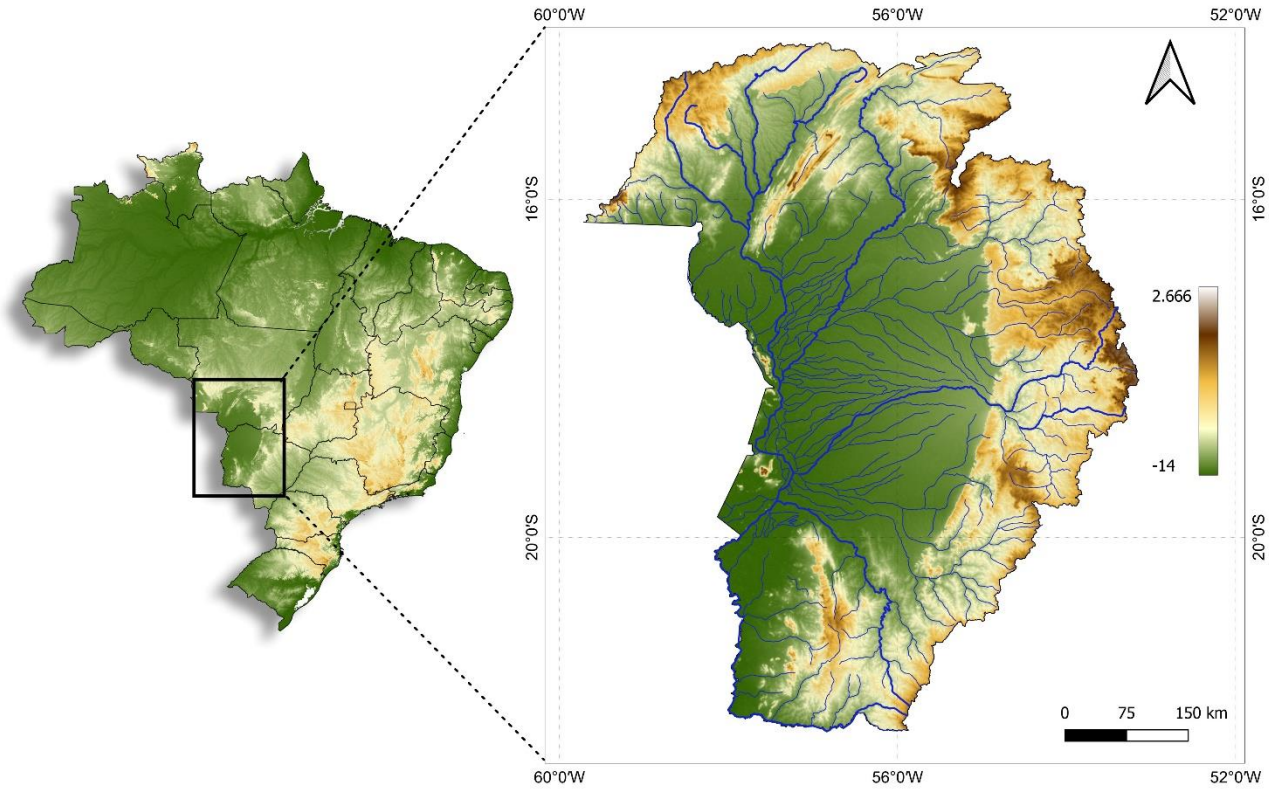

Figura 2. Bacia do Alto rio Paraguai em território brasileiro.

A bacia do Alto rio Paraguai compreende um mosaico de paisagens, com uma rede hidrográfica bastante heterogênea, composta por rios sinuosos em áreas de menor altitude (Boin *et al.*, 2019; Zumak *et al.*, 2021). Ao longo dessa bacia, por exemplo, observa-se a presença de diversos meandros abandonados (Carvalho, 1986), que correspondem a áreas alagadas (lagos) resultantes de desvios do curso d'água. Esses desvios ocorrem pela sinuosidade elevada dos rios, resultando em vazamento de água para áreas adjacentes, formando assim áreas fluviais isoladas (Menecozi, 2015). Durante períodos de cheias, por sua vez, esses meandros podem se reconectar ao rio (Boin *et al.*, 2019).

O rio Paraguai corresponde ao principal rio da bacia, se originando na porção norte (na Chapada dos Parecis, Estado do Mato Grosso), e seguindo para o sul (Carvalho, 1986) (Fig. 2). Ao longo de seu percurso, o rio Paraguai recebe corpos d'água de diversos afluentes, como os dos rios Jauru, Cabaçal e Sepotuba na porção norte, e os rios Cuiabá, Taquari, Miranda e Apa na porção sul (Carvalho, 1986). Na confluência com o Rio Apa, o rio Paraguai adentra o Paraguai, marcando assim o limite da bacia do Alto Paraguai (Carvalho, 1986).

Compondo a rede hidrográfica do Alto rio Paraguai, a bacia do rio Taquari abrange regiões bastante distintas entre si, com sua porção mais alta situada no planalto, estendendo-se desde as nascentes do Rio Taquari até um pouco além de sua confluência com o rio Coxim (Galdino *et al.*, 2006). Por ser uma área com intenso potencial erosivo, essa região compreende uma das maiores preocupações atuais quanto às questões erosivas da bacia do Alto Paraguai. A região mais baixa da bacia do rio Taquari, por sua vez, localiza-se na planície pantaneira, estendendo-se até a desembocadura do rio Taquari no rio Paraguai (Galdino *et al.*, 2006). Essa área, com menor potencial erosivo, consiste em um amplo espaço de deposição de sedimentos, formando uma das maiores rede de leques aluviais do planeta, representando cerca de 37% da planície pantaneira (Galdino *et al.*, 2006; Assine *et al.*, 2016).

A bacia do Alto Paraguai é caracterizada por uma diversidade de relevos, compreendendo planaltos e planícies, que abrangem aproximadamente 61% e 36% da área da bacia, respectivamente (Silva, Abdon, 1998). Os planaltos, que abrigam as nascentes dos principais tributários do rio Paraguai, são formados por terras altas de cadeias montanhosas, com altitudes variando entre 400 e 1.500 metros acima do nível do mar (Tucci *et al.*, 1995; Zumak *et al.*, 2021). Entre os locais que compõem o planalto da bacia do Alto Paraguai, destacam-se a Chapada dos Guimarães, Chapada dos Parecis, Serra de Maracaju, Serra da Bodoquena, e Maciço do Urucum (Boin *et al.*, 2019). Por outro lado, as planícies compreendem as terras baixas da bacia do Alto Paraguai, com altitude entre 80 e 200 metros acima do nível do mar, sendo regiões circundadas pelos planaltos (Boin *et al.*, 2019; Zumak *et al.*, 2021).

Essas planícies, como um todo, configuram a paisagem do Pantanal, uma área reconhecida como “Patrimônio Natural Mundial” e a maior região alagada contínua do mundo, com uma extensão de aproximadamente 150.000 km² (Unesco, 2000). Em relação à cobertura vegetal, o Pantanal é influenciado por diversos domínios fitogeográficos, como a Amazônia, Cerrado, Mata Atlântica e o Gran Chaco boliviano e paraguaio (ANA *et al.*, 2004). A formação da planície alagada é decorrente de uma combinação de fatores, como o tipo de solo e o regime pluviométrico da bacia do Alto Paraguai, apresentando chuvas sazonais (Carvalho, 1986; Tucci *et al.*, 1995; Boin *et al.*, 2019). Além disso, há o fator relacionado com a elevada vazão de água proveniente das terras altas que, ao adentrar a planície, sofre uma redução de sua velocidade em decorrência da acentuada diferença de declive entre os relevos

(Carvalho, 1986; Boin *et al.*, 2019). Essas condições, como um todo, contribuem para uma baixa capacidade de drenagem da planície (Carvalho, 1986; Tucci *et al.*, 1995), possibilitando um alagamento expressivo no Pantanal por aproximadamente cinco a seis meses do ano (Zumak *et al.*, 2021).

Ademais, uma vez que as planícies pantaneiras constituem áreas de deposição de sedimentos advindos das terras altas que as circundam, os processos erosivos e as pressões antrópicas que ocorrem nos planaltos afetam diretamente o Pantanal (Roque *et al.*, 2016; Boin *et al.*, 2019; Guerra *et al.*, 2020). Nas últimas décadas, a bacia do Alto Paraguai tem enfrentado crescentes pressões antrópicas, relacionadas principalmente a atividades agropecuárias, como o uso da terra para pastagem e produção de grãos. Além disso, a região é submetida a uma intensa atividade hidrelétrica, contendo atualmente cerca de 52 usinas em operação, sendo sete correspondentes a usinas hidrelétricas (UHEs), e 26 Pequenas Centrais Hidrelétricas (PCHs), além de mais de 80 PCHs em fase de estudo para construção (ECOA, 2024).

Tais influências antrópicas resultam em diversas questões ambientais, incluindo a perda de vegetação e a diminuição das matas de galeria, contribuindo assim para o aumento do potencial erosivo e consequente assoreamento dos rios (Guerra *et al.*, 2020). A bacia do rio Taquari, por exemplo, sofreu uma perda de mais de 860 mil hectares desde 1985 devido às atividades de uso do solo (Zumak *et al.*, 2021), sendo atualmente uma das maiores preocupações acerca dos problemas ambientais no Pantanal (Zumak *et al.*, 2021). Devido às características do solo e aos processos geomorfológicos, a bacia do rio Taquari é naturalmente propensa à erosão, sendo responsável pelo transporte de areia fina para o rio Paraguai (Galdino *et al.*, 2006). Porém, a intensificação do uso do solo ao longo das décadas ampliou o processo erosivo na região, acarretando o assoreamento do rio Taquari e a formação de uma abrangente área permanentemente inundada em sua planície, configurando um sistema de leques aluviais (Galdino *et al.*, 2006).

Dessa forma, projetos de conservação na bacia do Alto rio Paraguai são fundamentais tanto no âmbito socioeconômico, quanto no ambiental. O assoreamento de rios, assim como o aumento de regiões com inundação permanente, prejudica a manutenção do uso do solo, impactando nas atividades agropecuárias (Zumak *et al.*, 2021). Além disso, afeta diretamente a vida cotidiana da população local, resultando

na perda de moradias e no deslocamento forçado de famílias das áreas inundadas (Guerra *et al.*, 2020; Zumak *et al.*, 2021). Em termos ambientais, os impactos também são imensuráveis, afetando diretamente a qualidade da água e, consequentemente, a diversidade da ictiofauna na região.

A diversidade de peixes na bacia do Alto rio Paraguai também impulsiona o turismo e a pesca na região, compreendendo espécies de interesse de pesca comercial e esportiva, *e.g.*, curimbatá, *Prochilodus lineatus* (Valenciennes, 1837); dourado, *Salminus brasiliensis* (Cuvier, 1816); pintando, *Pseudoplatystoma corruscans* (von Spix & Agassiz, 1829); e piraputanga, *Brycon hilarii* (Valenciennes, 1850). Contudo, a bacia também apresenta numerosas espécies de menor porte que, embora não sejam de interesse para esse tipo de pesca, compõem a diversidade da região e desempenham importantes papéis para o funcionamento do ecossistema aquático (Gimênes-Junior, Rech, 2022). A bacia do Alto Paraguai apresenta uma notável diversidade biológica e altas taxas de endemismo, principalmente em terras altas. Com a maioria das espécies pertencentes às ordens Characiformes e Siluriformes, a bacia é habitat de cerca de 386 espécies de peixes (Carvalho, Albert, 2011; Gimênes-Junior, Rech, 2022), sendo pelo menos um terço delas consideradas endêmicas (Carvalho, Albert, 2011).

3. Justificativa e estruturação da dissertação

Como as espécies de *Pimelodella* apresentam uma morfologia altamente conservada, a delimitação e identificação de suas espécies torna-se um árduo processo (Slobodian *et al.*, 2017). Embora várias coletas tenham sido realizadas na bacia do rio Paraguai e integrem os acervos de coleções científicas, muitos exemplares permanecem indeterminados ao nível de gênero, ou foram identificados erroneamente (Slobodian *et al.*, 2017; obs. pess.). Além disso, observa-se uma lacuna em trabalhos taxonômicos com *Pimelodella*, apesar da evidente necessidade de estudos que visem elucidar os problemas relacionados à delimitação e identificação de suas espécies. Diante desse desafio taxonômico, o presente estudo visa contribuir para o conhecimento acerca da delimitação das espécies de *Pimelodella* que ocorrem na bacia do Alto rio Paraguai.

Assim, o primeiro capítulo concentra-se em estudar a delimitação das espécies de *Pimelodella* que ocorrem na bacia do Alto rio Paraguai a partir da morfometria geométrica. Este capítulo objetiva verificar se há variação de forma entre tais espécies e, caso sim, entender de que modo essa variação ocorre. O segundo capítulo, por sua vez, se refere a um artigo publicado na revista Neotropical Ichthyology, compreendendo a descrição de uma nova espécie de *Pimelodella* com ocorrência também na bacia do rio Paraguai, denominada *Pimelodella guato*. Além disso, é apresentada uma chave de identificação para as espécies do gênero que ocorrem nessa bacia. A descrição da nova espécie baseou-se na taxonomia tradicional (clássica), utilizando aspectos de morfometria linear e da osteologia. No entanto, dado que sua distribuição geográfica abrange a bacia estudada nesta dissertação, incluímos *P. guato* nas análises de morfometria geométrica, sendo uma das espécies também abordadas no primeiro capítulo.

Chapter 1

Geometric morphometrics in the delimitation of sympatric species of *Pimelodella* Eigenmann & Eigenmann, 1888 (Siluriformes: Heptapteridae)

Abstract

The genus *Pimelodella* is the most diverse within its family Heptapteridae, and the delimitation and identification of its species pose a challenge to the group due to highly conserved morphology and extensive geographical distribution. Geometric morphometrics, widely used in the field of Taxonomy, offers valuable insights into species delimitation, and may be valuable in resolving taxonomic issues of *Pimelodella*. Thus, this work aims to examine the applicability of geometric morphometrics, incorporating landmarks of both external morphology and osteology, in the delimitation of species of *Pimelodella* within the Upper rio Paraguai basin. Fourteen landmarks were selected for both photographs and radiographs in lateral view, as 12 were chosen for photographs in dorsal view. These landmarks correspond to fin insertions, skeletal structures, and the head region. Geometric morphometrics analyses revealed significant variation in body and head size among the species, with *P. gracilis* standing out as the largest species, while *P. griffini* was indicated as the smallest among those under investigation. In addition, the species varied significantly in shape, although partial superimposition of groups was also observed in the morphospace. Regarding body shape, variations were mainly associated with the positions of the dorsal and adipose fins alongside body depth, as head shape displayed changes ranging from bulkier and arrow-like shapes, along with variations in the position of the supraoccipital process. Overall, geometric morphometrics was an efficient method to delimit certain species of *Pimelodella*, such as *P. mucosa,* which was the species that most distinguished in shape among those analysed, as well as distinguishing *P. gracilis* from *P. griffini*. *Pimelodella mucosa* encompasses a deeper body shape throughout their entire length, with dorsal and adipose fins located more distant from each other. Conversely*, Pimelodella gracilis* exhibits a slender body shape, with dorsal and adipose fins closely positioned to each other. While linear morphometrics and meristic data are commonly utilized to delimit species of *Pimelodella*, geometric morphometrics complements this approach, aiding in the discussion of shape changes.

Keywords: Adipose fin, Freshwater ichthyofauna, Morphology, Shape variation, Taxonomy, Upper rio Paraguai basin.

Introduction

1. Family Heptapteridae and genus *Pimelodella* Eigenmann & Eigenmann, 1888

The Neotropical region exhibits the highest diversity of freshwater fishes in the world, encompassing over 6,000 species described (Dagosta, de Pinna, 2019; Albert *et al.*, 2020). However, current estimations suggest this diversity surpasses 9,000 species, with many yet to be described (Reis et al., 2016; Albert et al., 2020). One of the main components of Neotropical ichthyological diversity is the order Siluriformes, constituting approximately 38.7% of its overall diversity (Albert *et al.*, 2020). It includes a wide range of morphologies and sizes, either featuring fishes with naked bodies or covered with bony plates. Siluriformes is predominantly composed of freshwater fishes, and presently comprises 4,220 valid species distributed in 509 genera and 41 families (Fricke *et al.*, 2024).

Extending throughout the Neotropical region, the family Heptapteridae stands as one of the most prominent families within the order Siluriformes in terms of diversity, comprising 235 valid species distributed across 23 genera (Fricke *et al.*, 2024). Encompassing fishes of small or medium size (usually less than 20 cm SL), this family is characterized by a unique combination of features, including: skin naked, simple cephalic laterosensorial canals, three pairs of barbels (maxillary, inner and outer mentals), nares well separated and lacking barbels, gill membranes free, conspicuous adipose fin, usually with a free posterior lobe (or confluent with the caudal fin in some species), caudal fin usually bifurcated (Bockmann, Guazzelli, 2003; Bockmann, Slobodian, 2018).

Members of the family Heptapteridae are commonly known as *bagre*, *bagrinho*, *barbilla*, *chicote*, *chum-chum*, *cunshi*, *jundiá*, *komairu*, *lobó*, *mandi*, *mandi-chorão*, *mandizinho*, *puyapuya*, and other local names (Bockmann, Guazzelli, 2003; Bockmann, Slobodian, 2013; Slobodian *et al.*, 2022). Most species of this family exhibit benthic habits and are typically found in streams with well-preserved marginal vegetation. However, some species may also occupy the water column, such as those belonging to the genus *Brachyrhamdia* Myers, 1927, and *Pimelodella* Eigenmann & Eigenmann, 1888 (Bockmann, Guazzelli, 2003; Bockmann, Slobodian, 2013; Bockmann, Slobodian, 2018). Heptapteridae is endemic to the Neotropical region, with its distribution ranging in eastern drainages from the Gulf of Mexico to central

Argentina, and in western drainages from southern Mexico to central Peru (Bockmann, Guazzelli, 2003; Bockmann, Slobodian, 2018; Slobodian *et al.*, 2022).

At the species level, several genera have undergone thorough careful systematic studies over the years (see references in Slobodian, Bockmann, in press). Moreover, there are investigations concerning the phylogenetic relationships within the family, based on morphological (Bockmann, 1998) and molecular (*e.g.*, Silva *et al.*, 2021; Faustino-Fuster *et al.*, 2021) data. In general, the delimitation of genera and species of Heptapteridae primarily relies on osteological differences and on a combination of phenotypic characteristics, given the highly conserved external morphology observed in the majority of the genera (Lundberg, McDade, 1986; Bockmann, Guazzelli, 2003). Therefore, the challenges associated with the delimitation process may result in a potential underestimation of the diversity within the family. Bockmann and Guazzelli (2003) suggest an estimate of approximately 200 valid species constituting the family at the time, with approximately 50 species still awaiting formal descriptions.

Within the family Heptapteridae, the genus *Pimelodella* is the most species-rich. However, the highly conserved morphology observed across its various species complicates the determination of diagnostic characters (Slobodian *et al.*, 2017). This, associated with the widespread geographical distribution of the group, leads to considerable difficulties in the accurate description and identification of its species (Slobodian *et al.*, 2017). When compiling a list of Heptapteridae species in the rio Madeira based on available literature, Bockmann and Slobodian (2013) highlighted the obstacle in obtaining precise identifications of members of the genus *Pimelodella*. This intricacy arised from the superficiality of descriptions available in the literature, which, when compared with current taxonomic standards, proves inadequate for obtaining precise identifications (Bockmann, Slobodian, 2013).

The difficulties in the identification process are also evident in the materials housed within scientific collections, where numerous specimens of *Pimelodella* bear erroneous identifications or are undetermined at species-level (Slobodian *et al.*, 2017; pers. obs.). On speciesLink (2024), for instance, there are over 5,000 registers of vouchers of *Pimelodella* from several scientific collections, from which approximately 2,500 are identified solely as "*Pimelodella* sp.". In an unpublished thesis, Slobodian

(2017) conducted an extensive taxonomic revision of the genus *Pimelodella*, employing data from linear morphometrics, osteology, coloration, and genetics. This investigation underscores the necessity of utilizing osteological or molecular characters to delimitate some species, such as *P. avanhandavae* Eigenmann, 1917, *P. gracilis* (Valenciennes, 1835) and *P. taeniophora* (Regan, 1903). The necessity of relying on such characters for species identification complicates the task for non-specialists in accurately discerning these species, given that not all researchers may possess the recquired technical resources and experience. Consequently, it is crucial to investigate external morphological characters that may contribute to the taxonomy of the genus.

Presenting a widespread distribution from Panama to Argentina, the species of *Pimelodella* are found throughout the major neotropical basins, including the rio Paraguai basin. For this basin there are records of *P. gracilis*; *P. griffini* Eigenmann, 1917; *P. laticeps* Eigenmann, 1917; *P. megalura* Miranda Ribeiro, 1918; *P. mucosa* Eigenmann & Ward *in* Eigenmann *et al.*, 1907; *P. notomelas* Eigenmann, 1917; *P. parva* Güntert, 1942; *P. taeniophora*; *P. taenioptera* Miranda Ribeiro, 1914 (Eigenmann, 1917; Britski *et al.*, 1999, 2007; Koerber *et al.*, 2017; Mirande, Koerber, 2020; Slobodian *et al.*, 2022). Among these, solely *P. laticeps* and *P. parva* are not found in the upper reaches of the Paraguai basin, that is the focus area of this study.

Pimelodella gracilis was initially described under the genus *Pimelodus* Lacepède, 1803, based on an illustration (Valenciennes, 1835), followed by a subsequent textual description in 1847 (Valenciennes, 1847). The type was collected by d'Orbigny in the city of Corrientes, Argentina, within the rio Paraná. According to d'Orbigny, more individuals of this species were collected in the same region, consistently in rocky locations with robust water currents (Cuvier, Valenciennes, 1840). When the genus *Pimelodella* was described, Eigenmann and Eigenmann (1888) reclassified *Pimelodus gracilis* to this novel genus. Furthermore, the authors expanded its geographical distribution to Goiás State, Brazil. However, Eigenmann (1917), in his taxonomic revision of *Pimelodella*, expressed doubts about the corrected designation of these specimens from Goiás. Indeed, based on his descriptions, Slobodian (2017) suggests that these specimens may instead correspond to *P. laurenti* Fowler, 1941.

In fact, the geographical distribution of *P. gracilis* has been the subject of various discussions over the decades, due to similarities with other *Pimelodella* species, such as *P. cristata* (Müller & Troschel, 1849) and *P. steindachneri* Eigenmann, 1917. Due to the potentially wide distribution of *P. gracilis* (*i.e.* La Plata, Uruguai, Amazon, and Orinoco basins), Mees (1974) proposed either the synonymy of *P. cristata* with *P. gracilis* or a geographical delimitation between the species. In the latter scenario, *P. gracilis* would be distributed to the La Plata and Uruguai basins, while *P. cristata* would occur in Guianas, Orinoco and Suriname regions, and *P. steindachneri* in the Amazon basin (Mees, 1974). Moreover, Slobodian (2017) suggests *P. taenioptera* as a junior synonym of *P. gracilis*, since there was no success in distinguishing both species.

Among the species of *Pimelodella*, *P. gracilis* is one of the most investigated, comprising biological, ecological, molecular, and cytogenetic studies (*e.g.*, Santos *et al.*, 2006; Viana *et al.* 2006; Barros *et al.*, 2011; Nascimento *et al.*, 2011; Fernandes *et al.*, 2013; Hakamada, Penha, 2014; Shimabukuro-Dias *et al.*, 2017; Penha *et al.*, 2018), along with helminthological examination (*e.g.*, Núñez *et al.*, 2011; Arredondo, Núñez, 2013; Ramallo, Ailán-Choke, 2017). Nonetheless, it is not possible to confirm the identification of the specimens investigated, given the absence of voucher numbers or photographic evidence in the studies. Currently, the distribution range of *P. gracilis* encompasses rios Orinoco, Amazon, Paraguai and Paraná basins (Bockmann, Guazzelli, 2003; Ferraris, 2007; Fricke *et al.*, 2024), with specimens typically inhabiting the large rivers of the Pantanal region (Slobodian, 2017; Slobodian *et al.*, 2022).

Pimelodella griffini was described from mountain rills near the city of Sapucay, Paraguay, within the rio Paraguai basin (Eigenmann, 1917). This description primarily relied on the observation of a filamentous prolongation on the unbranched dorsal-fin ray, however, this filament was posteriorly indicated as a secondary sexual character of male adults (*e.g.*, Dahl, 1961; Souza-Shibatta *et al.*, 2013). Despite indications of *P. griffini* occurring in other regions, such as the Beni basin (Pearson, 1924; Fowler, 1940) and the Paraguai basin in Argentina (Castello, 1969; Lopez *et al.*, 2003; Mirande, Koerber, 2015, 2020), Slobodian (2017) suggests that the specimens observed in these studies probably refer to *P. gracilis*, due to their morphological descriptions. Thus, the distribution of *P. griffini* must be restrict to rio Paraguai basin, as well as *P. megalura*, *P. mucosa*, *P. notomelas* and *P. taeniophora* (Bockmann, Guazzelli, 2003; Ferraris, 2007; Fricke *et al.*, 2024; Slobodian *et al.*, 2022).

Pimelodella megalura was first described from São Luiz de Cáceres (currently Cáceres), based on 22 syntypes (Miranda Ribeiro, 1918), with the posterior designation of a lectotype (Miranda Ribeiro, 1953). This species presents a short supraoccipital process, not reaching the anterior prenuchal plate (Slobodian, 2017). This characteristic is found only in a few *Pimelodella* species, such as *P. bockmanni* Slobodian & Pastana, 2018; *P. itapicuruensis* Eigenmann, 1917; *P. leptosoma* (Fowler, 1914); *P. longipinnis* (Borodin, 1927); *P. metae* Eigenmann, 1917; *P. montana* Allen *in* Eigenmann and Allen, 1942; *P. peruensis* Fowler, 1915; *P. robinsoni* (Fowler, 1941); *P. tapatapae* Eigenmann, 1920; *P. wolfi* (Fowler, 1941); and *P. yuncensis* Steindachner, 1902 (Fowler, 1914; Borodin, 1927; Fowler, 1941; Slobodian, 2017; Slobodian, Pastana, 2018). Additionally, certain specimens of *P. megalura* exhibit hypural 5 fused to the dorsal hypural plate (3+4) (Slobodian, 2017), contrary to one of the putative synapomorphies of *Pimelodella*, with the hypural 5 remaining free and not fused to hypurals 3+4 (Slobodian, Pastana, 2018). Both of these features found in *P. megalura* are also somewhat similar to what is found in the genus *Rhamdella* Eigenmann & Eigenmann, 1888 (Slobodian, 2017; Bockmann, Slobodian, 2018).

Pimelodella mucosa was described from the rio Paraguai basin in Bahia Negra, Paraguay (Eigenmann *et al.*, 1907), and its known occurrence is confined to this basin, encompassing water bodies in Paraguay, Argentina and Brazil (Bockmann, Guazzelli, 2003; Ferraris, 2007; Aguilera, Azpelicueta, 2015; Slobodian *et al.*, 2022). While reports have been documented in the Bolivian Amazon (Chernoff *et al.*, 2000), specimens collected from this region may represent *P. serrata* Eigenmann, 1917, which inhabits the area and which *P. mucosa* shares some resemblance with (Slobodian, 2017). Both species share a unique characteristic within the genus, *i.e.*, openings of preoperculomandibular laterosensory canal at dentary large and conspicuous (Slobodian, 2017; Slobodian *et al.*, 2022).

Pimelodella notomelas was described from the rio Paraguai basin, in São Luiz de Cáceres (currently Cáceres), Brazil (Eigenmann, 1917). Its initial description was primarily based on the presence of a black spot on the dorsal fin (Eigenmann, 1917), which was posteriorly revised as the distal half of the dorsal fin being dark brown to black (Slobodian, 2017). The distribution of *P. notomelas* is known from the Upper Paraguai basin (Bockmann, Guazzelli, 2003; Ferraris, 2007; Slobodian *et al.*, 2022; Fricke *et al.*, 2024), with scarce occurrence (Slobodian *et al.*, 2022).

Pimelodella taeniophora was initially classified within the genus *Pimelodus,* based on two syntypes collected by Dr. Ternetz in Descalvados, Mato Grosso State (Regan, 1903). These two specimens have been maintained as syntypes to date, with Slobodian (2017) suggesting a lectotype. Moreover, a study comprising specimens of *Pimelodella* from the rio Miranda, in Upper Paraguai basin, detected the presence of cryptic species with the use of multiple techniques (*i.e.*, cytogenetic, molecular, morphological) (Souza-Shibatta *et al.*, 2013). The analyses indicated the differentiation of two groups, identified by the authors as *P. griffini* and *P. taenioptera* (Souza-Shibatta *et al.*, 2013). However, Slobodian (2017) pointed out that the specimens designated as *P. griffini* in that study actually correspond to *P. taeniophora*.

In summary, *Pimelodella* species delimitation and identification present various difficulties, and this is no different for the species found in the Upper rio Paraguai basin. For biological groups contending with these taxonomic questions, the use of complementary approaches to linear morphometrics, such as geometric morphometrics, may contribute to the delimitation of these species.

2. The geometric morphometrics

The investigation of shape variation is present in various fields of biology, proving relevant in comprehending the morphological distinctions associated with ontogenetic development and evolutionary processes, such as adaptation (Zelditch *et al.*, 2004). In the 20th century, the biometry, coined by Karl Pearson and Walter F. R. Weldon, emerged as a field to formally understand shape variation through the quantitative data primarily derived from measurements (Adams *et al.*, 2004). The quantification of shape introduced objectivity into the examination of shape variation, enhancing the explanatory potential of this approach. Posteriorly, in the 1960s, advancements in statistical analyses contributed to the development of morphological studies, giving rise to the field of Morphometrics (Adams *et al.*, 2004). Initially, this area consisted solely of linear morphometrics, also termed traditional morphometrics (Marcus, 1990), which quantifies shape based on linear distance, angles, ratios, and counts (Rohlf, 1990; Adams *et al.*, 2004).

Despite being an effective method for its purpose and widespread adopted in morphological studies, linear morphometrics still retains inherent limitations (Rohlf,

1990; Zelditch *et al.*, 2004). Due to dealing with linear measures, the differentiation between size and shape is more difficult, with shape being represented by ratios derived from distance measurements (Rohlf, 1990; Zelditch *et al.*, 2004). Consequently, there arose a challenge in the geometric understanding of shape, as the method would not afford, for instance, a throughout comprehension of how curved dimensions are shaped between two extremities of a linear measure (Rohlf, 1990; Rohlf, Marcus, 1993; Zelditch *et al.*, 2004; Mitteroecker, Gunz, 2009). Thus, there arose the need for a method that transcends these limitations (Rohlf, Marcus, 1993).

Geometric morphometrics is a technique employed to quantify and analyze shape variations while maintaining geometric information, thereby facilitating a deeper understanding of morphological differences between groups (Bookstein, 1991; Mitteroecker, Gunz, 2009). This technique became widespread predominantly in the early 1990s with the advent of computer programs for morphometric analyses (Monteiro, Reis, 1999). Thus, it was indicated as a revolution in morphometric studies, since previous methods had mainly relied on distance measurements (Rohlf, 1990; Rohlf, Marcus, 1993). Geometric morphometrics, on the other hand, relies on the configuration of anatomical landmarks, detecting shape variations in any direction of the morphospace without interference from size, position, or orientation (Bookstein, 1991).

Landmarks are Cartesian coordinates that define the shape of structures or specimens, and are related to homologous points identified across all analyzed specimens (Bookstein, 1991; Zelditch *et al.*, 2004). Consequently, landmark configurations are superimposed, and shape differences are analyzed based on the positional variations among homologous landmarks of the specimens under consideration (Bookstein, 1991; Zelditch *et al.*, 2004).

In the field of geometric morphometrics, shape is defined as what persists when all effects of size, orientation, and position are removed (Kendall, 1977, 1984; Goodall, 1991; Zelditch *et al.*, 2004). Diverse approaches address this elimination, with the Generalized Procrustes Analysis (GPA) being the most widely used, comprising three sequential stages (Rohlf, Slice, 1990; Goodall, 1991; Zelditch *et al.*, 2004): Initially, translation is performed, whereby all configurations of landmarks are superimposed, thus removing the position effect (Rohlf, Slice, 1990; Goodall, 1991). Subsequently,

scaling is carried out, whereby the sizes of all point configurations are reduced to a singular magnitude, denominated the centroid size (Rohlf, Slice, 1990; Goodall, 1991). This is obtained through a mathematical computation, corresponding to the square root of the summed squared distances of the landmarks relative to their centroid (center of gravity) (Rohlf, Slice, 1990; Goodall, 1991). Finally, the ultimate step, termed rotation, is executed to eradicate orientation effects. This stage involves rotating the landmark configurations to minimize the mean distance between homologous landmarks (Rohlf, Slice, 1990; Goodall, 1991).

Geometric morphometrics emerges as an effective method in separating shape and size, facilitating the visualization of shape changes through graphical means, such as lollipops and wireframes (Klingenberg, 2013). Thus, it is a method that has notably advanced over the years, expanding into diverse spheres of biology, including the domain of Taxonomy.

2.1. Application of geometric morphometrics in taxonomic studies

Geometric morphometrics is increasingly being employed in Taxonomy, contributing to the identification and delimitation of species. Taxonomic studies utilizing this method are found across various zoological groups, such as insects (*e.g.*, Jaramillo-o *et al.*, 2014); amphibians and reptiles (*e.g.*, Leaché *et al.*, 2009; Ruane, 2015; see more references in Kaliontzopoulou, 2011); and mammals (*e.g.*, Fadda, Corti, 2001; Evin *et al.*, 2008; Abiadh *et al.*, 2010). In the field of Ichthyology, this taxonomic technique has also been explored in several taxa, including groups of Osteoglossiformes (*e.g.*, Feulner *et al.*, 2007), Characiformes (*e.g.*, Sidlauskas *et al.*, 2011; Barreto *et al.*, 2016; Barreto *et al.*, 2018; Silva *et al.*, 2021), Siluriformes (*e.g.*, Bichuette *et al.*, 2014; Anjos *et al.*, 2019; Arroyave, Cruz-Fernández, 2021; Arroyave *et al.*, 2021), Gymnotiformes (*e.g.*, Craig *et al.*, 2017; Craig *et al.*, 2018a; Craig *et al.*, 2018b; Herrera-Collazos *et al.*, 2020), Cichliformes (*e.g.*, Maderbacher *et al.*, 2008; Chiozzi *et al.*, 2018; Argolo *et al.*, 2020), and Perciformes (*e.g.*, Cruz-Aguero *et al.*, 2015; Garcia-Rodriguez *et al.*, 2019).

Regarding the family Heptapteridae, only four studies in the literature employed this method (Bichuette *et al.*, 2014; Arroyave, Cruz-Fernández, 2021; Arroyave *et al.*, 2021; Cortés-Hernández, Ramírez-Gil, 2024), three of them focusing on subterranean

species. Bichuette *et al.* (2014) observed, through geometric morphometric analyses, the existence of two distinct populations of *Rhamdiopsis krugi* Bockmann & Castro, 2010, within caves in two regions of Chapada Diamantina, in Brazil. The authors attributed the isolation among the individuals of this species to geological and hydrological barriers. Furthermore, they employed this method to associate variations in body shape with habitat, suggesting then a hypothesis of vertical colonization of the subterranean environment by this species in two sequential phases: first, colonization through the stream-dwelling habitat to hyporheic zones, and later extending to the hypogean habitat (Bichuette *et al.*, 2014). Moreover, the study conducted by Arroyave *et al.* (2021) investigated the shape variation among different subspecies of *Rhamdia guatemalensis* (Günther, 1864), distributed in karstic aquifers of the Yucatán Peninsula, in Mexico. The authors concluded that the observed shape variation among the groups is insufficient to indicate speciation (Arroyave *et al.*, 2021). In a parallel study of the same genus, Arroyave and Cruz-Fernández (2021) asserted that the shape of the troglobitic species of *Rhamdia* Bleeker, 1858, does not exhibit significant variance from *Rhamdia laticauda* (Kner, 1858), its closest phylogenetic congener.

Concerning the genus *Pimelodella*, however, only one recent study implementing geometric morphometrics in species delimitation was found (Cortés-Hernández, Ramírez-Gil, 2024). In this work, the authors examined the morphological variation of seven species of *Pimelodella* inhabiting the rio Orinoco basin in Colombia, *i.e.*, *P. cristata*, *P. cruxenti* Fernández-Yépez, 1950, *P. figueroai* Dahl, 1961, *P. longibarbata* Cortés-Hernández *et al.*, 2020, *P. megalops* Eigenmann, 1912, *P. metae*, and specimens maintained as "*Pimelodella* sp." (Cortés-Hernández, Ramírez-Gil, 2024). Overall, the analyses of geometric morphometrics revealed shape variations among groups, notably distinguishing *P. cristata*, *P. cruxenti*, and *P. longibarbata* in the morphospace, while some overlap was observed among the remaining species (Cortés-Hernández, Ramírez-Gil, 2024).

For groups beyond Heptapteridae, studies employing geometric morphometrics as a species delimitation technique are ascertainable. In a work concerning members of the family Loricariidae, Anjos *et al.* (2019) analyzed three endemic species of *Hypostomus* Lacepède, 1803, utilizing various approaches, such as geometric morphometrics, meristics, and molecular techniques. Based on this integrative

taxonomy, a relocation of *Hypostomus chrysostiktos* (Birindelli *et al.*, 2007) to the genus *Pterygoplichthys* Gill, 1858, was carried out (Anjos *et al.*, 2019).

Furthermore, concerning the order Gymnotiformes, Herrera-Collazos *et al.* (2020) applied integrative taxonomy to describe three new species within the complex of *Eigenmannia trilineata* López & Castello, 1966, with geometric morphometrics contributing to this delimitation process. Therefore, geometric morphometrics may also be a valuable technique in resolving taxonomic problems across other ichthyological groups, including applications in *Pimelodella*.

3. Objectives

The primary objective of the present research is to examine the applicability of geometric morphometrics, incorporating landmarks of both external morphology and osteology, in the delimitation of species of *Pimelodella* within the Upper rio Paraguai basin. To this end, the following specific objectives were aimed to be achieved:

• Verify the occurrence of *Pimelodella* species in the Upper rio Paraguai basin, through the examination of specimens disposed in scientific collections;

• Investigate the shape variations within species of *Pimelodella* occurring in this basin through geometric morphometric analyses, utilizing external morphological and osteological landmarks.

Material and Methods

1. Sample and identification of specimens

The material in this research are specimens of *Pimelodella* of species occurring in the Upper rio Paraguai basin, and which constitute materials deposited in the following scientific collections: Coleção de Peixes da Universidade Federal de Mato Grosso (CPUFMT), Coleção de Peixes do Museu de Ciências e Tecnologia (MCP-Peixes), Coleção Ictiológica da Universidade de Brasília (CIUnB), Coleção Ictiológica do Núcleo de Pesquisas em Limnologia, Ictiologia e Aquicultura (NUPELIA), Coleção Zoológica da Universidade Federal de Mato Grosso do Sul (ZUFMS-PIS), Laboratório de Ictiologia de Ribeirão Preto (LIRP), Museu de Zoologia da Universidade de São

Paulo (MZUSP), and Museu de Zoologia da Universidade Estadual de Londrina (MZUEL-Peixes).

The identification of specimens follows Slobodian (2017), employing external morphological and osteological characteristics observed with the assistance of a Leica S8 APO stereomicroscope and X-ray images, respectively. Subsequently, specimens were meticulously selected for geometric morphometrics analysis, primarily based on their preservation state, whereby those exhibiting deformities or substantial damage were excluded from the analyses.

Furthermore, efforts were made to include only adult specimens of *Pimelodella*. However, there are no studies addressing the length at first maturity of the species encompassed within this study, and assessing gonad maturation would necessitate specimen dissection, which was not possible for all the species. Therefore, we used the upper 40% of the Standard Length for each species, as a proxy for maturity. This approach does not guarantee the inclusion of solely adult specimens, but facilitates the exclusion of smaller (and potentially juveniles) ones.

2. Geometric morphometrics

2.1. Data acquisition

The selected specimens underwent geometric morphometric analyses utilizing both external morphology and osteological data to obtain information regarding their variations in body and head shape. Body shape was assessed through external morphology and osteological data from lateral views of photographs and radiographs, whereas head shape was evaluated based on external morphology data from dorsal view of photographs. The lists of specimens analyzed for each dataset are provided in Tables 1, 2 and 3, and the geographic distribution of all specimens analysed is shown in Figure 1.

Table 1. List of specimens included in the geometric morphometrics analyses for the external lateral view. N = number of specimens.

Scientific collection	Lot	N	Species
CIUnB	1772	7	*Pimelodella guato*
CPUFMT	850	1	*Pimelodella gracilis*

CPUFMT	870	2	*Pimelodella taeniophora*
CPUFMT	1800	1	*Pimelodella gracilis*
CPUFMT	2306	3	*Pimelodella gracilis*
CPUFMT	3569	1	*Pimelodella mucosa*
CPUFMT	3714	2	*Pimelodella mucosa*
CPUFMT	3870	1	*Pimelodella mucosa*
CPUFMT	4003	3	*Pimelodella taeniophora*
LIRP	9528	6	*Pimelodella mucosa*
LIRP	9534	1	*Pimelodella taeniophora*
MCP-Peixes	10924	2	*Pimelodella taeniophora*
MCP-Peixes	15620	6	*Pimelodella megalura*
MCP-Peixes	15708	4	*Pimelodella taeniophora*
MCP-Peixes	15775	15	*Pimelodella taeniophora*
MCP-Peixes	26120	1	*Pimelodella gracilis*
MCP-Peixes	36117	10	*Pimelodella griffini*
MZUEL-Peixes	3829	2	*Pimelodella megalura*
MZUEL-Peixes	3830	8	*Pimelodella griffini*
MZUEL-Peixes	6457	1	*Pimelodella gracilis*
MZUEL-Peixes	6460	2	*Pimelodella griffini*
MZUEL-Peixes	9034	2	*Pimelodella griffini*
MZUEL-Peixes	9035	3	*Pimelodella griffini*
MZUEL-Peixes	11088	2	*Pimelodella guato*
MZUEL-Peixes	11185	2	*Pimelodella gracilis*
MZUEL-Peixes	11190	2	*Pimelodella gracilis*
MZUEL-Peixes	13217	1	*Pimelodella mucosa*
MZUEL-Peixes	14001	2	*Pimelodella gracilis*
MZUEL-Peixes	14055	2	*Pimelodella mucosa*
MZUEL-Peixes	16829	1	*Pimelodella guato*
MZUSP	100564	2	*Pimelodella griffini*
MZUSP	24856	1	*Pimelodella gracilis*
MZUSP	25091	1	*Pimelodella mucosa*
MZUSP	82381	1	*Pimelodella gracilis*
NUP	1067	9	*Pimelodella mucosa*
NUP	3390	11	*Pimelodella taeniophora*
NUP	3408	8	*Pimelodella gracilis*
NUP	3473	8	*Pimelodella gracilis*
NUP	3505	6	*Pimelodella gracilis*
NUP	3506	2	*Pimelodella taeniophora*

NUP	11390	3	*Pimelodella taeniophora*
NUP	13590	3	*Pimelodella mucosa*
NUP	14189	15	*Pimelodella taeniophora*
NUP	14201	10	*Pimelodella mucosa*
NUP	14295	1	*Pimelodella guato*
NUP	14355	8	*Pimelodella mucosa*
NUP	14702	1	*Pimelodella megalura*
NUP	19919	3	*Pimelodella guato*
NUP	21860	1	*Pimelodella taeniophora*
ZUFMS-PIS	615	2	*Pimelodella megalura*
ZUFMS-PIS	647	4	*Pimelodella guato*
ZUFMS-PIS	676	9	*Pimelodella guato*
ZUFMS-PIS	838	2	*Pimelodella gracilis*
ZUFMS-PIS	876	18	*Pimelodella griffini*
ZUFMS-PIS	1401	1	*Pimelodella griffini*
ZUFMS-PIS	1417	14	*Pimelodella megalura*
ZUFMS-PIS	1428	9	*Pimelodella megalura*
ZUFMS-PIS	1433	1	*Pimelodella griffini*
ZUFMS-PIS	1477	1	*Pimelodella megalura*
ZUFMS-PIS	1607	14	*Pimelodella griffini*
ZUFMS-PIS	1613	1	*Pimelodella mucosa*
ZUFMS-PIS	3256	2	*Pimelodella mucosa*
ZUFMS-PIS	3269	1	*Pimelodella mucosa*
ZUFMS-PIS	3696	1	*Pimelodella griffini*
ZUFMS-PIS	3900	5	*Pimelodella megalura*
ZUFMS-PIS	4194	1	*Pimelodella mucosa*
ZUFMS-PIS	4329	3	*Pimelodella taeniophora*
ZUFMS-PIS	4703	1	*Pimelodella megalura*
ZUFMS-PIS	4843	2	*Pimelodella guato*
ZUFMS-PIS	5911	1	*Pimelodella megalura*
ZUFMS-PIS	6008	1	*Pimelodella mucosa*
ZUFMS-PIS	6320	9	*Pimelodella taeniophora*
ZUFMS-PIS	6370	2	*Pimelodella guato*
ZUFMS-PIS	6442	1	*Pimelodella taeniophora*
ZUFMS-PIS	6488	7	*Pimelodella gracilis*
ZUFMS-PIS	6678	2	*Pimelodella gracilis*
ZUFMS-PIS	6746	1	*Pimelodella megalura*
ZUFMS-PIS	7677	2	*Pimelodella mucosa*

ZUFMS-PIS	8342	1	*Pimelodella taeniophora*
ZUFMS-PIS	8515	1	*Pimelodella guato*
ZUFMS-PIS	8516	3	*Pimelodella guato*

Table 2. List of specimens included in the geometric morphometrics analyses for the osteological lateral view. N = number of specimens.

Scientific collection	Lot	N	Species
CIUnB	1772	3	*Pimelodella guato*
CPUFMT	1800	1	*Pimelodella gracilis*
CPUFMT	2306	2	*Pimelodella gracilis*
MCP-Peixes	15708	4	*Pimelodella taeniophora*
MCP-Peixes	15775	15	*Pimelodella taeniophora*
MCP-Peixes	26120	1	*Pimelodella gracilis*
MZUEL-Peixes	3829	2	*Pimelodella megalura*
MZUEL-Peixes	6457	1	*Pimelodella gracilis*
MZUEL-Peixes	6460	2	*Pimelodella griffini*
MZUEL-Peixes	9035	2	*Pimelodella griffini*
MZUSP	25091	1	*Pimelodella mucosa*
NUP	1067	9	*Pimelodella mucosa*
NUP	3408	6	*Pimelodella gracilis*
NUP	3473	3	*Pimelodella gracilis*
NUP	3505	4	*Pimelodella gracilis*
NUP	14189	2	*Pimelodella taeniophora*
NUP	14201	8	*Pimelodella mucosa*
NUP	14702	1	*Pimelodella megalura*
ZUFMS-PIS	615	2	*Pimelodella megalura*
ZUFMS-PIS	647	4	*Pimelodella guato*
ZUFMS-PIS	648	1	*Pimelodella taeniophora*
ZUFMS-PIS	838	2	*Pimelodella gracilis*
ZUFMS-PIS	876	18	*Pimelodella griffini*
ZUFMS-PIS	1401	1	*Pimelodella griffini*
ZUFMS-PIS	1417	11	*Pimelodella megalura*
ZUFMS-PIS	1428	6	*Pimelodella megalura*
ZUFMS-PIS	1465	1	*Pimelodella griffini*
ZUFMS-PIS	1477	1	*Pimelodella megalura*
ZUFMS-PIS	1607	4	*Pimelodella griffini*
ZUFMS-PIS	1613	1	*Pimelodella mucosa*

ZUFMS-PIS	3256	2	*Pimelodella mucosa*
ZUFMS-PIS	3269	1	*Pimelodella mucosa*
ZUFMS-PIS	3696	1	*Pimelodella griffini*
ZUFMS-PIS	3900	5	*Pimelodella megalura*
ZUFMS-PIS	4194	1	*Pimelodella mucosa*
ZUFMS-PIS	4329	3	*Pimelodella taeniophora*
ZUFMS-PIS	4703	1	*Pimelodella megalura*
ZUFMS-PIS	4843	2	*Pimelodella guato*
ZUFMS-PIS	5549	2	*Pimelodella taeniophora*
ZUFMS-PIS	6008	1	*Pimelodella mucosa*
ZUFMS-PIS	6320	5	*Pimelodella taeniophora*
ZUFMS-PIS	6370	2	*Pimelodella guato*
ZUFMS-PIS	6442	1	*Pimelodella taeniophora*
ZUFMS-PIS	6488	4	*Pimelodella gracilis*
ZUFMS-PIS	6678	2	*Pimelodella gracilis*
ZUFMS-PIS	6746	1	*Pimelodella megalura*
ZUFMS-PIS	8515	1	*Pimelodella guato*
ZUFMS-PIS	8516	3	*Pimelodella guato*

Table 3. List of specimens included in the geometric morphometrics analyses for the external dorsal view. N = number of specimens.

Scientific collection	Lot	N	Species
CIUnB	1772	7	*Pimelodella guato*
CPUFMT	850	2	*Pimelodella gracilis*
CPUFMT	870	2	*Pimelodella taeniophora*
CPUFMT	1800	1	*Pimelodella gracilis*
CPUFMT	2306	3	*Pimelodella gracilis*
CPUFMT	3081	1	*Pimelodella mucosa*
CPUFMT	3569	1	*Pimelodella mucosa*
CPUFMT	3714	2	*Pimelodella mucosa*
CPUFMT	3870	1	*Pimelodella mucosa*
CPUFMT	4003	2	*Pimelodella taeniophora*
LIRP	9528	7	*Pimelodella mucosa*
MCP-Peixes	10924	2	*Pimelodella taeniophora*
MCP-Peixes	15620	6	*Pimelodella megalura*
MCP-Peixes	15708	4	*Pimelodella taeniophora*
MCP-Peixes	15775	9	*Pimelodella taeniophora*

MCP-Peixes	26120	1	*Pimelodella gracilis*
MCP-Peixes	36117	10	*Pimelodella griffini*
MZUEL-Peixes	3829	2	*Pimelodella megalura*
MZUEL-Peixes	3830	8	*Pimelodella griffini*
MZUEL-Peixes	6457	1	*Pimelodella gracilis*
MZUEL-Peixes	6460	2	*Pimelodella griffini*
MZUEL-Peixes	9034	2	*Pimelodella griffini*
MZUEL-Peixes	9035	3	*Pimelodella griffini*
MZUEL-Peixes	11088	2	*Pimelodella guato*
MZUEL-Peixes	11185	2	*Pimelodella gracilis*
MZUEL-Peixes	11190	2	*Pimelodella gracilis*
MZUEL-Peixes	13217	2	*Pimelodella mucosa*
MZUEL-Peixes	14001	2	*Pimelodella gracilis*
MZUEL-Peixes	14055	2	*Pimelodella mucosa*
MZUEL-Peixes	16829	1	*Pimelodella guato*
MZUSP	100564	2	*Pimelodella griffini*
MZUSP	24856	1	*Pimelodella gracilis*
MZUSP	25091	1	*Pimelodella mucosa*
MZUSP	82381	1	*Pimelodella gracilis*
NUP	1067	12	*Pimelodella mucosa*
NUP	3390	10	*Pimelodella taeniophora*
NUP	3408	9	*Pimelodella gracilis*
NUP	3473	9	*Pimelodella gracilis*
NUP	3505	9	*Pimelodella gracilis*
NUP	3506	2	*Pimelodella taeniophora*
NUP	11390	3	*Pimelodella taeniophora*
NUP	13590	3	*Pimelodella mucosa*
NUP	14189	14	*Pimelodella taeniophora*
NUP	14201	10	*Pimelodella mucosa*
NUP	14295	1	*Pimelodella guato*
NUP	14355	14	*Pimelodella mucosa*
NUP	14702	1	*Pimelodella megalura*
NUP	19919	3	*Pimelodella guato*
NUP	21860	1	*Pimelodella taeniophora*
ZUFMS-PIS	615	2	*Pimelodella megalura*
ZUFMS-PIS	647	4	*Pimelodella guato*
ZUFMS-PIS	676	14	*Pimelodella guato*
ZUFMS-PIS	838	1	*Pimelodella gracilis*

ZUFMS-PIS	876	20	*Pimelodella griffini*
ZUFMS-PIS	1401	1	*Pimelodella griffini*
ZUFMS-PIS	1417	14	*Pimelodella megalura*
ZUFMS-PIS	1428	9	*Pimelodella megalura*
ZUFMS-PIS	1433	1	*Pimelodella griffini*
ZUFMS-PIS	1477	1	*Pimelodella megalura*
ZUFMS-PIS	1607	19	*Pimelodella griffini*
ZUFMS-PIS	1613	1	*Pimelodella mucosa*
ZUFMS-PIS	3256	2	*Pimelodella mucosa*
ZUFMS-PIS	3269	1	*Pimelodella mucosa*
ZUFMS-PIS	3696	1	*Pimelodella griffini*
ZUFMS-PIS	3900	5	*Pimelodella megalura*
ZUFMS-PIS	4194	1	*Pimelodella mucosa*
ZUFMS-PIS	4329	3	*Pimelodella taeniophora*
ZUFMS-PIS	4703	1	*Pimelodella megalura*
ZUFMS-PIS	4843	2	*Pimelodella guato*
ZUFMS-PIS	5911	1	*Pimelodella megalura*
ZUFMS-PIS	6008	1	*Pimelodella mucosa*
ZUFMS-PIS	6320	9	*Pimelodella taeniophora*
ZUFMS-PIS	6370	2	*Pimelodella guato*
ZUFMS-PIS	6442	1	*Pimelodella taeniophora*
ZUFMS-PIS	6488	7	*Pimelodella gracilis*
ZUFMS-PIS	6678	2	*Pimelodella gracilis*
ZUFMS-PIS	6746	1	*Pimelodella megalura*
ZUFMS-PIS	7677	2	*Pimelodella mucosa*
ZUFMS-PIS	8342	1	*Pimelodella taeniophora*
ZUFMS-PIS	8515	1	*Pimelodella guato*
ZUFMS-PIS	8516	3	*Pimelodella guato*

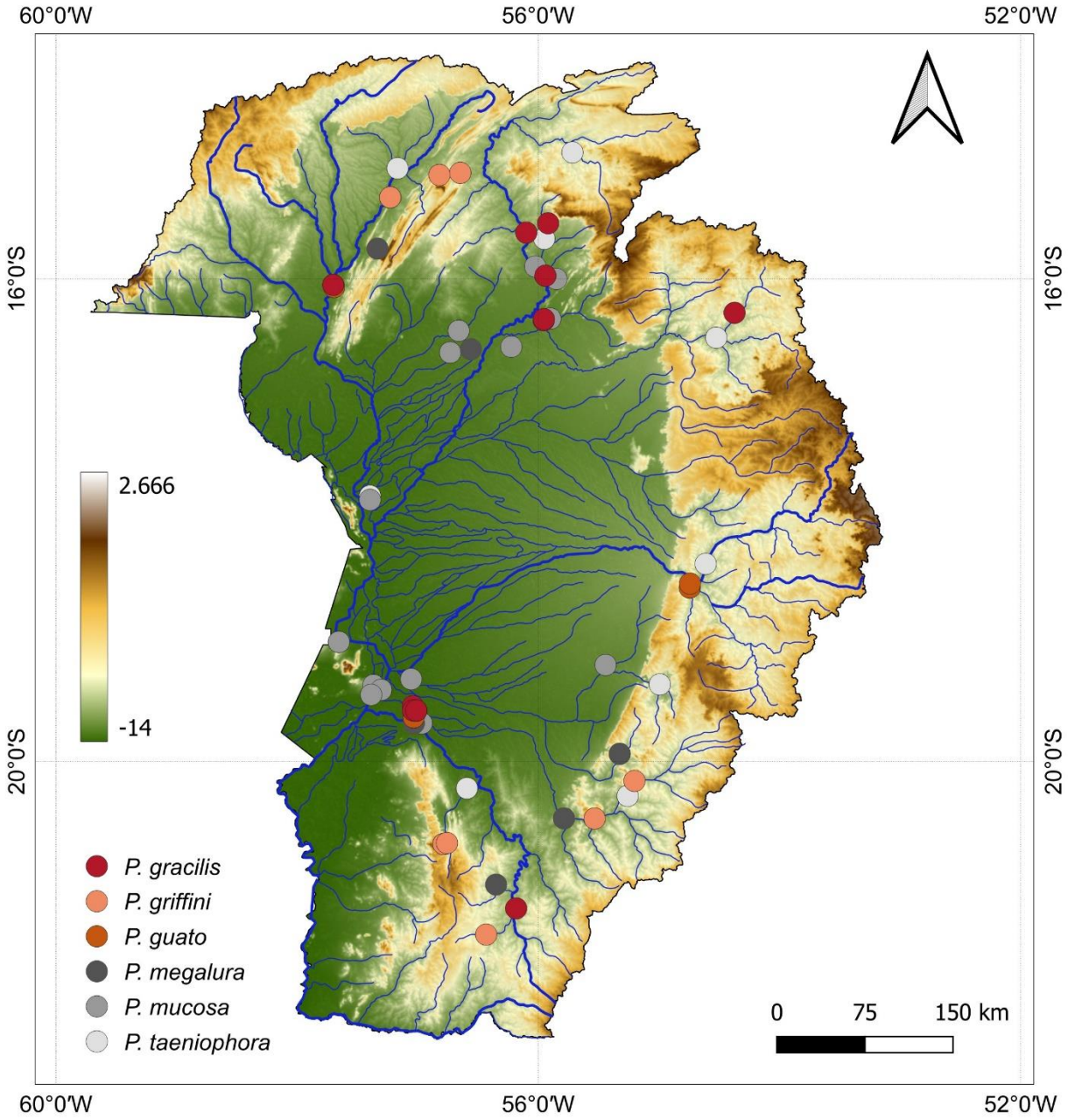

Figure 1. Map of the Upper rio Paraguai basin, in Brazil, showing the geographic distribution of the specimens of *Pimelodella* analysed. The symbols might represent more than one voucher specimen each.

Photographs were captured using a Canon EOS 5D Mark II camera, in collaboration with the Laboratório de Anatomia Comparada dos Vertebrados (LACV) at the Universidade de Brasília (UnB). Radiographs were taken in lateral view utilizing the Faxitron LX-60 digital X-ray equipment, in collaboration with LIRP and the Instituto de Biodiversidade e Sustentabilidade – NUPEM/UFRJ. All images were captured following standardized procedures (Zelditch *et al.*, 2004). For photographs, the camera

was mounted on a stand to maintain parallel alignment with both the table and the specimen. Also, the specimens were carefully positioned at the center of the frame to mitigate distortions near the edges (Zelditch *et al.*, 2004). Due to notable differences in specimen sizes, photographs were taken at varying scales. However, the scale of each image was posteriorly documented within the software programs utilized, ensuring data integrity across analyses.

2.2. Landmarks

A set of landmarks was initially defined and digitized, but subsequent preliminary analyses led to the removal of certain landmarks due to their unreliability in the provided information (Mitteroecker, Schaefer, 2022). Concerning the images in lateral view, which comprise the body shape, 14 landmarks were defined for both the photographs (Fig. 2) and radiographs (Fig. 3). Regarding the photographs in dorsal view, encompassing the head region, 12 landmarks were selected (Fig. 4). The landmarks for the photographs were determined based on literature sources (Bichuette *et al.*, 2014; Arroyave, Cruz-Fernández, 2021; Arroyave *et al.*, 2021) and correspond to the head and anteriormost fin insertions. Meanwhile, the digital radiographs comprised nine landmarks selected based on literature (Sidlauskas *et al.*, 2011), and five proposed within this study (*i.e.*, landmarks 2, 7, 8, 12 and 14). These landmarks are associated with the head, fin insertions, and skeletal structures, such as vertebral counts.

Figure 2. Lateral view of *Pimelodella gracilis*, MZUEL-Peixes 14001, 93.7 mm SL, with the positions of the 14 landmarks (red dots): (1) snout tip; (2) anterior origin of dorsal-fin base at the spinelet; (3) posterior end of dorsal-fin base; (4) anterior insertion of adipose fin; (5) posterior insertion of adipose fin; (6) insertion of middle caudal-fin rays; (7) posterior insertion

of anal-fin base; (8) anterior insertion of anal-fin base; (9) ventralmost end of the branchiostegal membrane; (10) insertion of first ray (unbranched) of the pectoral fin; (11) posteriormost tip of the branchiostegal membrane; (12) anterior limit of the left posterior nostril; (13) anterior limit of the left eye; (14) posterior limit of the left eye.

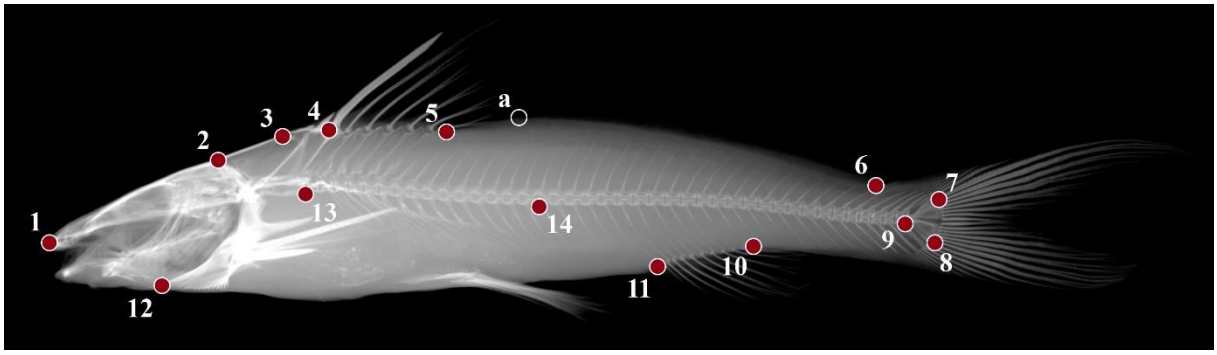

Figure 3. Radiograph of *Pimelodella gracilis*, NUP 3505, 95.4 mm SL, with the positions of the 14 landmarks (red dots): (1) anterior limit of premaxila; (2) anterior limit of supraoccipital process; (3) posterior limit of supraoccipital process; (4) anterior limit of the articular condyle of the dorsal-fin spine; (5) basal radial of the sixth ray of the dorsal fin; (6) posterior insertion of adipose fin; (7) posterodorsal tip of hypural 5; (8) posteroventral tip of hypural 1+2; (9) anteroventral tip of compound caudal centrum (PU1+U1); (10) insertion of posteriormost anal-fin ray; (11) insertion of anteriormost anal-fin ray; (12) anteromedial tip of cleithrum; (13) posteroventral tip of fifth vertebra of Weberian apparatus; (14) posteroventral tip of 20th vertebra. The white circumference, designated by the letter “a”, shows the landmark excluded from the analyses, corresponding to the origin of adipose fin.

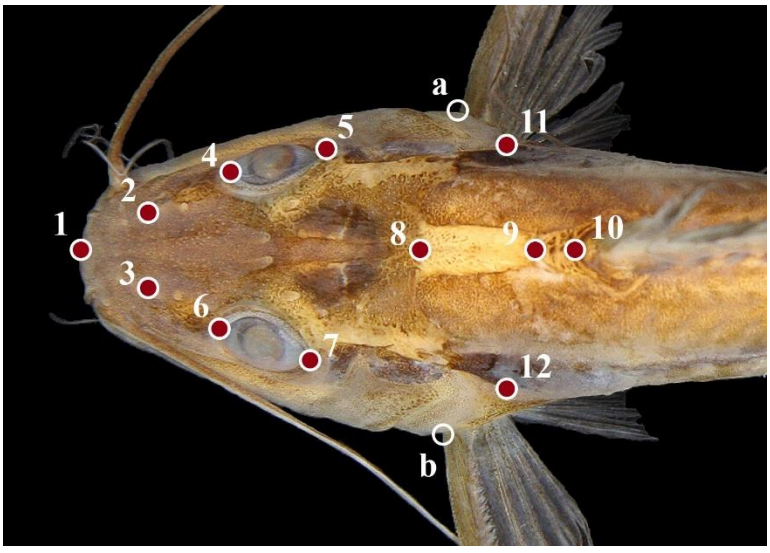

Figure 4. Dorsal view of *Pimelodella mucosa*, ZUFMS-PIS 3256, 75.3 mm SL, with the positions of the 12 landmarks (red dots): (1) snout tip; (2) anterior limit of the right posterior nostril; (3) anterior limit of the left posterior nostril; (4) anterior limit of the right eye; (5) posterior limit of the right eye; (6) anterior limit of the left eye; (7) posterior limit of the left eye; (8) anterior limit of the supraoccipital process; (9) posterior limit of the supraoccipital process; (10) origin of dorsal fin at the spinelet; (11) posterior limit of the right branchiostegal membrane; (12) posterior limit of the left branchiostegal membrane. The white circumferences, designated by

the letters “a” and “b”, show the landmarks excluded from the analyses, corresponding to the origins of pectoral-fin spines.

From the photographs and radiographs obtained, image banks were created using software TpsUtil 1.82 (Rohlf, 2022) and imported into tpsDig 2.32 (Rohlf, 2021), where the landmarks were digitized. The images were arranged in a random order, aiming to minimize bias in digitization across specimens of the same species.

Moreover, the precision of landmark digitization was assessed by repeating the digitization of landmarks to verify measurement error. Measurement error was calculated for both lateral and dorsal views of the photographs and for the radiographs. This procedure aims to ascertain the extent of measurement error, as an elevated value may artificially inflate the amount of variance and consequently reduce statistical robustness (Fruciano, 2016). For this purpose, a set of 30 images was randomly selected, replicated three times, and digitized to subsequently comparison of landmark position across these replicas. This comparison was computed using a Procrustes ANOVA within the MorphoJ 1.07a (Klingenberg, 2011) software, wherein the mean squares of error were expected to be inferior to the mean squares of the individual (Viscosi, Cardini, 2011; Fruciano, 2016).

2.2. Geometric morphometrics analyses

Separate analyses were equally performed for lateral and dorsal views of photographs and for the radiographs. The landmarks were subjected to a Generalized Procrustes Analysis (GPA), where they were translated, scaled and rotated, in order to analyze shape variation without the influence of other variables, such as position, size and orientation (Klingenberg, 2011). At the end of this analysis, Procrustes coordinates and Centroid Size were obtained, representing solely shape and size variation, respectively.

Using the centroid sizes obtained through GPA, the variation in body size was assessed by analyzing species as the sources of variation in an Analysis of Variance (ANOVA), with subsequent generation of boxplots displaying the centroid size for each species. Furthermore, pairwise comparisons among the species were conducted using Tukey's multiple comparison tests, based on the results of the ANOVA.

Although shape and size are distinct variables, it is important to verify their correlation to evaluate the effect of size on shape, a concept known as allometry (Mosimann, 1970). To examine allometry, a multivariate regression was conducted, utilizing Procrustes coordinates as dependent variables and log-transformed centroid size as independent variable (Monteiro, 1999; Viscosi, Cardini, 2011; Klingenberg, 2016). This regression was performed using a permutation test with 10,000 rounds, and pooling the regression within groups of species (Klingenberg, 2016). The log transformation is required when dealing with a wide range of sizes among specimens, while pooled within-group regression is recommended in situations where, for instance, multiple species are being analyzed and size corrections for taxonomic objectives may be necessary (Viscosi, Cardini, 2011; Mitteroecker *et al.*, 2013; Klingenberg, 2016).

In cases where allometric effects are elevated, a size correction must be executed to prevent a reduction in statistical power and finding shape variations across groups due to size influences (Sidlauskas *et al.*, 2011; Klingenberg, 2016). This correction can be achieved through a Principal Component Analyses (PCA) utilizing the covariance matrix of the regression residuals (Sidlauskas, 2011; Klingenberg, 2016). On the other hand, in situations where the size is weakly influencing in shape, the correction is not necessary and the PCA may be performed using the covariance matrix of the Procrustes coordinates.

Shape variation was assessed by conducting a PCA using the covariance matrix. The PCA, an explanatory analysis, aims to reduce data dimensionality while retaining maximal information content (James, McCulloch, 1990; Jolliffe, 1990). This process involves replacing the original correlated variables (*i.e.*, Procrustes coordinates) with a lower set of Principal Components (PCs) (James, McCulloch, 1990; Zelditch *et al.*, 2004). Thus, PCA enables the summarization of data dimensionality while maintaining the count of original variables and maximizing the explained variance across the entire sample (James, McCulloch, 1990; Zelditch *et al.*, 2004; Viscosi, Cardini, 2011).

PCA affords low-dimension graphical visualization with the PCs as axes. Since PCA ordinates the PCs based on retained variance, the first PC represents the most data variation, followed by subsequent PCs (Jolliffe, 1990; Davies, Fearn, 2004). In geometric morphometrics, PCA generates scatterplots displaying shape variations

among specimens, allowing the observation of potential clusters across the morphospace, thereby identifying group differences (Marcus, 1991). Eigenvalues quantify the extent of variance contained within each PC, while scores depict shape observations projected onto PCs (Jolliffe, 1990).

Moreover, the visualization of shape changes was facilitated by plotting the wireframes of the first PCs. This graphical representation corresponds to connections between landmarks using straight lines and aims to compare average shape configurations with observed shapes (Klingenberg, 2013).

Finally, the statistical evaluation of shape variation among groups was assessed through Multivariate Analysis of Variance (MANOVA) using Pillai's trace. This analysis allows to verify whether the observed shape variation among groups significantly distinguishes species from each other, utilizing all the PC scores obtained from PCA as dependent variables and species as the independent variable.

Pairwise comparisons between the species were also analyzed. For this purpose, first a Procrustes Anova was executed to evaluate the effect of species on Procrustes shape variables, employing 9,999 iterations to determine significance level through a permutation test. Based on this model, pairwise comparisons between least squares means of Procrustes distances were assessed among all the species (Collyer, Adams, 2018). Since this test comprises multiple comparisons, an adjustment on significance levels must be applied and, as the pairwise comparisons derived from Procrustes ANOVA did not incorporate this adjustment, a Bonferroni correction was computed separately. This correction was acquired by calculating α / n, where α = the significance level (set at 0.05 for all statistical analyses) and n = number of comparisons (15 in this study, as it encompasses six species being compared with each other). Consequently, a critical value equal to 0.0033 was employed to evaluate the results of the pairwise comparisons.

All analyses were conducted using MorphoJ 1.07a (Klingenberg, 2011), R 4.3.1 (R Core Team, 2023) and RStudio 2023.06.1+524 (RStudio Team, 2023) using the packges "geomorph" 4.0.6 (Baken *et al.*, 2021; Adams *et al.*, 2023) and "RRPP" 1.4.0 (Collyer, Adams, 2018, 2023).

3. Examined material

Imparfinis sp. – CPUFMT 1800, 18, 1 examined, 54.2 mm SL, Brazil, Mato Grosso, Rondonópolis municipality, rio Paraguai basin, Córrego Arareau (urban area), 16º16'53"S, 54º22'19"W.

Pimelodella australis – MZUSP 14214, 3, 2 examined, 98.0–116,5 mm SL, Brazil, Rio Grande do Sul, Osório municipality, Lagoa dos Quadros, 29º43'00"S, 50º06'59".

Pimelodella avanhandavae – All from Brazil. CPUFMT 1800, 18, 12 examined, 1 xr, 41.3–87.1 mm SL, Mato Grosso, Rondonópolis municipality, rio Paraguai basin, Córrego Arareau (urban area), 16º16'53"S, 54º22'19"W; CPUFMT 1911, 1, xr, 99.1 mm SL, Mato Grosso, Alto Araguaia municipality, Upper rio Paraguai basin, rio Ariranha, at the MT-465 highway bridge, next to Arlindo's bar, 17º56'58"S, 53º44'16"W; MCP-Peixes 36119, 7, xr, 81.5–101.3 mm SL, Mato Grosso, Pontes e Lacerda municipality, rio Pindaituba (tributary of rio Guaporé) at BR-174, between Pontes e Lacerda and Comodoro, 15º00'41"S, 59º17'18"W. ZUFMS-PIS 1417, 51, 1 examined, 63.6 mm SL, Mato Grosso do Sul, Corguinho municipality, Córrego São João, 19º56'11"S, 55º19'28"W.

Pimelodella cristata – MZUSP 50519, 1, 120.1 mm SL, Brazil, Acre, Foz do Bajé, rio Tejo, 8º56'00"S, 72º33'59"W.

Pimelodella gracilis – CPUFMT 679, 3, 106.8–133.5 mm SL, Brazil, Mato Grosso, Diamantino municipality, rio Tapajós basin, rio Claro, near the sinkhole of rio Claro, future PCH Jacutinga, 13º48'51"S, 56º41'30"W; CPUFMT 850, 4, 100.2–135.2 mm SL, Brazil, Mato Grosso, Juara municipality, rio Tapajós basin, bridge over the rio São João da Barra, 10º18'46"S, 57º38'44"W; CPUFMT 1546, 1, 162.6 mm SL, Brazil, Mato Grosso, Nobres municipality, Upper rio Paraguai basin, rio Nobres, 14º43'42"S, 56º19'08"W; CPUFMT 1800, 18, 5 examined, xr, 68.1–83.7 mm SL, Brazil, Mato Grosso, Rondonópolis municipality, rio Paraguai basin, Córrego Arareau (urban area), 16º16'53"S, 54º22'19"W; CPUFMT 2306, 3, 107.0–107.3 mm SL, Brazil, Mato Grosso, Cuiabá municipality, rio Paraguai basin, Córrego Aricazinho, 15º32'21"S, 55º55'07"W; LIRP 9531, 1, 88.4 mm SL, Brazil, Mato Grosso do Sul, Corumbá municipality, rio Paraguai, in Amolar, Parque Nacional do Pantanal, 17º52'42"S, 57º28'43"W; MCP-Peixes 26120, 2, 1 xr, 96.9–97.6 mm SL, Brazil, Mato Grosso, Cáceres municipality,

rio Paraguai in Cáceres its surroundings, 16º02'59"S, 57º42'00"W; MZUEL-Peixes 6457, 2, 1 examined, xr, 90.0 mm SL, Brazil, Mato Grosso do Sul, Corumbá municipality, rio Paraguai basin, rio Miranda, 19º34'36"S, 57º01'05"W; MZUEL-Peixes 11185, 7, 5 examined, 136.5–185.8 mm SL, Brazil, Mato Grosso do Sul, Bonito municipality, rio Paraguai basin, rio Miranda, 21º13'00"S, 56º11'00"W; MZUEL-Peixes 11190, 8, 6 examined, 72.3–119,7 mm SL, Brazil, Mato Grosso do Sul, Corumbá municipality, rio Paraguai basin, corixo in bridge 11, 19º32'29S", 57º02'23"W; MZUEL-Peixes 14001, 9, 6 examined, 56.9–93,65 mm SL, Brazil, Mato Grosso do Sul, Corumbá municipality, rio Paraguai basin, rio Miranda, along the right bank at Base de Estudos do Pantanal (BEP), 19º34'35"S, 57º01'04"W; MZUSP 337, 5, 2 examined, 100.4–113.3 mm SL, Argentina, Entre Rios, Paraná; MZUSP 23195, 1, 189.3 mm SL, Brazil, Mato Grosso, rio Taquari, approximately 150 km from Coxim municipality, 18º3'00"S, 55º10'00"W; MZUSP 24856, 2, 1 examined, 107.8 mm SL, Brazil, Mato Grosso, Cuiabá municipality, rio Cuiabá approximately 500m downstream from the new bridge, 15º37'00"S, 56º05'59"W; MZUSP 27728, 3, 2 examined, 137.4–205.8 mm SL, Brazil, Mato Grosso do Sul, Coxim municipality, rio Taquari, 18º30'00"S, 54º45'00"W; MZUSP 38033, 7, 3 examined, 65.0–71.6 mm SL, Brazil, Mato Grosso do Sul, Corumbá municipality, rio Paraguai, Morrinhos, 19º00'00"S, 57º39'00"W; MZUSP 82381, 1, 114.7 mm SL, Brazil, São Paulo, Porto Cabral, rio Paraná, 22º15'00"S, 52º30'00"W; MZUSP 87788, 1, 147.1 mm SL, Brazil, Mato Grosso, Tangará da Serra municipality, rio Paraguai basin, rio Sepotuba, Salto Maciel, 15º55'59"S,57º39'00"W; NUP 2231, 8, 94.4–158.5 mm SL, Brazil, Mato Grosso, Rosário Oeste municipality, rio Paraguai basin, Reservatório Manso, tributary of rio Manso, 14º49'54"S, 55º37'09"W; NUP 3408, 16, 8 xr, 10 examined, 98.1–118.4 mm SL, Brazil, Mato Grosso, Barão de Melgaço municipality, rio Paraguai basin, rio Cuiabá (Cb4), tributary of rio Cuiabá, 16º20'37"S, 55º57'17"W; NUP 3473, 25, 15 examined, 4 xr, 87.8–103.1 mm SL, Brazil, Mato Grosso, Santo Antônio de Leverger municipality, rio Paraguai basin, Baía de Chacororé, tributary of rio Cuiabá, 16º20'02"S, 55º57'10"W; NUP 3505, 19, 9 examined, 4 xr, 90.3–114.0 mm SL, Brazil, Mato Grosso, Santo Antônio de Leverger municipality, rio Paraguai basin, rio Cuiabá (Cb3), tributary of rio Paraguai, 15º58'26"S, 55º56'26"W; NUP 14300, 10, 56.7–71.7 mm SL, Brazil, Mato Grosso, Cáceres municipality, rio Paraguai basin, Baía de Cáceres, tributary of rio Paraguai, 18º58'42"S, 57º43'43"W; ZUFMS-PIS 620, 1, xr, 144.1 mm SL, Brazil, Mato Grosso do Sul, Aquidauana municipality, stream near Piraputanga, 20º28'16"S,

55º47'14"W; ZUFMS-PIS 838, 2, xr, 101.8–127.5 mm SL, Brazil, Mato Grosso do Sul, Corumbá municipality, rio Miranda, across from the BEP, Passo do Lontra, 19°34'37"S, 57°00'42"W; ZUFMS-PIS 1417, 51, 1 examined, 68.9 mm SL, Brazil, Mato Grosso do Sul, Corguinho municipality, Córrego São João, 19º56'11"S, 55º19'28"W; ZUFMS-PIS 6488, 12, 6 xr, 49.4–166.4 mm SL, Brazil, Mato Grosso do Sul, Corumbá municipality, rio Miranda, under the bridge, during a surge, 19º34'35"S, 57º02'17"W; ZUFMS-PIS 6678, 4, xr, 135.2–156.6 mm SL, Brazil, Mato Grosso do Sul, Corumbá municipality, rio Miranda, 19°34'37"S, 57°00'42"W.

Pimelodella griffini – All from Brazil. CPUFMT 5352, 6, 46.4–58.9 mm SL, Mato Grosso, Indiavaí municipality, Upper rio Paraguai basin, rio Jauru, 15º23'48"S, 58º36'11"W; CPUFMT 4629, 57, Mato Grosso, Tangará da Serra municipality, Upper rio Paraguai basin, rio Formoso, 14º40'00"S, 57º50'50"W; LIRP 11407, 2, 44.7–51.6 mm SL, Mato Grosso do Sul, Coxim municipality, rio Taquari, 18º31'36"S, 54º44'24"W; MCP-Peixes 36117, 19, 10 examined, 46.9–59,7 mm SL, Mato Grosso, Nova Lacerda municipality, Córrego Retiro (tributary of rio Guaporé) on BR-174, 14º48'07"S, 59º19'24"W; MCP-Peixes 36127, 35, 15 examined, 39.2–53.7 mm SL, Mato Grosso, Pontes e Lacerda municipality, Ribeirão (tributary of rio Guaporé) on BR-174, between Pontes e Lacerda and Comodoro, 14º55'15"S, 59º17'29"W; MZUEL-Peixes 3830, 11, 9 examined, 43.2–56.5 mm SL, Mato Grosso, Porto Estrela municipality, rio Paraguai basin, Ribeirão Salobo, 15º19'28"S, 57º13'39"W; MZUEL-Peixes 6460, 9, 2 examined, xr, 71.4–74.6, Mato Grosso do Sul, Corumbá municipality, rio Paraguai basin, rio Miranda BEP/UFMS, 19º34'36"S, 57º01'05"W; MZUEL-Peixes 7748, 4, 3 examined, 40.4–56.1, Mato Grosso, Barra do Garças municipality, bacia do rio Amazonas, rio Taquaral, Araguaia, 15º40'41"S, 52º17'52"W; MZUEL-Peixes 9034, 2, 47.6–60.7 mm SL, Mato Grosso, Jangada municipality, rio Paraguai basin, rio Chiqueirão, tributary of rio Cuiabá, 15º07'16"S, 56º38'48"W; MZUEL-Peixes 9035, 4, 3 examined, xr, 51.1–63.6 mm SL, Mato Grosso, Barra do Bugres municipality, rio Paraguai basin, rio Currupira, tributary of rio Paraguai, 15º08'18"S, 56º49'10"W; MZUSP 44487, 64, 10 examined, 41.7–54.2 mm SL, Mato Grosso, Pontes e Lacerda municipality, rio Guaporé and adjacent flooded area in Pontes e Lacerda (tributary of rio Madeira), 15º14'00"S, 59º19'59"W; MZUSP 90671, 34, 10 examined, 40.1–50.1 mm SL, Mato Grosso, Cáceres municipality, rio Sepotuba (middle stretch), 15º16'35"S, 57º42'50"; MZUSP 100564, 12, 2 examined, 67.7–81.1 mm SL, Mato Grosso, Aripuanã

municipality, rio Aripuanã, Fishermen's port, below the Dardanelos/Andorinhas waterfall, 10º10'06"S, 59º26'50"W; NUP 11627, 10, 52.8–62.9 mm SL, Mato Grosso, Tangará da Serra municipality, rio Paraguai basin, rio Sepotuba, tributary of rio Paraguai, 14º41'35"S, 57º48'14"W; NUP 21728, 3, 47.9–51.7 mm SL, Mato Grosso do Sul, Pedro Gomes municipality, rio Paraguai basin, Middle rio Taquari, tributary of rio Taquari, 18º10'45"S, 54º29'18"W; ZUFMS-PIS 876, 20, 18 xr, 45.9–60.0 mm SL, Mato Grosso do Sul, Bodoquena municipality, rio Salobra, 20°40'31"S, 56°45'25"W; ZUFMS-PIS 1401, 1, xr, 64.2 mm SL, Mato Grosso do Sul, Bodoquena municipality, Córrego Salobrinha, 20°41'00"S, 56°47'10"W; ZUFMS-PIS 1417, 51, 4 examined, 37.3–53.8 mm SL, Mato Grosso do Sul, Corguinho municipality, Córrego São João, 19º56'11"S, 55º19'28"W; ZUFMS-PIS 1428, 6, 46.8–57.9 mm SL, Mato Grosso do Sul, Corguinho municipality, Córrego São João, 19º56'11"S, 55º19'28"W; ZUFMS-PIS 1433, 1, 55.3 mm SL, Mato Grosso do Sul, Aquidauana municipality, Riacho Lageado, approximately 30 km from Cipolândia, 20°09'38"S, 55°12'06"W; ZUFMS-PIS 1465, 10, 5 xr, 43.9–70.6 mm SL, Mato Grosso do Sul, Aquidauana municipality, Córrego Piraputanguinha, Piraputanga, 20°28'21"S, 55°31'57"W; ZUFMS-PIS 1607, 35, 20 examined, 5 xr, 55.4–86.1 mm SL, Mato Grosso do Sul, Bodoquena municipality, Córrego Salobrinha, 20°41'00"S, 56°47'10"W; ZUFMS-PIS 3696, 1, xr, 94.8 mm SL, Mato Grosso do Sul, Jardim municipality, rio da Prata, 21°26'03"S, 56°25'55"W; ZUFMS-PIS 3900, 2, xr, 69.0–73.3 mm SL, Mato Grosso do Sul, Corguinho municipality, Córrego Periquito, 19º56'13"S, 55º19'28"W; ZUFMS-PIS 4329, 1, xr, 67.5 mm SL, Mato Grosso do Sul, Terenos municipality, Upper rio Paraguai basin, Pesqueiro in rio Aquidauana, 20°17'07"S, 55°15'30"W.

Pimelodella guato – All from Brazil, Upper rio Paraguai basin. ZUFMS-PIS 8515, 1, xr, 78.5 mm SL, holotype, Mato Grosso do Sul, Corumbá municipality, rio Miranda, sandy beaches at Passo do Lontra region, 19°34'37"S, 57°00'42"W; CIUnB 1772, 7, 3 xr, 79.1–99.9 mm SL, 1 c&s, 91.2 mm SL, paratypes, Mato Grosso do Sul, Corumbá municipality, rio Miranda, sandy beaches at Passo do Lontra region, 19°34'37"S, 57°00'42"W; MZUEL-Peixes 11088, 1, 103.7 mm SL, Mato Grosso do Sul, Corumbá municipality, corixo, fifth bridge after the entrance to Passo do Lontra, Estrada Parque, 19°38’00"S, 57°02’00"W; MZUEL-Peixes 16829, 2, 1 examined, 79.6 mm SL, paratype, Mato Grosso do Sul, Corumbá municipality, rio Miranda BEP/UFMS, 19º34'36"S, 57º01'05"W; NUP 14295, 1, 72.3 mm SL, Mato Grosso, Cáceres

municipality, Baía de Cáceres, tributary of rio Paraguai, 16°04'02"S, 57°41'38"W; NUP 19919, 3, 64.8–83.2 mm SL, paratypes, Mato Grosso do Sul, Coxim municipality, rio Coxim, tributary of rio Taquari, 18º33'32"S, 54º44'37"W; ZUFMS-PIS 647, 5, xr, 37.1–94.3 mm SL, paratypes, Mato Grosso do Sul, Corumbá municipality, rio Miranda, across from the BEP, Passo do Lontra, 19°34'37"S, 57°00'42"W; ZUFMS-PIS 676, 15, 62.3–107.4 mm SL, paratypes, Mato Grosso do Sul, Corumbá municipality, rio Miranda, sandy beaches at Passo do Lontra region, 19°34'37"S, 57°00'42"W; ZUFMS-PIS 4843, 2, xr, 64.6–65.4 mm SL, paratypes, Mato Grosso do Sul, Corumbá municipality, rio Miranda, across from the BEP, 19°34'37"S, 57°00'42"W; ZUFMS-PIS 6370, 2, xr, 98.6–127.9 mm SL, paratypes, Mato Grosso do Sul, Coxim municipality, rio Taquari, 18°31'32"S, 54°44'30"W; ZUFMS-PIS 8516, 4, xr, 49.7–109.0 mm SL, paratypes, Mato Grosso do Sul, Corumbá municipality, rio Miranda, sandy beaches at Passo do Lontra region, 19°34'37"S, 57°00'42"W.

Pimelodella megalura – All from Brazil. MCP-Peixes 15620, 6, 45.1–72.6 mm SL, Mato Grosso, Cáceres municipality, arroio along the Barra do Bugres/Cáceres road, approximately 99 km south of Barra do Bugres (tributary of rio Paraguai), 15º45'00"S, 57º19'59"W; MCP-Peixes 15708, 1, 74.3 mm SL, Mato Grosso, Barra do Bugres municipality, rio Bugres, in Barra do Bugres (tributary of rio Paraguai), 15º04'59"S, 57º10'00"W; MZUEL-Peixes 3829, 4, 2 examined, xr, 69.9–79.1 mm SL, Mato Grosso, municipality Porto Estrela, rio Paraguai basin, Ribeirão Salobo, 15º19'28"S, 57º13'39"W; NUP 14702, 26, 15 examined, 1 xr, 42.6–63.9 mm SL, Mato Grosso, Santo Antônio de Leverger municipality, rio Paraguai basin, rio Aricá Mirim, tributary of rio Cuiabá, 16º35'00"S, 56º33'33"W; ZUFMS-PIS 615, 2, xr, 84.8–89.5 mm SL, Mato Grosso do Sul, Aquidauana municipality, rio Aquidauana, 20º28'16"S, 55º47'14"W; ZUFMS-PIS 1417, 51, 14 examined, 5 xr, 52.9–81.9 mm SL, Mato Grosso do Sul, Corguinho municipality, Córrego São João, 19º56'11"S, 55º19'28"W; ZUFMS-PIS 1428, 3, xr, 58.6–67.8 mm SL, Mato Grosso do Sul, Corguinho municipality, Córrego São João, 19º56'11"S, 55º19'28"W; ZUFMS-PIS 1477, 1, 66.6 mm SL, Mato Grosso do Sul, Aquidauana municipality, Córrego Cipolândia, 20º28'16"S, 55º47'14"W; ZUFMS-PIS 3900, 3, xr, 71.5–79.7 mm SL, Mato Grosso do Sul, Corguinho municipality, Córrego Periquito, 19º56'13"S, 55º19'28"W; ZUFMS-PIS 4703, 106, 1 examined, xr, 80.8 mm SL, Mato Grosso do Sul, Bodoquena municipality, Córrego Salobrinha, 20º40'59"S, 56º47'07"W; ZUFMS-PIS 5911, 1, 66.1 mm SL, Mato

Grosso do Sul, Corumbá municipality, floodplain on the banks of MS-325, 19°41'02"S, 57°01'54"W; ZUFMS-PIS 6746, 1, xr, 115.3 mm SL, Mato Grosso do Sul, Bonito municipality, tributary of Córrego Retiro, 21º01'12"S, 56º20'59"W.

Pimelodella mucosa – All from Brazil. CPUFMT 3081, 1, 66.7 mm SL, Mato Grosso, Poconé municipality, Upper rio Paraguai basin, rio Bento Gomes on MT-060 (Transpantaneira highway), 16º25'48"S, 56º39'36"W; CPUFMT 3569, 1, 70.3 mm SL, Mato Grosso, Poconé municipality, Upper rio Paraguai basin, rio Claro, 16º36'36"S, 56º43'48"W; CPUFMT 3714, 2, 87.6–97.1 mm SL, Mato Grosso, municipality Santo Antônio do Leverger, Baía do Pereira, 15º53'48"S, 56º01'30"W; CPUFMT 3870, 1, 92.8 mm SL, Mato Grosso, Santo Antônio do Leverger municipality, Upper rio Paraguai basin, flooded areas of Campo de Fora, 16º00'00"S, 55º51'00"W; LIRP 9528, 7, 46.3–66.8 mm SL, Mato Grosso, Poconé municipality, Baía do Burro, Parque Nacional do Pantanal, 17º49'52"S, 57º23'43"W; MZUEL-Peixes 13217, 4, 3 examined, 55.1–78.0 mm SL, Mato Grosso do Sul, Corumbá municipality, rio Paraguai basin, Base de Estudos do Pantanal; 19º34'35"S, 57º01'08"W; MZUEL-Peixes 14055, 2, 45.5–57.5 mm SL, Mato Grosso do Sul, Corumbá municipality, rio Paraguai basin, Baía da Medalha, in Base de Estudos do Pantanal, 19º34'32"S, 57º00'53"W; MZUSP 25091, 2, 1 examined, xr, 86.1 mm SL, Mato Grosso, Corumbá municipality, fifth bridge after the rio Miranda (south), 19º40'59"S, 56º58'00"W; NUP 1067, 12, 9 xr, 58.8–101.7 mm SL, Mato Grosso, Barão de Melgaço municipality, rio Paraguai basin, Baía Sinhá Mariana, tributary of rio Cuiabá, 16º19'48"S, 55º54'00"W; NUP 13590, 3, 50.3–59.7 mm SL, Mato Grosso do Sul, Porto Murtinho municipality, Lagoa Figueirinha, 19º22'00"S, 57º22'00"W; NUP 14201, 26, 10 examined, 8 xr, 56.5–82.4 mm SL, Mato Grosso do Sul, Porto Murtinho municipality, Lagoa 12, 19º24'21"S, 57º18'11"W; NUP 14355, 26, 15 examined, 66.5–91.9 mm SL, Mato Grosso do Sul, Porto Murtinho municipality, Lagoa Piúva, tributary of rio Paraguai, 19º26'47"S, 57º23'10"W; ZUFMS-PIS 1613, 1, xr, 44.8 mm SL, Mato Grosso do Sul, Corumbá municipality, bay 24 km from the Base de Estudos do Pantanal (BEP), 19º00'33"S, 57º39'12"W; ZUFMS-PIS 3256, 2, xr, 75.3–75.4 mm SL, Mato Grosso do Sul, Corumbá municipality, Baía da Medalha, 19°34'34"S, 57°00'46"W; ZUFMS-PIS 3269, 1, xr, 56.5 mm SL, Mato Grosso, Barão de Melgaço municipality, flooded areas of rio Cuiabá basin, 16°33'46.2"S, 56°13'25"W; ZUFMS-PIS 4194, 60, 1 examined, 81.6 mm SL, Mato Grosso do Sul, Corumbá municipality, rio Miranda, during surge, 19º34'46"S,

57º01'11"W; ZUFMS-PIS 6008, 1, xr, 86.7 mm SL, Mato Grosso do Sul, Corumbá municipality, bay in Pousada Arara Azul, 19°19'00"S, 57°03'14"W; ZUFMS-PIS 7677, 1, 96.9 mm SL, Mato Grosso do Sul, Rio Verde de Mato Grosso municipality, Baía Santa Virgínia, 19º12'00"S, 55º26'29"W.

Pimelodella notomelas – All from Brazil. MZUEL-Peixes 7743, 5, 3 examined, 43.9–52.6 mm SL, Mato Grosso, Barra do Garças municipality, rio Amazonas basin, rio Corrente, Araguaia, 15º29'57"S, 52º42'40"W; MZUEL-Peixes 9032, 1, 39.7 mm SL, Mato Grosso, Barão De Melgaço municipality, rio Paraguai basin, flooded area on road between Porto de Fora and Mimoso, 16º09'21"S, 55º48'19"W; MZUEL-Peixes 9694, 1, 33.0 mm SL, Mato Grosso do Sul, Corumbá municipality, bacia do rio Miranda, corixo near bridge 17 in Estrada Parque, 19º30'06"S, 57º02'32"W; NUP 3557, 1, 36.2 mm SL, Mato Grosso, Alto Garças municipality, rio Tocantins-Araguaia basin, rio das Garças, tributary of rio Araguaia, 15º34'54"S, 53º24'50"W; ZUFMS-PIS 5438, 2, xr, 34.3–34.4 mm SL, Mato Grosso do Sul, Porto Murtinho municipality, Upper rio Paraguai basin, Córrego Rapadura in Fazenda Estrela, 21°29'47"S, 57°32'42"W.

Pimelodella roccae – MZUSP 100564, 12, 3 examined, 80.3–92.8 mm SL, Brazil, Mato Grosso, Aripuanã municipality, rio Aripuanã, Fishermen's port, below the Dardanelos/Andorinhas waterfall, 10º10'06"S, 59º26',50"W; MZUSP 110494, 3, 1 examined, 156.1 mm SL, Peru, Huánuco, Tingo Maria, left bank of rio Huallaga downstream from the mouth of Quebrada Acerradero, near the Balneário, 9º15'13"S, 76º00'33"W.

Pimelodella serrata – All from Brazil. LIRP 10022, 4, 71.3–83.6 mm SL, Rondônia, Costa Marques municipality, rio Guaporé, near the mouth of rio Cautário, 12º13'37"S, 64º31'30"W; LIRP 10029, 15, 12 examined, 66.7–83.9 mm SL, Rondônia, Guajara-Mirim municipality, rio Mamoré, near Guajará-Mirim, 11º30'09"S, 65º11'17"W.

Pimelodella taeniophora – All from Brazil. CPUFMT 870, 3, 36.8–68.3 mm SL, Mato Grosso, Vila Bela da Sta Trindade municipality, rio Guaporé basin, Serra da Borda, rio Areias, 14º52'44"S, 59º52'44"W; CPUFMT 4003, 8, 60.4–75.7 mm SL, Mato Grosso, Poconé municipality, Upper rio Paraguai basin, rio Bento Gomes in MT-060 (Transpantaneira highway), 16º25'48"S, 56º39'36"W; LIRP 9528, 2, 47.9–61.2 mm SL, Mato Grosso, Poconé municipality, Baía do Burro, Parque Nacional do Pantanal, 17º49'52"S, 57º23'43"W; LIRP 9533, 2, 51.3–55.8 mm SL, Mato Grosso do Sul,

Corumbá municipality, corixo Boca do Ricardo, Parque Nacional do Pantanal, 17º51'36"S, 57º24'06"W; LIRP 9534, 7, 53.9–71.4 mm SL, Mato Grosso, Poconé municipality, Baía do Nove, Parque Nacional do Pantanal, 17º47'58"S, 57º23'42"W; LIRP 9535, 7, 6 examined, 50.4–63.3 mm SL, Mato Grosso, Poconé municipality, Baía do Morro, Parque Nacional do Pantanal; LIRP 10024, 4, 45.1–52.1 mm SL, Rondônia, Costa Marques municipality, mouth of rio São Domingos, 12º26'44"S, 63º52'32"W; MCP-Peixes 10924, 2, 91.2–91.6 mm SL, Mato Grosso, Cuiabá municipality, Córrego Pindaival approximately 25 km east of Cuiabá (rio Paraguai system), 15º40'00"S, 55º57'00"W; MCP-Peixes 15708, 4, 64.8–86.1 mm SL, Mato Grosso, Barra do Bugres municipality, rio Bugres, in Barra do Bugres (tributary of rio Paraguai), 15º04'59"S, 57º10'00"W; MCP-Peixes 15775, 62, 30 examined, 15 xr, 35.8–79.9 mm SL, Mato Grosso, Cáceres municipality, rio Paraguai in Cáceres and its surroundings, 16º02'59"S, 57º42'00"W; MCP-Peixes 36138, 9, 33.7–54.3 mm SL, Mato Grosso, Poconé municipality, rio Sangradouro on BR-070 highway, between Cuiabá and Cáceres, 15º56'32"S, 57º06'15"W; MZUSP 44289, 1, 61.1 mm SL, Mato Grosso, Jangada municipality, rio Paraguai basin, Ribeirão Chiqueirão, approximately 21 km west of Jangada (tributary of Jangada, rio Cuiabá), 15º07'00", 56º38'00"W; NUP 3390, 16, 56.6–107.0 mm SL, Mato Grosso, Santo Antônio de Leverger municipality, rio Paraguai basin, rio Cuiabá (Cb3), tributary of rio Paraguai, 15º58'27"S, 55º56'27"W; NUP 3506, 4, 72.6–110.1 mm SL, Mato Grosso, Santo Antônio de Leverger municipality, rio Paraguai basin, rio Cuiabá (Cb3), tributary of rio Paraguai, 15º58'27"S, 55º56'27"W; NUP 11390, 5, 70.0–80.0 mm SL, Mato Grosso, Rosário Oeste municipality, rio Paraguai basin, rio Casca (Ca3), tributary of rio Cuiabá, 14º57'07"S, 55º42'59"W; NUP 12222, 2, 38.5–50.2 mm SL, Mato Grosso, Rondonópolis municipality, rio Paraguai basin, rio Vermelho, tributary of rio São Lourenço, 16º29'45"S, 53º37'59"W; NUP 14189, 21, 15 examined, 2 xr, 55.1–66.9 mm SL, Mato Grosso do Sul, Porto Murtinho municipality, rio Paraguai basin, Lagoa 12, tributary of rio Paraguai, 19º24'21"S, 57º18'11"W; NUP 21860, 2, 79.5–83.5 mm SL, Mato Grosso, Rondonópolis municipality, Upper rio Paraguai basin, rio Vermelho, tributary of rio São Lourenço, 16º29'16"S, 54º31'25"W; ZUFMS-PIS 648, 1, xr, 51.6 mm SL, Mato Grosso do Sul, Corumbá municipality, marginal lagoon at MS-325 highway, 19º00'33"S, 57º39'12"W; ZUFMS-PIS 4329, 2, xr, 82.4–104.5 mm SL, Mato Grosso do Sul, Terenos municipality, Upper rio Paraguai basin, Pesqueiro in Rio Aquidauana, 20°17'07"S, 55°15'30"W; ZUFMS-PIS 5549, 3, xr, 45.6–50.0 mm SL, Mato Grosso do

Sul, Rio Negro municipality, Upper rio Paraguai basin, rio Garimpo na MS-080, 19°21'40"S, 54°59'33"W; ZUFMS-PIS 6320, 9, 5 xr, 66.8–82.3 mm SL, Mato Grosso do Sul, Coxim municipality, Upper rio Paraguai basin, rio Taquari, at Palmeiras waterfall, 18°21'44"S, 54°36'41"W; ZUFMS-PIS 6327, 1, xr, 51.0 mm SL, Mato Grosso do Sul, Coxim municipality, Upper rio Paraguai basin, rio Taquari, 18°31'36"S, 54°44'26"W; ZUFMS-PIS 6442, 1, xr, 69.8 mm SL, Mato Grosso do Sul, Miranda municipality, Upper rio Paraguai basin, rio Salobra, 20°13'17"S, 56°35'29"W; ZUFMS-PIS 6488, 6, 16.1–64.7 mm SL, Mato Grosso do Sul, Corumbá municipality, rio Miranda, under the bridge, during low water, 19º34'35"S, 57º02'17"W; ZUFMS-PIS 7677, 2, 63.5–66.1 mm SL, Mato Grosso do Sul, Rio Verde de Mato Grosso municipality, Baía Santa Virgínia, 19º12'00"S, 55º26'29"W; ZUFMS-PIS 8342, 1, xr, 76.8 mm SL.

Pimelodella sp. – All from Brazil. CPUFMT 2306, 1, 68.0 mm SL, Mato Grosso, Cuiabá municipality, rio Paraguai basin, Córrego Aricazinho, 15º32'21"S, 55º55'07"W; MCP-Peixes 15602, 5, 43.4–52.6 mm SL, Mato Grosso, Barra do Bugres municipality, rio Jauquara in Jauquara (tributary of rio dos Pássaros, rio Paraguai), 15º10'00"S, 57º04'59"W; MZUEL-Peixes 6458, 11, 5 examined, 60.0–97.1 mm SL, Mato Grosso do Sul, Corumbá municipality, rio Miranda, 19º34'36", 57º01'05"W; NUP 3506, 9, 65.2–86.1 mm SL, Mato Grosso, Santo Antônio de Leverger municipality, rio Paraguai basin, rio Cuiabá (Cb3), tributary of rio Paraguai, 15º58'27"S, 55º56'27"W; NUP 3566, 3, 103.0–122.1 mm SL, Mato Grosso, Rosário Oeste municipality, rio Paraguai basin, Reservatório Manso, tributary of rio Manso, 15º06'50"S, 55º40'38"W; NUP 14295, 1, 73.2 mm SL, Mato Grosso, Cáceres municipality, rio Paraguai basin, Baía de Cáceres, tributary of rio Paraguai, 18º58'42"S, 57º43'43"W; ZUFMS-PIS 618, 4, xr, 57.8–66.3 mm SL, Mato Grosso do Sul, Corumbá municipality, Upper rio Paraguai basin, rio Miranda, sandy beaches at Passo do Lontra region, 19°34'37"S, 57°00'42"W; ZUFMS-PIS 676, 2, 1 xr, 75.8–87.5 mm SL, Mato Grosso do Sul, Corumbá municipality, rio Miranda, sandy beaches at Passo do Lontra region, 19°34'37"S, 57°00'42"W; ZUFMS-PIS 1477, 2, 63.9–68.3 mm SL, Mato Grosso do Sul, Aquidauana municipality, Córrego Cipolândia, 20º28'16"S, 55º47'14"W; ZUFMS-PIS 3445, 7, xr, 28.9–40.2 mm SL, Mato Grosso, municipality Santo Antônio do Leverger, flooded areas of rio Cuiabá basin, 16°15'07"S, 55°47'20"W; ZUFMS-PIS 3478, 3, 31.0–48.1 mm SL, Mato Grosso, Barão de Melgaço municipality, flooded areas of rio Cuiabá basin, 16º32'36"S,

56º13'41"W; ZUFMS-PIS 4194, 60, 19 examined, 15 xr, 29.1–90.5 mm SL, Mato Grosso do Sul, Corumbá municipality, rio Miranda, during low water, 19º34'46"S, 57º01'11"W; ZUFMS-PIS 4703, 106, 19 examined, 53.6–91.4 mm SL, Mato Grosso do Sul, Bodoquena municipality, Córrego Salobrinha, 20º40'59"S, 56º47'07"W; ZUFMS-PIS 4843, 11, 2 examined, xr, 57.5–60.1 mm SL, Mato Grosso do Sul, Corumbá municipality, Upper rio Paraguai basin, rio Miranda, across from the BEP, 19°34'37"S, 57°00'42"W; ZUFMS-PIS 4862, 1, xr, 73.5 mm SL, Mato Grosso do Sul, Corumbá municipality, Upper rio Paraguai basin, Baía das Pedras, marginal lagoon at MS-184, 19°24'00"S, 57°02'00"W.

Pimelodus sp. – All from Brazil, in Upper rio Paraguai basin. ZUFMS-PIS 6679, 7, Mato Grosso do Sul, Corumbá municipality, rio Miranda, across from the BEP, 19°34'37"S, 57°00'42"W; ZUFMS-PIS 6680, 1, Mato Grosso do Sul, Coxim municipality, rio Taquari, 18°31'32"S, 54°44'30"W.

Results

Among the species occurring within the Upper rio Paraguai basin, 786 specimens were assessed from the previously cited, corresponding to the following species: *P. avanhandavae* (n = 21), *P. gracilis* (n = 126), *P. griffini* (n= 210), *P. megalura* (n = 50), *P. mucosa* (n = 65), *P. notomelas* (n = 8), *P. taeniophora* (n = 148), and *Pimelodella* sp. (n = 83) (Fig. 5). Moreover, 43 specimens were identified as pertaining to a new species within the genus, which was described and named *P. guato* Pierre & Slobodian, 2024. The detailed description of this species is addressed in Chapter 2, corresponding to the associated publication (Pierre, Slobodian, 2024).

Figure 5. Lateral view of species of *Pimelodella* found in the Upper rio Paraguai basin. **A.** *P. avanhandavae*, MCP-Peixes 36119, 89.4 mm SL; **B.** *P. gracilis*, MZUEL-Peixes 14001, 93.7 mm SL; **C.** *P. griffini*, ZUFMS-PIS 1607, 69.4 mm SL; **D.** *P. guato*, holotype, ZUFMS-PIS 8515, 78.5 mm SL; **E.** *P. megalura*, MCP-Peixes 15708, 74.3 mm SL; **F.** *P. mucosa*, ZUFMS-PIS 3256, 76.3 mm SL; **G.** *P. notomelas*, MZUEL-Peixes 7743, 52.6 mm SL; and **H.** *P. taeniophora*, MCP-Peixes 15708, 74.33 mm SL.

A notable proportion of the beforementioned material was remarkably bent, and therefore inadequate for geometric morphometric analyses. Consequently, the number of specimens utilized in the analyses was reduced compared to the total provided (sample sizes further addressed). Furthermore, since *P. griffini* and *P. taeniophora* presented a relatively higher number of specimens compared to the other species, some of them were excluded from the analyses to prevent substantial discrepancies in sample size across groups. Additionally, *P. avanhandavae* and *P. notomelas* were omitted from the analysis due to the small number of available specimens.

The repeatability of landmark digitization was high across photographs (both lateral and dorsal views) and radiographs. In all datasets, the Procrustes ANOVA indicated that individual differences had a greater influence on both size and shape variations than measurement error (*i.e.*, differences in digitization between replicas), with the mean squares of error being lower than the mean squares of the individual (Tab. 4). This analysis suggests a high degree of precision in the digitization of all landmarks, enabling the geometric morphometrics analyses.

Table 4. Results of the Procrustes ANOVA for centroid size and shape variation across three replicas of 30 *Pimelodella* specimens per view (lateral in photographs and radiographs; dorsal in photographs), distinguishing individual variation from measurement error. SS = sum of squares; MS = mean squares; df = degrees of freedom; F = F statistics; *p* = significance level.

	View	Effect	SS	MS	df	F	*p*
Centroid Size	Lateral view (Photos)	Individual	403.52	13.91	29	1247.71	< 0.0001
		Error	0.67	0.01	60		
	Lateral view (X-ray)	Individual	53282.21	1837.32	29	47013.82	< 0.0001
		Error	2.34	0.04	60		
	Dorsal view (Photos)	Individual	27.97	0.96	29	870.75	< 0.0001
		Error	0.07	0.00	60		
Shape	Lateral view (Photos)	Individual	0.21	0.000304	696	58.00	< 0.0001
		Error	0.01	0.000005	1440		
	Lateral view (X-ray)	Individual	0.26	0.000377	696	390.6	< 0.0001
		Error	0.00	0.000001	1440		
	Dorsal view (Photos)	Individual	0.15	0.000251	580	28.35	< 0.0001
		Error	0.01	0.000009	1200		

1. Shape variation of the body in lateral view

1.1. Photographs

A total of 313 specimens were analyzed for external lateral view, encompassing the following species: *P. gracilis* (n = 48), *P. griffini* (n = 71), *P. guato* (n = 34), *P. megalura* (n = 36), *P. mucosa* (n = 52), and *P. taeniophora* (n = 72) (Tab. 1).

The ANOVA detected significant size variation among the species (F = 83.46; df = 5; $p < 2e\text{-}16$). Subsequently, the Tukey's test revealed significant differentiation in centroid sizes among all pairs of species ($p < 0.001$), except between *P. megalura*, *P. mucosa* and *P. taeniophora* ($p > 0.05$). This consistent pattern is visually evident in the boxplot of the centroid sizes (Fig. 6), where *P. gracilis* exhibits the largest size, followed by *P. guato*.

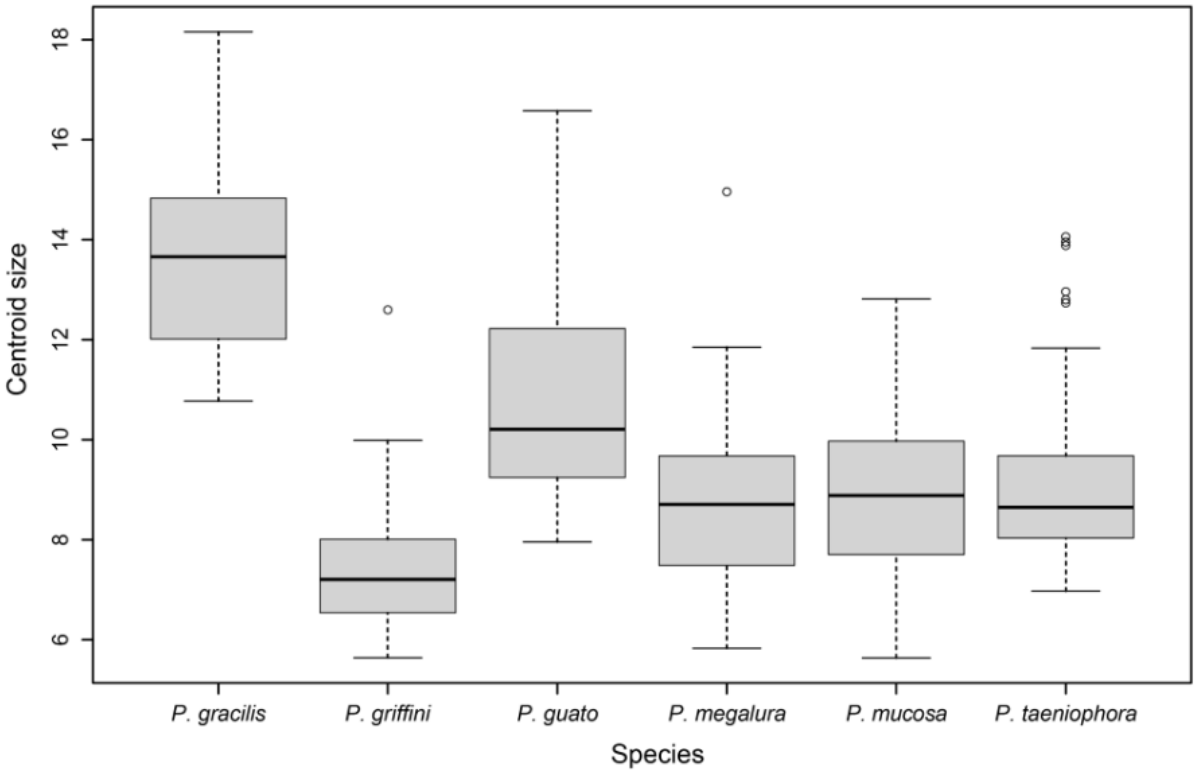

Figure 6. Boxplot of centroid size for each species of *Pimelodella* in external lateral view. The circles represent the outliers.

The pooled within-group regression showed that size influenced 5.8% of the total shape variation, with a significant permutation test ($p < 0.0001$). Despite the pronounced significance of the *p* value, the proportion of the allometric effect remained notably low, and the PCA derived from the regression residuals (Fig. 7) was very similar compared to the PCA following GPA (further addressed). Therefore, the analyses here presented were proceeded without size correction.

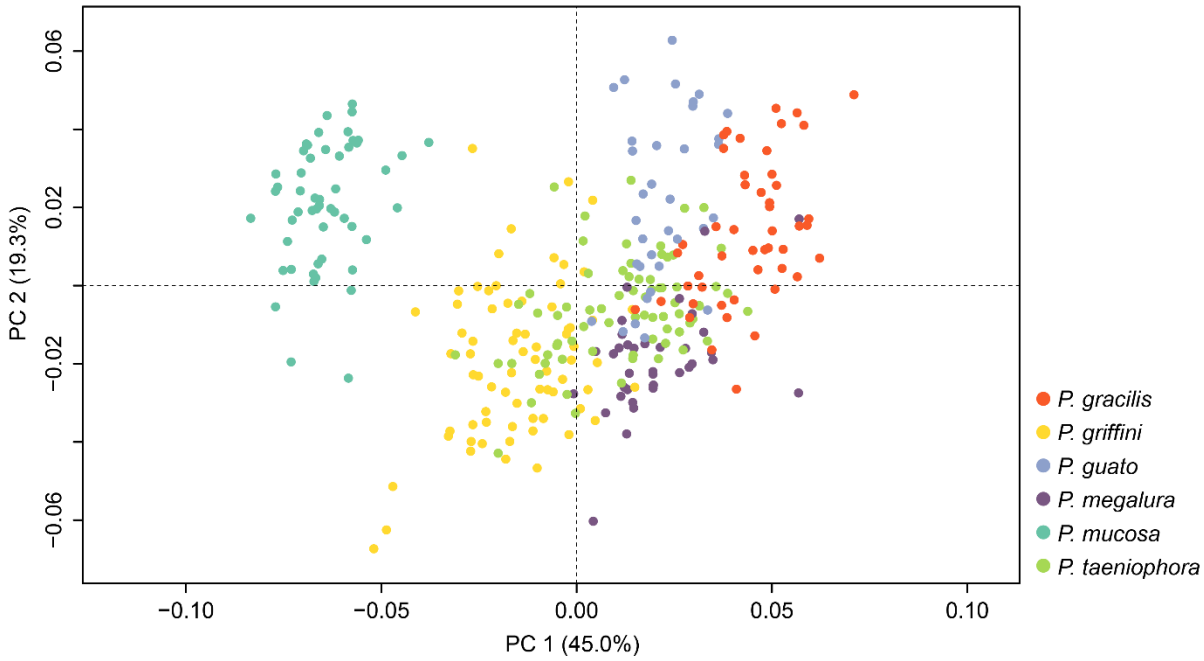

Figure 7. Scatterplot of Principal Components one (PC1) and two (PC2) from the residuals of the allometric regression in external lateral view. The variance percentage for each PC is provided in parentheses.

Regarding the shape analyses, The PCA detected that shape variation corresponding to the external lateral view was distributed across 24 PCs, with 75.3% of the total variance concentrated in the first three PCs. The PCA graphics revealed that, despite some overlapping points, notable shape differences among certain groups can be visualized (Fig. 8). *Pimelodella mucosa* emerged as the species most distinctly separated in the morphospace, differentiating from all other species. Further, *P. griffini* and *P. gracilis* demonstrated great separation from each other along the PC1 axis (Fig. 8). While in PC2 axis no group patterns were discernible (Fig. 8A), in the PC3 axis there is a tendency for separation between *P. griffini* and *P. gracilis* (Fig. 8B). It is also evident that *P. guato* exhibits a strong separation from *P. griffini* and *P. gracilis* along the PC1 axis. Conversely, *P. megalura* and *P. taeniophora* overlapped with all the species, except *P. mucosa*.

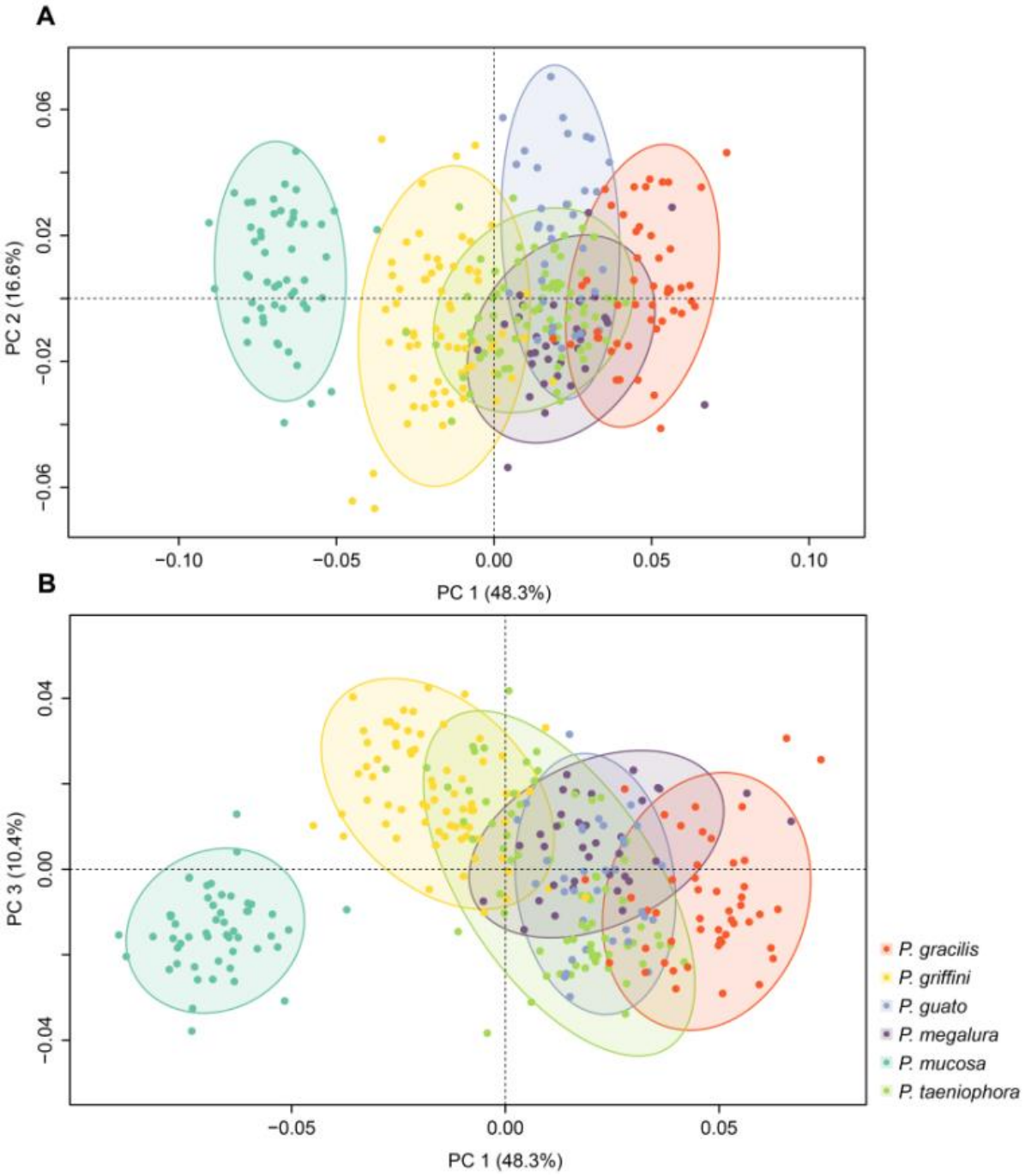

Figure 8. Scatterplot of Principal Components **A.** One (PC1) and two (PC2); and **B.** One and three (PC3), from the Principal Components Analysis (PCA) in external lateral view, with frequency ellipses of 90%. The variance percentage for each PC is provided in parentheses.

Shape variations related to the first three PCs are shown in Figure 9. PC1 explained 48.3% of the variation, primarily describing changes in landmarks corresponding to the insertions of dorsal and adipose fins (*i.e.*, landmarks 2, 3 and 4) (Fig. 9A). The overall variation in landmark positions is translated as changes related to the body depth. Specimens of *P. mucosa* presented the most negative scores on

the PC1 axis (Fig. 8), denoting a deeper body shape, with the dorsal fin and origin of adipose fin positioned more posteriorly in the body, and distantly from each other (Fig. 9A). Conversely, specimens of *P. gracilis* were displayed in the opposite extreme of the PC1 axis, presenting the most positive scores (Fig. 8). These specimens present a slender body shape, with the dorsal fin and origin of adipose fin situated more anteriorly in the body, and closer from each other (Fig. 9A). Additionally, specimens at this extreme tended to present the anal-fin base more aligned with the verticals through adipose-fin terminus compared to specimens at the negative extreme (Fig. 9A).

PC2 contributed 16.6% to the shape variation and described the curvature of the body and snout tip position (Fig. 9B). However, no species were separated along this axis (Fig. 8A). The negative extreme of the axis corresponded to specimens with a downward curved body shape, with more ventral positions of the snout tip and caudal peduncle, and a straight dorsal-fin base (Fig. 9B). Meanwhile, the positive extreme of the axis comprised specimens with more dorsal positions of the snout tip and caudal peduncle coupled with an inclined profile of the dorsal-fin base, imparting an impression of an upward curved body (Fig. 9B).

PC3 retained 10.4% of the total variance. Although species did not distinctly vary in shape along this axis due to overlap (Fig. 8B), PC3 displayed a somewhat similar aspect of shape change observed in PC1 (Figs. 9A,C). The variations in the positions of landmarks on the dorsal and adipose fins (*i.e.*, landmarks 2, 3 and 4) describe dorsal and adipose fins more near to each other in the extreme negative score, and more distant to each other in extreme positive score (Fig. 9C).

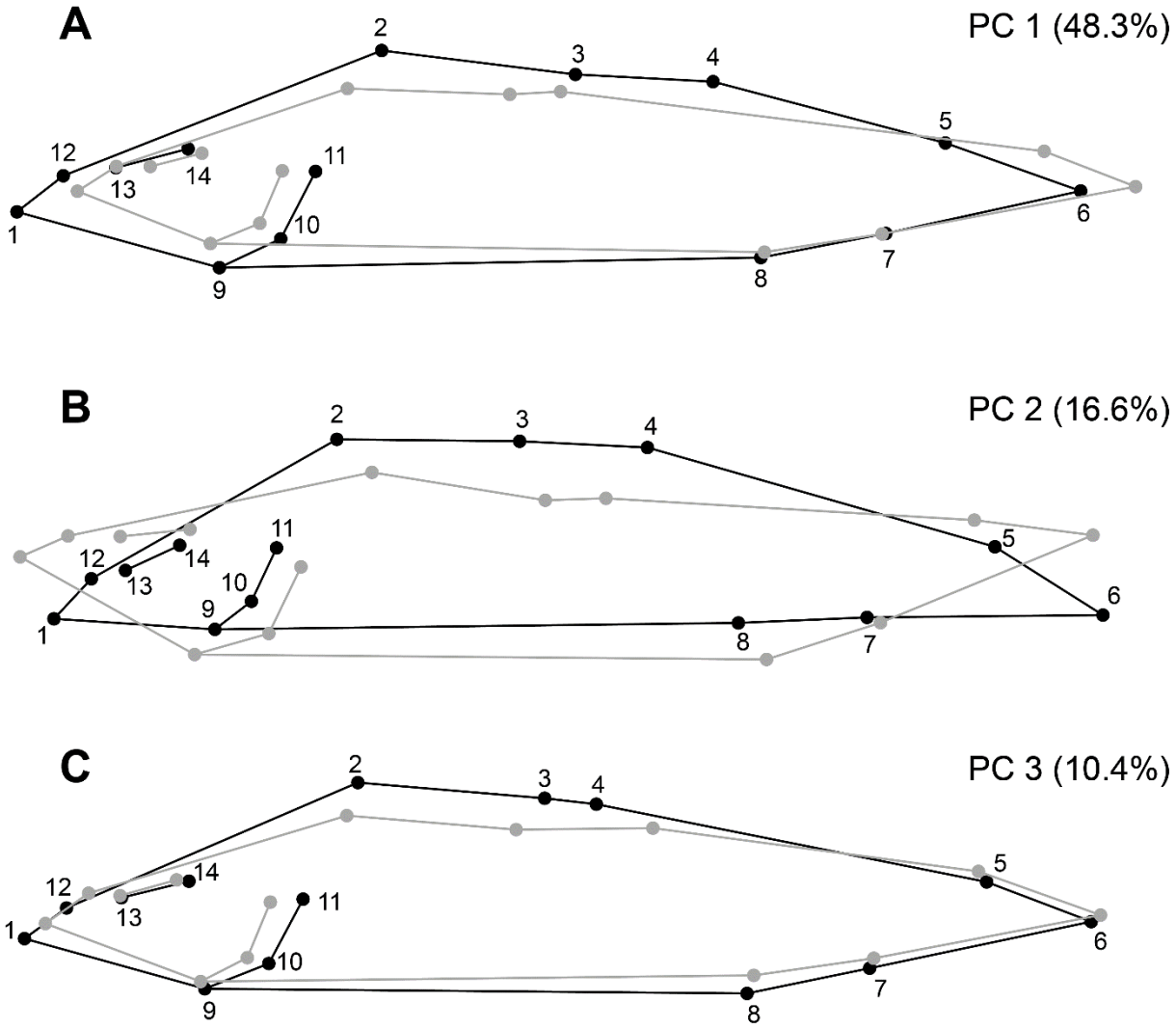

Figure 9. Wireframe visualizations of shape variation between the extremes of **A.** Principal Component 1 (PC1) axis; **B.** Principal Component 2 (PC2) axis and **C.** Principal Component 3 (PC3) axis in lateral photographic view. Black wireframe illustrates the shape configuration at the negative extreme of each PC axis. Gray wireframe represents the shape configuration at the positive extreme of each PC axis. Variance percentages of each PC are provided in parentheses.

A MANOVA of the PCs scores suggested a significant variation in shape among the species (Pillai's trace = 3.27; approx. F = 22.76; num df = 120; p < 2.2e-16). Additionally, significant shape differences were observed between all pairs of species, as elucidated by the results of the pairwise comparisons (Tab. 5). This latter test was performed based on a Procrustes ANOVA, which assessed the effect of species on Procrustes shape variables (R^2 = 0.55; F = 76.00; p = 0.0001; Z = 12.0). The statistical significance of the pairwise p values followed Bonferroni correction (<0.0033), and they

were significant in all species pairs, with *p* values ranging between 0.0001–0.0003 (Tab. 5).

Table 5. Results of pairwise comparisons between least squares means of Procrustes distances, based on Procrustes ANOVA, comparing body shape variation among species of *Pimelodella* in external lateral view. The values below the diagonal correspond to pairwise *p* values based on 10.000 permutations, while the values above the diagonal represent pairwise effect sizes (Z scores).

	Pimelodella gracilis	*Pimelodella griffini*	*Pimelodella guato*	*Pimelodella megalura*	*Pimelodella mucosa*
P. gracilis		5.47	3.67	3.57	6.77
P. griffini	0.0001		4.64	4.26	5.50
P. guato	0.0001	0.0001		3.96	6.21
P. megalura	0.0001	0.0001	0.0001		6.13
P. mucosa	0.0001	0.0001	0.0001	0.0001	
P. taeniophora	0.0001	0.0001	0.0003	0.0001	0.0001

1.2. Radiographs

The lateral view regarding the radiographs (therefore osteological lateral view) included 157 specimens, representing the following species: *P. gracilis* (n = 26), *P. griffini* (n = 35), *P. guato* (n = 15), *P. megalura* (n = 26), *P. mucosa* (n = 24), and *P. taeniophora* (n = 31) (Tab. 2). The lower number of specimens compared to the photographs data is due to limitations employed by the X-ray equipment, which restricted the maximum number of specimens that could be radiographed.

Concerning the size variation, the ANOVA underscored a significant difference in size among the species ($F = 38.06$; $df = 5$; $p < 2e\text{-}16$). Subsequently, Tukey's test indicated that all species sizes differ significantly when compared pairwise ($p < 0.05$), except for the comparisons between *P. griffini* and *P. mucosa*, as well as between *P. megalura*, *P. mucosa* and *P. taeniophora* ($p > 0.05$). This same pattern is corroborated by the boxplot of the centroid sizes (Fig. 10), in which the results are similar to those of the external lateral view (Fig. 6).

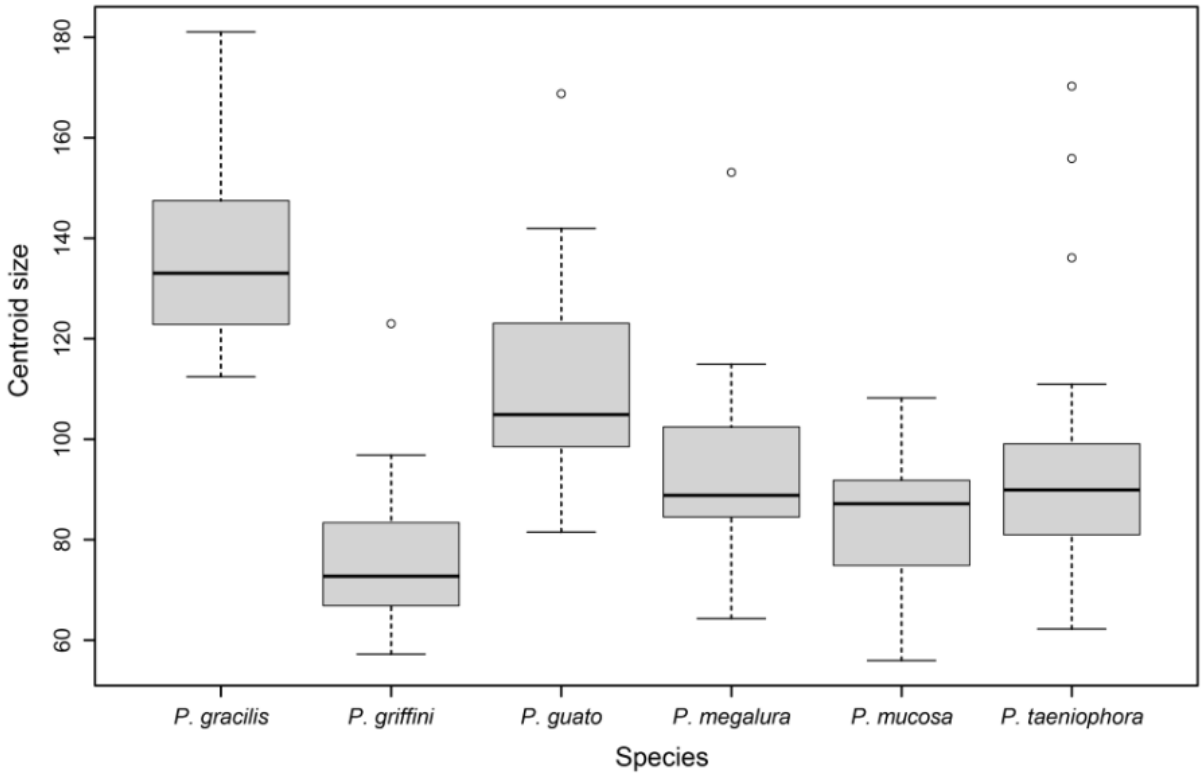

Figure 10. Boxplot of centroid size for each species of *Pimelodella* in osteological lateral view. The circles represent the outliers.

The pooled-regression analysis showed that 5.3% of shape variation is influenced by size, with a permutation test with $p = 0.0001$. As in the external lateral view, the *p* value demonstrated significance, but with a low allometric effect proportion and noticeable similarities between the PCA based on regression residuals (Fig. 11) and the one without the correction for allometric effect (further addressed). Thus, the analyses also proceeded without size correction.

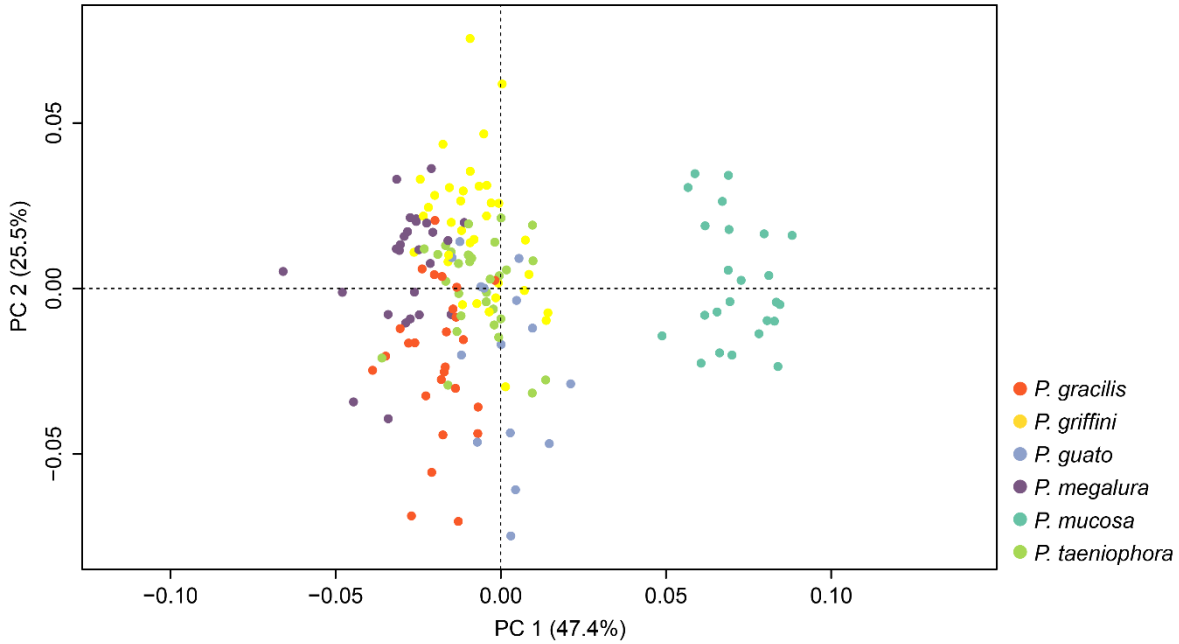

Figure 11. Scatterplot of Principal Components one (PC1) and two (PC2) from the residuals of the allometric regression in osteological lateral view. The variance percentage for each PC is provided in parentheses.

The PCA detected that the shape variation corresponding to the lateral radiographic view was distributed across 24 PCs, with the first three PCs explaining 81.1% of the total variance. The PCA plots revealed an overall overlap between the species, except for *P. mucosa*, which was the one with the most distinct shape, differentiating from all other species in PC1 axis (Fig. 12). Moreover, *P. griffini* and *P. gracilis* presented a partial separation when plotted on PC1 *vs.* PC2 (Fig. 12A), a differentiation that became more accentuated in PC1 *vs.* PC3 (Fig. 12B), resulting in complete segregation between the two species. Also, some species presented shape differences along the PC3 axis (Fig. 12B). In this axis, it was evident that *P. gracilis* and *P. megalura* exhibited similarities in shape, which were more distinct compared to *P. griffini* and *P. guato*. *Pimelodella taeniophora*, conversely, overlapped with all the species, except *P. mucosa*, across all axes (Fig. 12).

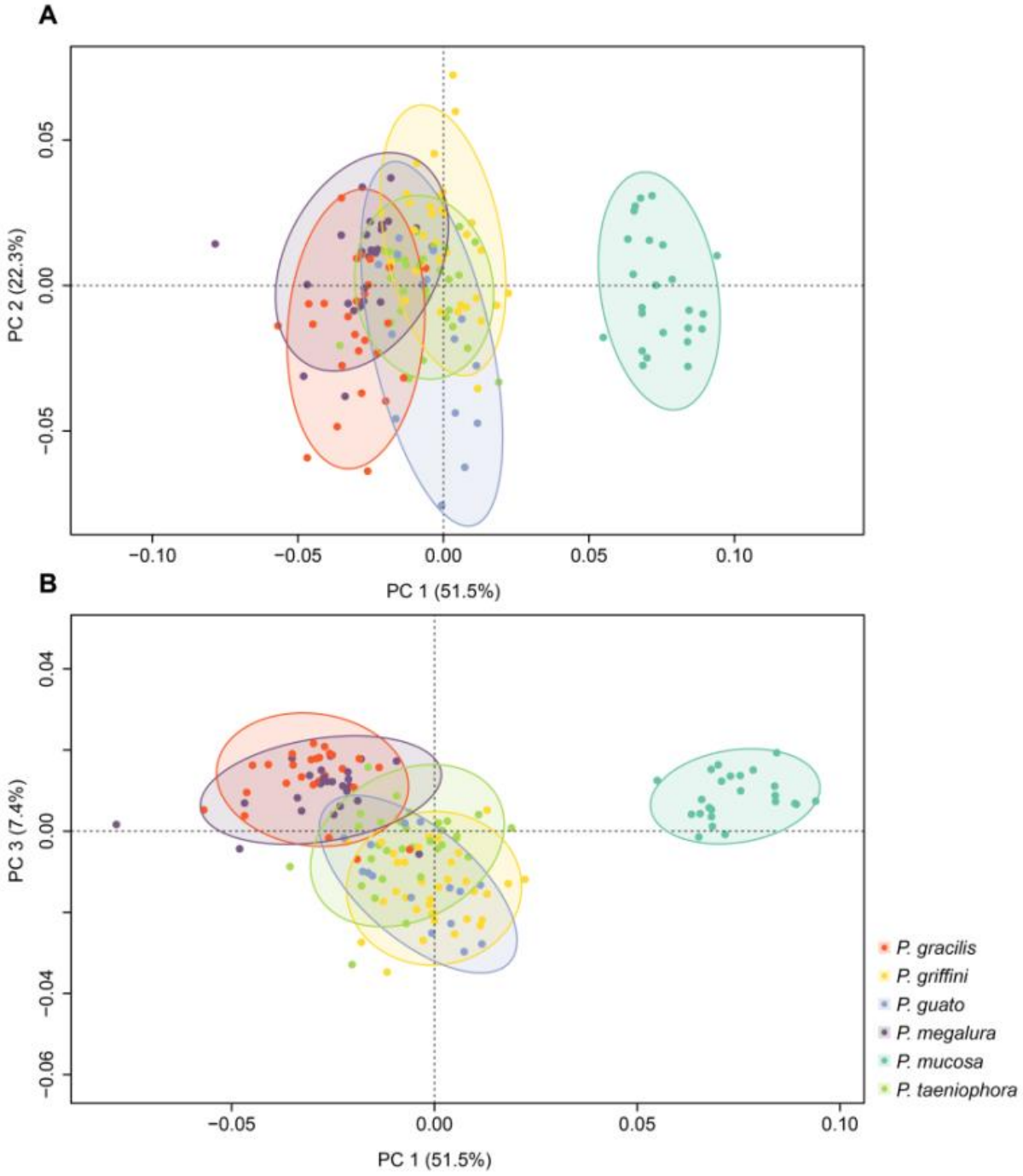

Figure 12. Scatterplot of Principal Components **A.** One (PC1) and two (PC2) and **B.** One and three (PC3) from the Principal Components Analysis (PCA) in osteological lateral view, with frequency ellipses of 90%. The variance percentage for each PC is provided in parentheses.

The variations in shape related to the first three PCs are illustrated in Figure 13. In general, the observed variations share notable similarities with the external lateral view addressed in the preceding section. PC1 explained 51.5% of the variation and described changes associated with body depth and comparative head size (Fig. 13A).

Specimens of *P. gracilis* and *P. megalura* displayed the most negative scores of the PC1 axis (Fig. 12). These specimens comprise a slender body shape, proportionally smaller heads, the posterior end of the Weberian apparatus at the first one fourth of the body length, and the 20th vertebra positioned midway between the snout and the compound caudal centrum (PU1+U1) (Fig. 13A). On the other hand, specimens of *P. mucosa* exhibited the most positive scores on the PC1 axis (Fig. 12), representing a deeper body shape, proportionally larger heads, the posterior end of the Weberian apparatus at the first third of the body length, and the 20th vertebra situated at the posteriormost third of the body, closer to the compound caudal centrum (Fig. 13A).

PC2 accounted for 22.3% of the shape variation and described the dorsal curvature of the body (Fig. 13B). All species superimpose massively on this axis (Fig. 12A), the negative extreme of the axis corresponded to specimens with an upward curvature, with a more dorsal position of the premaxila and the compound caudal centrum (Fig. 13B). Conversely, the specimens at the positive extreme of the axis comprised a downward curvature, with a more ventral position of the premaxila and the compound caudal centrum (Fig. 13B). Finally, PC3 explained 7.4% of the total variance, reflecting subtle differences in the premaxilla position, more ventral in the extreme positive scores, and caudal peduncle length, shorter in the extreme positive scores (Fig. 13C).

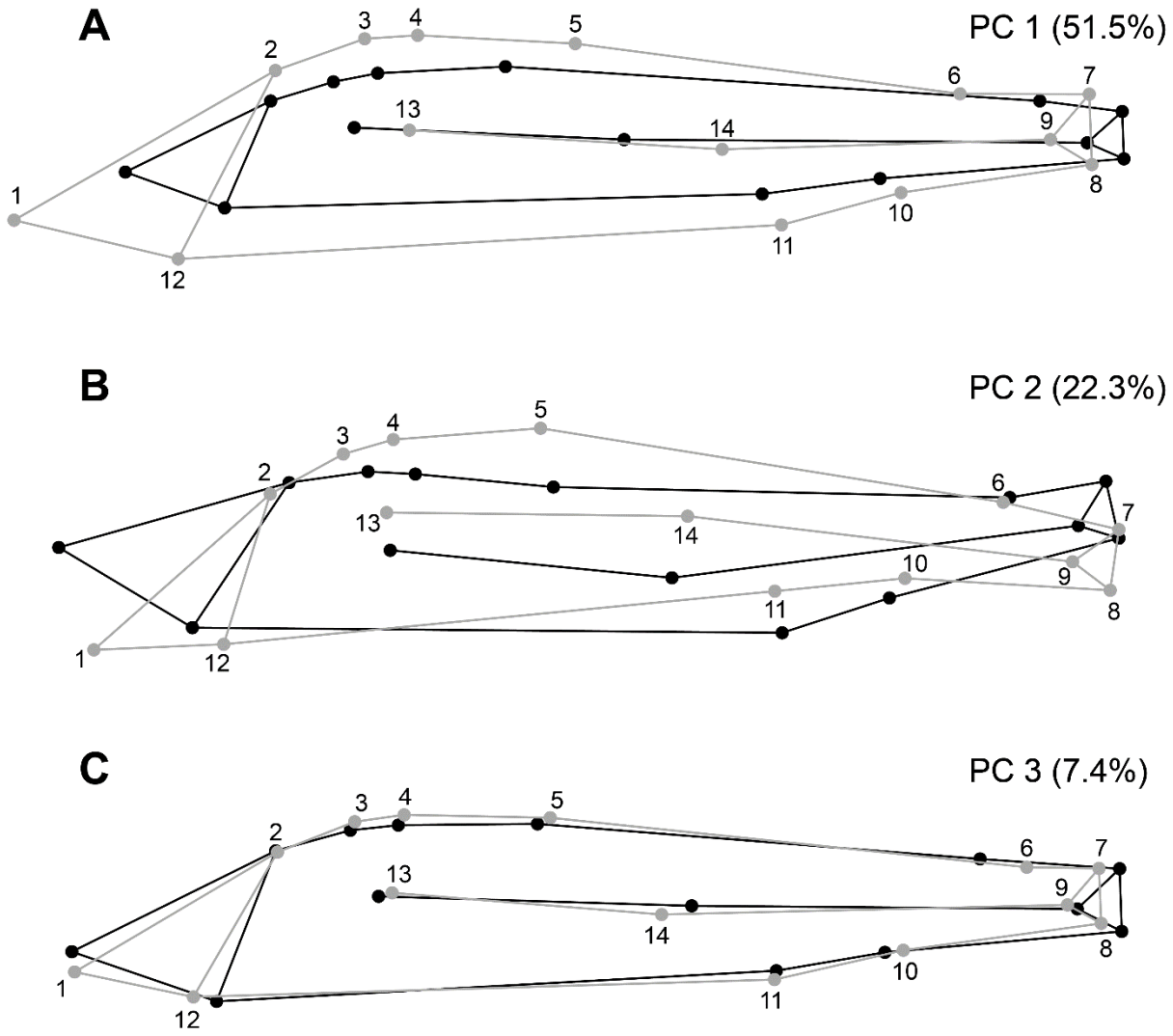

Figure 13. Wireframe visualizations of shape variation between the extremes of **A.** Principal Component 1 (PC1) axis; **B.** Principal Component 2 (PC2) axis; and **C.** Principal Component 3 (PC3) axis in osteological lateral view. Black wireframe illustrates the shape configuration at the negative extreme of each PC axis. Gray wireframe represents the shape configuration at the positive extreme of each PC axis. Variance percentages of each PC are provided in parentheses.

A MANOVA of the PCs scores suggested that shape differs significantly among the species (Pillai's trace = 3.52; approx. F = 13.09; num df = 120; p < 2.2e-16), and significant shape variation was observed between almost all pairs of species, with few exceptions, as shown in the results of the pairwise comparisons (Tab. 6). This latter test was conduct based on a Procrustes ANOVA, which evaluated the effect of species on Procrustes shape variables (R^2 = 0.61; F = 46.98; p = 0.0001; Z = 11.46). The statistical significance of the pairwise p values was adjusted utilizing Bonferroni correction (< 0.0033), indicating that shape differs significantly among all species pairs,

with *p* values ranging between 0.0001–0.0029, except for the pairs *P. gracilis-P. megalura* and *P. guato-P. taeniophora* (Tab. 6).

Table 6. Results of pairwise comparisons between least squares means of Procrustes distances, based on Procrustes ANOVA, comparing body shape variation among species of *Pimelodella* in osteological lateral view. The values below the diagonal correspond to pairwise *p* values based on 10.000 permutations, while the values above the diagonal represent pairwise effect sizes (Z scores).

	Pimelodella gracilis	*Pimelodella griffini*	*Pimelodella guato*	*Pimelodella megalura*	*Pimelodella mucosa*
P. gracilis		4.27	2.82	2.41	6.28
P. griffini	0.0001		2.97	3.48	5.35
P. guato	0.0012	0.0009		3.42	5.23
P. megalura	0.0056	0.0001	0.0001		6.00
P. mucosa	0.0001	0.0001	0.0001	0.0001	
P. taeniophora	0.0003	0.0029	0.0414	0.0004	0.0001

2. Shape variation of the head in dorsal view

A total of 332 specimens were included in the analyses regarding the external dorsal view, pertaining to the following species: *P. gracilis* (n = 53), *P. griffini* (n = 78), *P. guato* (n = 39), *P. megalura* (n = 36), *P. mucosa* (n = 64), and *P. taeniophora* (n = 62) (Tab. 3).

The ANOVA indicated significant size variation among the species (F = 93.48; df = 5; $p < 2e\text{-}16$), and the Tukey's test showed significant differentiation in centroid sizes among all pairs of species ($p < 0.05$), except for the pairs *P. guato-P. mucosa* and *P. megalura-P. taeniophora* ($p > 0.05$). In Figure 14 is observed the boxplot for centroid size. *Pimelodella gracilis*, *P. guato* and *P. mucosa* exhibited a broader size range, while *P. griffini*, *P. megalura* and *P. taeniophora* were smaller and displayed a more restricted size range.

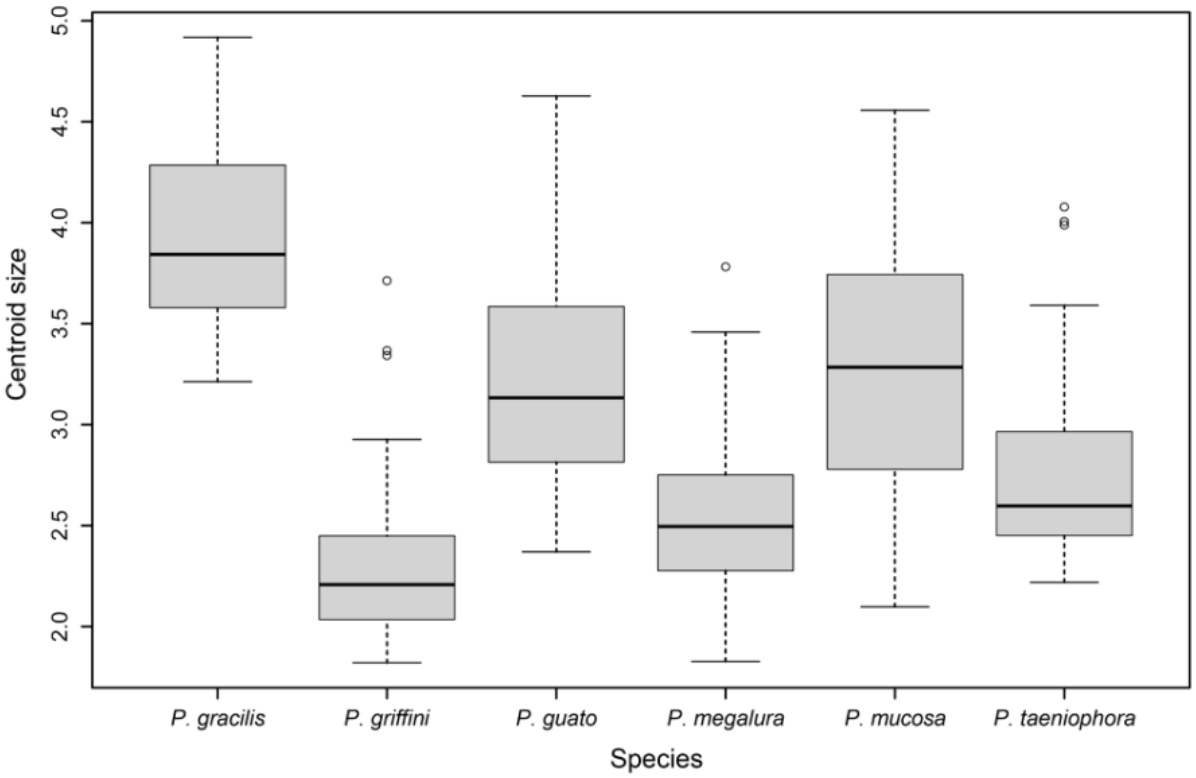

Figure 14. Boxplot of centroid size for each species of *Pimelodella* in external dorsal view. The circles represent the outliers.

The pooled within-group regression revealed that size influenced 11.0% of the total head shape variation, with a significant permutation test ($p < 0.0001$). The proportion of the allometric effect here was higher compared to the external and osteological lateral views, and the analyses based on the regression residuals differed from those without the correction for allometric effect. In this context, to prevent erroneous biological interpretation, the size correction was conducted, and all the subsequent analyses were based on the regression residuals.

The PCA detected that shape variation corresponding to the external dorsal view was distributed across 20 PCs, with 60.1% of the total variance distributed in the first three PCs. The PCA graphics indicated that, despite substantial overlap among the species, it was evident that *P. mucosa*, *P. gracilis* and *P. guato* separated from *P. griffini* and *P. megalura* along the PC1 axis (Fig. 15). Although presenting shape similarities with *P. gracilis* and *P. guato*, *P. mucosa* completely segregates from *P. griffini* and *P. megalura*, and almost completely separates from *P. taeniophora* (Fig. 15). Furthermore, no discernible patterns for species differentiation could be distinguished along the PC2 and PC3 axes (Fig. 15).

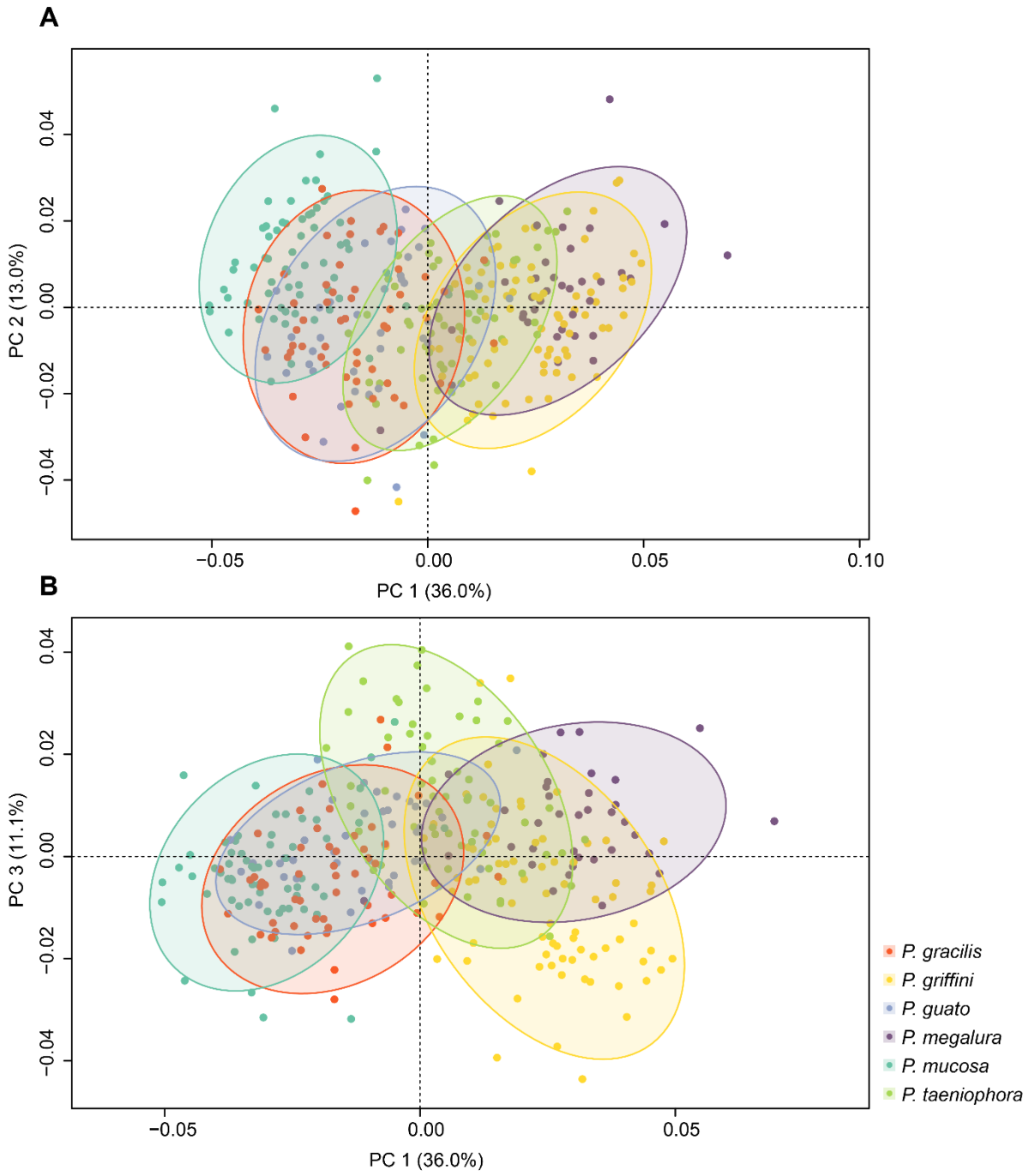

Figure 15. Scatterplot of Principal Components **A.** One (PC1) and two (PC2) and **B.** One and three (PC3) from the Principal Components Analysis (PCA) based on the regression residuals in external dorsal view, with equal frequency ellipses of 90%. The variance percentage for each PC is provided in parentheses.

Shape variations regarding the first three PCs are shown in Figure 16. The PC1 explained 36.0% of the variation and was associated with the posterior region of the

head and the position of the dorsal fin (Fig. 16A). Negative scores along the PC1 axis, exemplified by *P. mucosa* at its extreme (Fig. 15), described a homogeneous head shape characterized by a larger snout width maintained along the head (Fig. 16A). Additionally, a closer proximity between the posterior tip of the supraoccipital process and the origin of the dorsal fin was observed (Fig. 16A). The opposite was true for the positive extreme of the axis, represented by *P. megalura* (Fig. 15), thus indicating an "arrow" head shape, characterized by a narrower snout width and wider head width at the branchiostegal membrane (Fig. 16A). Also, a larger distance between the posterior tip of the supraoccipital process and the origin of the dorsal fin was observed (Fig. 16A). A similar pattern was recovered to a lesser extent in PC2, which accounted for 13.0% of the variation (Fig. 16B). In PC2, the extreme negative score indicates a pattern somewhat similar to the extreme positives scores of PC1. However, the extreme positive scores of PC2 shows comparatively narrower heads, but with long supraoccipital process (Fig. 16B). PC3, responsible for 11.1% of the total variance, mainly described the changes in the anterior region of the head, corresponding to a longer snout at the extreme negative scores (Fig. 16C). Nevertheless, neither PC2 nor PC3 could distinguish the shape among the species (Fig. 15).

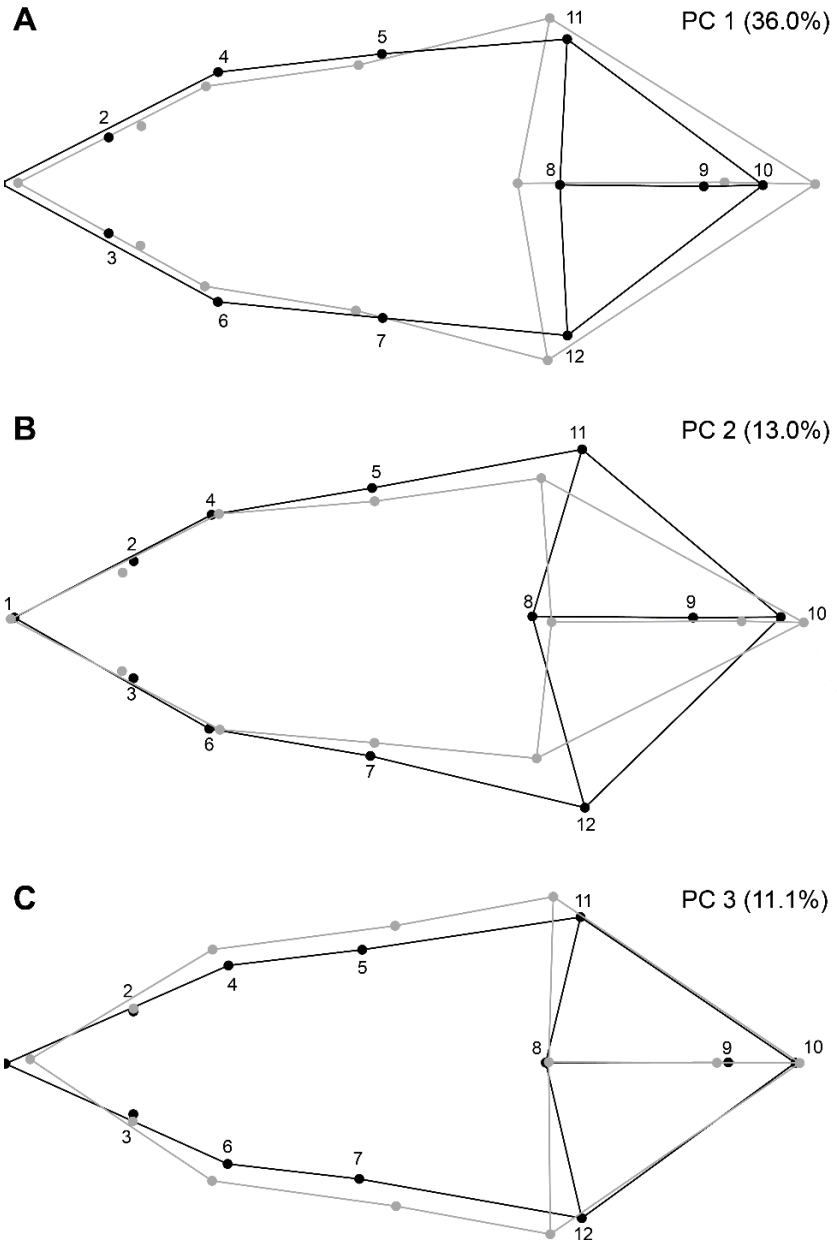

Figure 16. Wireframe visualizations of shape variation between the extremes of **A.** Principal Component 1 (PC1) axis; **B.** Principal Component 2 (PC2) axis and **C.** Principal Component 3 (PC3) axis in external dorsal view. Black wireframe illustrates the shape configuration at the negative extreme of each PC axis. Gray wireframe represents the shape configuration at the positive extreme of each PC axis. Variance percentages of each PC are provided in parentheses.

Despite considerable overlap in the PCA plots, a MANOVA of the PCs scores suggested a significant variation in shape among the species (Pillai's trace = 2.00; approx. F = 10.40; num df = 100; p < 2.2e-16). In addition, significant shape differences were observed between all pairs of species, as evidenced by the results of the pairwise comparisons (Tab. 7). This test was performed based on a Procrustes ANOVA, which

assessed the effect of species on Procrustes shape variables (R^2 =0.36; F = 37.37; *p* = 0.0001; Z = 11.9). The significance of the pairwise *p* values was adjusted following Bonferroni correction (<0.0033), and they were significant in all species pairs, with *p* values ranging between 0.0001–0.0004 (Tab. 7).

Table 7. Results of pairwise comparisons between least squares means of Procrustes distances, based on Procrustes ANOVA, comparing body shape variation among species of *Pimelodella* in external dorsal view. The values below the diagonal correspond to pairwise *p* values based on 10.000 permutations, while the values above the diagonal represent pairwise effect sizes (Z scores).

	Pimelodella gracilis	*Pimelodella griffini*	*Pimelodella guato*	*Pimelodella megalura*	*Pimelodella mucosa*
P. gracilis		6.35	3.22	6.34	4.52
P. griffini	0.0001		5.75	3.32	7.57
P. guato	0.0004	0.0001		5.94	4.92
P. megalura	0.0001	0.0003	0.0001		7.06
P. mucosa	0.0001	0.0001	0.0001	0.0001	
P. taeniophora	0.0001	0.0001	0.0001	0.0001	0.0001

3. PCA plots without specimens of *Pimelodella taeniophora*

In all datasets (external and osteological lateral views, as well as external dorsal view), *Pimelodella taeniophora* was the species that overlapped the most in all PCA plots. Therefore, Figure 17 shows the PCA plots with the same parameters employed in the preceding analyses, but with the omission of *P. taeniophora*. This exclusion aims to improve the clarity of groups visualization within the morphospace.

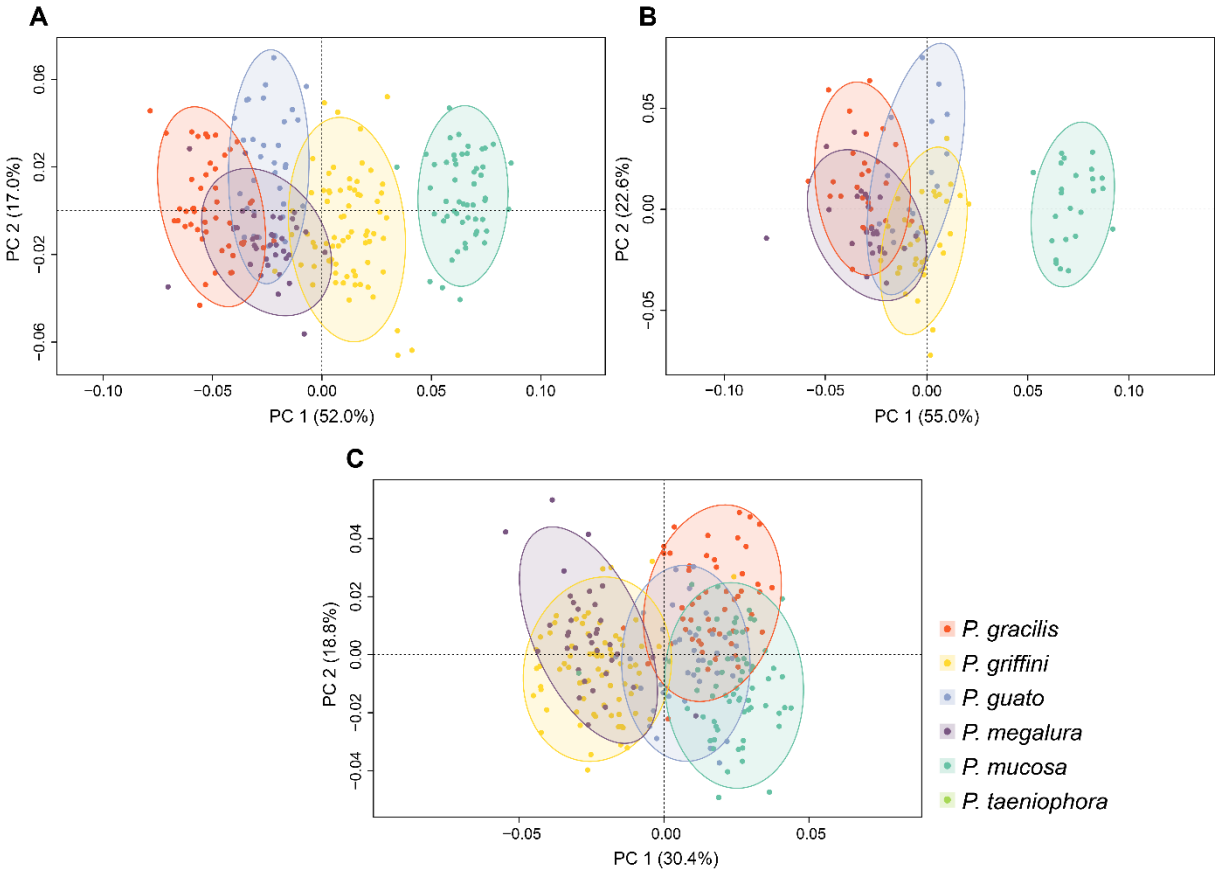

Figure 17. Scatterplot of Principal Components one (PC1) and two (PC2) with frequency ellipses of 90% of **A.** External lateral view; **B.** Osteological lateral view and **C.** External dorsal view. The variance percentage for each PC is provided in parentheses.

Discussion

The notable conservative morphology between species of the genus *Pimelodella* results in a challenging task for their delimitation and identification (Slobodian *et al.*, 2017; Slobodian, Pastana, 2018). Despite recent works addressing taxonomic issues in *Pimelodella* (*e.g.*, Souza-Shibatta *et al.*, 2013; Conde-Saldaña, 2016; Slobodian, 2017; Slobodian *et al.*, 2017, 2021, 2022; Slobodian, Pastana, 2018; Conde-Saldaña *et al.*, 2019; Cortés-Hernández *et al.*, 2020, 2023; Cortés-Hernández, Ramírez-Gil, 2024), the challenge in its species' delimitation may lead to misidentifications or undetermined specimens at the species level. Among the materials obtained from scientific collections examined in this work, approximately 56.2% were incorrectly identified, and 10.6% were indicated as indetermined at the species level. Additionally, it has been observed that certain specimens identifyied as *Pimelodella* actually belong to other genus from the family (*i.e.*, *Imparfinis* Eigenmann

& Norris, 1900), or are even from another family (*i.e.*, *Pimelodus*, family Pimelodidae) (see Examined Material).

Furthermore, despite all recently described *Pimelodella* species used linear morphometric data for the comparison with congeners, they also indicated a superimposition of this kind of data and demanded osteology, coloration patterns or other data in order to differ the described species from known ones (*e.g*., Slobodian *et al.*, 2017; Slobodian, Pastana, 2018; Conde-Saldaña *et al.*, 2019; Cortés-Hernández *et al.*, 2020, 2023). Given this scenario, this study aimed to assess if geometric morphometrics could be a method for description of the shape differences and helpful in delimiting species of *Pimelodella.* Therefore, we choose the species found in the Upper rio Paraguai basin as our case of study. This basin was chosen due to the extensive sampling in several scientific collections and because the basin had species ranging the different morphotypes found in the genus: shorter maxillary babel as *P. griffini*, with enlarged preoperculomandibular cephalic lateral-line canal openings as *P. mucosa*, with shorter supraoccipital process as *P. megalura*, among other.

All species reported to occur in the rio Paraguai basin were represented among the examined materials, with the exception of *P. laticeps* and *P. parva*, which do not inhabit the Upper rio Paraguai basin and are only known from lower reaches, for the first, and the type material, for the second. Further, some specimens collected in this basin were identified as *P. avanhandavae*, a species previously documented only in the rio Tietê basin in Upper rio Paraná basin (Bockmann, Guazzelli, 2003; Ferraris, 2007; Fricke *et al.*, 2024), but demand a more throughout investigation. Additionally, certain specimens were identified as pertaining to a new species, named *P. guato*, as detailed in chapter 2 (Appendix I). Thus, our work focused on species from the Upper rio Paraguai instead of encompassing all rio Paraguai basin.

Also, the high number of specimens misidentified at the species level posed a challenge in obtaining an adequate sample size for each species through collection loans. *Pimelodella notomelas* and *P. avanhandavae*, although found in the rio Paraguai basin, were excluded from the analyses due to their low representation. Moreover, the use of geometric morphometrics faces limitations, such as the requisite for specimens in great preservation state and without deformities, such as bent bodies

(commonly found among *Pimelodella* material). These conditions further reduced the number of specimens included in the analyses compared to the total available.

Regarding the size variation, some patterns were observed. *Pimelodella gracilis* emerged as the largest species, followed by *P. guato*, with both species displaying the greatest variability in size range (Figs. 6, 10). Conversely, *P. griffini* was consistently indicated as the smallest species among those analyzed (Figs. 6, 10). Furthermore, the analyses revealed overlapping size ranges for *P. megalura*, *P. mucosa* and *P. taeniophora* (Figs. 6, 10). These similarities in size range are also evident in the material analyzed by Slobodian (2017), wherein specimens of *P. gracilis* exhibited a size range of 75.1–170.1 mm SL, while *P. griffini* ranged from 43.8–69.9 mm SL, *P. megalura* ranged from 70.0–143.6 mm SL, and *P. taeniophora* ranged from 59.1–92.7 mm SL (Slobodian, 2017). Although *P. notomelas* was not included in the analyses of the present work, this species appears to be the smallest among *Pimelodella* species occurring in Upper rio Paraguai basin (see in Examined Material; Eigenmann, 1917; Britski *et al.*, 1999, 2007; Slobodian, 2017: Tabel 52).

The larger size found in *P. gracilis* and *P. guato* is unusual for heptapterids, that are usually small, but specimens of *Goeldiella* Eigenmann & Norris, 1900, *Heptapterus* Bleeker, 1858, *Pimelodella*, *Rhamdia*, and *Rhamdioglanis* Ihering, 1907, were reported to exceed this length (Bockmann, Guazzelli, 2003). Certainly, the only *Pimelodella* species distributed in the Upper rio Paraguai basin that did not surpass a size of 100 mm SL were *P. griffini* and *P. notomelas*. Body size is frequently associated with various biological and ecological traits, such as the habitat depth and predation risks (Harvey, Stewart, 1991), as well as the body composition (Breck, 2014). However, given the lack of ecological studies concerning the *Pimelodella* species, including those inhabiting the rio Paraguai basin, direct assumptions regarding their body size are a difficult task.

Additionally, it is pertinent to point out some considerations regarding their conservation status. While all species under investigation are currently classified as Least Concern in the IUCN Red List of Threatened Species (2024), and none of them is included in the Red Book of Threatened Brazilian Fauna (ICMBio, 2018; MMA, 2022), the scarce taxonomic, biological, and population studies results in considerable gaps for understanding the true status of these species (IUCN, 2024). The vulnerability

of freshwater fishes is usually associated with commercial fisheries or impacts to their environment (Allan *et al.*, 2005; Xenopoulos *et al.*, 2005; Dudgeon *et al.*, 2006). Although *Pimelodella* species, in general, are not targeted in recreational and commercial activities due to their small sizes, primarily consisting of ornamental fishes (Bockmann, Guazzelli, 2003), certain species analyzed herein may have a restricted distribution to the Upper rio Paraguai basin (*i.e.*, *P. griffini*, *P. megalura*, *P. mucosa*, *P. taeniophora*), an area intensely subjected to intense anthropic pressures (Roque *et al.*, 2016; Boin *et al.*, 2019; Guerra *et al.*, 2020). This context highlights an urgency in elucidating taxonomic issues of *Pimelodella*, since taxonomic studies may directly impact species conservation.

The allometric effects observed in the body shape from external and osteological lateral views were considerably negligible. However, the allometric effect for the dorsal head shape was more pronounced. Therefore, allometric correction was exclusively conducted in analyses related to head shape in dorsal view. Despite the necessity of this adjustment, the influence of size on shape remained relativity low (11.0%). This result is probable attributable to the endeavor to only select adult specimens. While several studies have assessed allometric effects and employed adjustments (*e.g.*, Sidlauskas *et al.*, 2011; Arroyave *et al.*, 2020; Herrera-Collazos *et al.*, 2020; Cortés-Hernández, Ramírez-Gil, 2024), there are also certain investigations that have indicated a low influence of size on shape and proceeded with the analyses without correction (*e.g.*, White, 2009; Alhajeri *et al.*, 2019).

Our decision in working with adult specimens was in order to isolate the taxonomic differences from other sources of shape differences, such as ontogeny or sex. Despite few works reporting sex differences in heptapterids (*e.g.*, Mees, 1974; Souza-Shibatta, 2013; Pierre, Slobodian, 2024), ontogenetic changes were already suggested (*e.g.*, Eigenmann, 1917; Bockmann, Slobodian, 2013; Deprá, Slobodian, 2024). Overall, it is essential to at least examine these effects when conducting geometric morphometrics studies, as failing to correct for high allometry could jeopardize the analyses. Additionally, considering the employment of this adjustment is quite pertinent especially when investigating diverse taxonomic groups (Sidlauskas *et al.*, 2011; Klingenberg, 2016), and the decision of non-adjustment in the present work was due to the low allometry detected in our selection.

Overall, the findings presented herein that despite the partial superimposition in some axes of the data sets, the species vary significantly in shape, what can be observed statistically in the pairwise comparisons. Therefore, geometric morphometrics effectively recovered shape differences between some taxa, mainly along the PC1 axes (that retained most of the variance), despite the challenges for others. It is no surprise the species analyzed here superimpose in the morphospace. The delimitation difficulties are inherent to the genus, as can be observed in literature (Miranda Ribeiro, 1914; Eigenmann, 1917; Fowler, 1915, 1940, 1941; Britski *et al.*, 1999, 2007; Souza-Shibatta *et al.*, 2013; Slobodian, 2017; Cortés-Hernández, Ramírez-Gil, 2024), and are not different for the Upper rio Paraguai species.

The first works to try to distinguish these species were those of Britski *et al.* (1999, 2007), that listed six species of *Pimelodella* from Pantanal (*i.e.*, *Pimelodella gracilis*, *P. griffini*, *P. megalura*, *P. mucosa*, *P. notomelas*, *P. taenioptera*). Despite the great advancement to *Pimelodella* identification given by these works, the species were differentiated by characteristics related to the length of the dorsal lobe of the caudal fin and coloration features (*e.g.*, body stripes) (Britski *et al.*, 1999, 2007). Those traits, despite contributing to the delimitation of species alongside other diagnostic characters, usually overlap between part of *Pimelodella* species and cannot be successfully used exclusively. Furthermore, the presence of an elongated filamentous on the dorsal fin, also attributed as a diagnostic feature for *P. griffini,* (Britski *et al.*,1999, 2007), probably corresponds to a secondary sexual dimorphism trait presented in male adults (Dahl, 1961; Souza-Shibatta *et al.*, 2013; Pierre, Slobodian, 2024).

Based on Britski *et al.* (1999, 2007) diagnoses, Souza-Shibatta *et al.* (2013) identified four species of *Pimelodella* among material collected in the rio Miranda, in the Upper rio Paraguai basin, corresponding to *P. gracilis*, *P. griffini*, *P. megalura*, and *P. taenioptera*. However, analyses integrating cytogenetic, molecular, and morphological data revealed that the material comprised two species. Cytogenetic analyses verified two groups with distinct chromosomal numbers (2n = 46 and 2n = 52 chromosomes) and were corroborated by molecular and linear morphometrics data, which also recovered two groups encompassing the same specimens (Souza-Shibatta *et al.*, 2013): *Pimelodella griffini* and *P. taenioptera*. The authors highlighted that, despite the differentiation of the two groups, overlap existed between them regarding several body proportions. Posteriorly to this work, Slobodian (2017) revised the

material and suggested that *P. taenioptera* would probably be a junior-synonym of *P. gracilis,* meanwhile the specimens identified as *P. griffini* would indeed correspond to *P. taeniophora*.

Regarding the overlapping characteristics among *Pimelodella* species, Slobodian (2017) also evidenced that diagnostic characteristics related to meristic counts and linear morphometrics, as well as molecular data, generally intersect among numerous species, including those under investigation herein. In the case of *P. taenioptera*, for instance, the overlap of characteristics with *P. gracilis* was so elevated that a synonymization was proposed, with *P. taenioptera* being the junior synonym (Slobodian, 2017), and this synonymy was taken into account for the present work. Thus, the similarities in linear morphometric data between *P. taeniophora* and *P. gracilis* indicated by Souza-Shibatta *et al.* (2013) and Slobodian (2017) were also evidenced by the partial superimposition of both species in our morphospaces.

The variations in body shape in lateral view were primarily associated with the relative position of the dorsal and adipose fins, as well as body depth (Figs. 9, 13). These changes were evident along PC1 and PC3 axes in both external and osteological lateral views (Figs. 9A,C, 13A,C), suggesting they are relevant to taxonomic delimitation. Those characteristics are relevant to *Pimelodella* species delimitation, despite possible overlaps in the morphospace or linear morphometric ranges.

Other important characters were the body part proportions visualized by the vertebral relative position. It is evident, for instance, differences in the positions of the posterior end of the Weberian apparatus and of the 20th vertebra in relation to body length between *P. gracilis* and *P. mucosa*. In *P. gracilis* (as well as in *P. megalura*), the posterior end of the Weberian apparatus is positioned at the first one fourth of the body length, whereas in *P. mucosa*, it is situated at the first third of the body length (Fig. 13A). Meanwhile, the 20th vertebra is located midway between the snout and the compound caudal centrum (PU1+U1) in the former species, but at the posteriormost third of the body in the latter (Fig. 13A). Although vertebral counts are already used in species delimitation (*e.g.*, Slobodian 2017, Slobodian *et al*., 2017), this is the first work to integrate characteristics related to body proportion and vertebral count. We think this kind of data can be useful in *Pimelodella* taxonomy.

However, in PC2 (Figs. 9B, 13B), shape variations likely represent artifacts, possibly corresponding to fixation effects, such as the presence of bent specimens. This can be inferred by the relatively high variance (16.6% and 22.3% in external and osteological lateral views, respectively), meanwhile all species similarly superimpose in these axes. Given the absence of clear patterns among points in morphospace and the observable shifts in body curvature in the wireframes, it is possible that fixation or euthanasia methods influenced shape. The occurrences of some individuals being fixed with their mouths wide open may have impacted body shape variation, as landmark 1 might have been digitized in an elevated position. Further, an inadequate fixation may have resulted in an overall curved or bent body aspect. Despite the confounding influence of fixation on assessing shape changes, such effects were mostly captured in PC2, while PC1 and PC3 explained the variation related to biological variables (*i.e.*, species).

It is worth mentioning that, despite external and osteological lateral views summing up similar results regarding body shape, the osteological landmarks made clear some patterns, such as the elongation pattern of the body related to vertebral count, and facilitate the identification of shape changes regarding the head length and dorsal-fin insertions. Nevertheless, we can conclude that in the absence of radiographs, external lateral view landmarks can be gathered successfully for *Pimelodella*, but with a loss to the explanatory power of the differences in body shape along the axes.

Regarding the head dorsal view, despite the heightened overlap of species in the morphospace, analyses showed gradual delimitation along the PC1 axis, describing bulkier heads with longer supraoccipital processes in an extreme, to arrow-shaped ones with shorter supraoccipital processes in the other (Fig. 16A). This underscores that the analyzed species indeed share several similarities, as shown in their diagnostic features (Slobodian, 2017), although some distinctions in head shape can be visualized between them. For instance, some *Pimelodella* species were described or can be delimited by the shorter supraoccipital process length, *i.e.*, *P. bockmanni*, *P. itapicuruensis*, *P. leptosoma*, *P. longipinnis*, *P. megalura*, *P. metae*, *P. montana*, *P. peruensis*, *P. robinsoni*, *P. tapatapae*, *P. wolfi* and *P. yuncensis* (Fowler, 1914; Borodin, 1927; Fowler, 1941; Slobodian, 2017; Slobodian, Pastana, 2018).

In a similar pattern to the lateral view, the head dorsal view patterns observed in PC2 are also probably related to euthanasia or fixation artifacts. The euthanasia by asphyxiation can result in mouth and opercles wide open, what can be translated in the branchiostegal landmarks (11 and 12) so much wider in the negative extreme of PC2 than in the positive extreme. We can observe that this pattern of a wider posterior portion of the head is different from the "arrow-shaped" obtained in PC1, in which the landmarks related to branchiostegal rays are in similar positions in the two extremes of the axis. The shape changes recovered in PC3 (Fig. 16C) may also correspond to euthanasia or fixation artifacts, as no clear patterns can be observed in the morphospace (Fig. 15B).

Initially, 15 landmarks were selected for the X-ray images, and 14 for the photographs taken in dorsal view. In the former dataset, the landmark corresponding to the origin of the adipose fin (Fig. 3, letter a) was omitted from the final analyses due to difficulties in visualizing this area in numerous radiographs. As for the external dorsal view, the landmarks related to the insertion of pectoral-fin spine (Fig. 4, letters a and b) were also excluded. Differences in opened or closed pectoral fins were observed to exert influence on the shape change of this region, retaining much of the variation in PC1. Thereby, despite these landmarks possibly contributing to a better delimitation of shape, their inclusion in the analyses was not possible.

Pimelodella mucosa is the species that exhibited the most distinguishable shape among those examined. Its specimens feature a deeper body shape throughout their entire length, with dorsal and adipose fins notably located more distant from each other. Additionally, the terminus of the Weberian Complex is situated proportionally posteriorly compared to the other species, probably due to the bulkier head and body. This species comprises a deeper and continuous head shape, with the origin of the supraoccipital process positioned posteriorly on the head and its posterior tip near the dorsal-fin insertion.

Among the species of *Pimelodella*, *P. mucosa* stands out for a unique diagnostic trait, characterized by enlarged preoperculomandibular cephalic lateral-line canal openings (Eigenmann *et al.*, 1907; Aguilera, Azpelicueta, 2015; Slobodian, 2017). This feature is also observed to some degree in *P. serrata* and *P. longibarbata*, with the former occurring in the rio Madeira basin (Lauzanne, Loubens, 1985; Chernoff *et al.*,

2000; Bockmann, Slobodian, 2013), as well as in the Amazon basin (Cortés-Hernandez *et al.*, 2023), while the latter inhabits the western rio Orinoco basin (Cortés-Hernández *et al.*, 2020). Moreover, the adipose fin of *P. mucosa* is short, roughly 3.5 times in SL (Slobodian, 2017). This, combined with its more posterior positioning on the body, may contribute to the geometric morphometric findings concerning its greater distance from the dorsal fin.

Molecular analyses indicated that *P. mucosa* is more closely related to other genera of Heptapteridae than to *Pimelodella* (Slobodian, 2017). While Slobodian (2017) attributed this finding to a possible bias related to missing data, the author also underscored the morphological differences of *P. mucosa* from other *Pimelodella* species. Given that the specimens of *P. mucosa* were the most distinguishable in the morphospace presented here, it is reasonable to conclude that geometric morphometrics can corroborate with future taxonomic displacements of *P. mucosa*.

Specimens of *P. gracilis*, occupied the extreme opposite position of *P. mucosa* in the morphospace in external and osteological lateral views (Figs. 8, 12). *Pimelodella gracilis* exhibits a slender body shape, with dorsal and adipose fins closely positioned to each other. The head is proportionally shorter, which is consistent with the higher number of vertebrae in this species, *i.e.*, 46, rarely 45 (Slobodian, 2017). Nonetheless, the head in dorsal view resembled that of *P. mucosa* in shape, implying that while body shape may diverge markedly within some species, the head shape does not necessarily accompany the same pattern. In addition, the adipose fin of *P. gracilis* is very long, measuring slightly more than 2–2.5 times in SL (Slobodian, 2017), which may reflect in a closer proximity to the dorsal fin, as detected by geometric morphometrics. Therefore, notwithstanding the overlap, geometric morphometrics recovered an elongated body shape in *P. gracilis*, along with distinctive fin positions to facilitate species identification. The anal fin of *P. gracilis*, for instance, tends to be notably situated anterior to the adipose-fin terminus, suggesting the body elongation given by the higher number of vertebrae occurs more pronouncedly in the caudal peduncle.

The challenge of delimiting *P. gracilis* goes beyond geometric morphometrics. Linear morphometrics were also insufficient to separate *P. gracilis* from *P. cristata*, and molecular analyses have indicated *P. gracilis* might constitute a paraphyletic group,

even among specimens from the rio Paraguai basin (Slobodian, 2017). These analyses have recovered certain specimens of *P. gracilis* from the rio Paraguai basin as phylogenetically closer to *P. taeniophora*, while other from the rios Paraguai and Paraná basins were displayed closer to *P. avanhandavae* (Slobodian, 2017). Nevertheless, the author indicated that not all specimens had radiographs, and the identification of some *P. gracilis* based exclusively on external morphology might have been erroneous (Slobodian, 2017).

Pimelodella gracilis and *P. avanhandavae*, in general, share various similarities, with the number of vertebrae being the most distinctive trait (46, rarely 45 in *P. gracilis vs.* 41–45 in *P. avanhandavae*). However, counting vertebrae requires X-ray or CT scans images, or clearing and staining procedures, thereby introducing limitations into the identification process. The employment of geometric morphometrics to examine shape variation between both species could offer notably insights. Unfortunately, the reduced availability of specimens of *P. avanhandavae* has hindered their inclusion in the study.

Furthermore, geometric morphometrics detected that *P. griffini* mostly differed from *P. mucosa* and *P. gracilis*, while it appeared to share similarities in head shape with *P. megalura* (Figs. 8, 12, 15). *Pimelodella griffini* and *P. megalura* present a more arrow-shaped head with a narrower snout width. Despite the similarities in head shape, *P. megalura* presents a diagnostical characteristic that is unique among the *Pimelodella* species within the rio Paraguai basin, which is the supraoccipital process does not reach the pre-nuchal plate (Slobodian, 2017). Unfortunately, since the external morphology data could not accurately assess the posterior tip of the supraoccipital process, the analyses concerning the head region did not capture this variation. However, in the osteological lateral view, it is evident an anteriorly position of the anterior tip of the supraoccipital process relative to the negative extreme of the PC1 axis (Figure 13A), which may be attributable to the specimens of *P. megalura* also encompassing this extreme.

Pimelodella guato, in a general sense, shares several similarities with sympatric species of *Pimelodella*. Nonetheless, it stands as a relatively easy to identify species due to other attributes, such as the morphology of the pectoral-fin spine. One of the most difficult species to differentiate from *P. guato* is *P. taeniophora*, which, in fact, is

the species with the most pronounced overlaps with all other species. This difficulty in delimitating *P. taeniophora* is also reflected in its diagnose, wherein several diagnostic characters intersect with those of other species, such as the extent of the supraoccipital process, the lengths of maxillary barbel and adipose fin, and the number of vertebrae (Slobodian, 2017).

Indeed, during the identification of *Pimelodella* species from the rio Paraguai basin, discriminate *P. taeniophora* becomes a quite challenge due to the similarity of morphological characteristics. Such problem was noted in a study conducted by Souza-Shibatta *et al.* (2013), where specimens of *P. taeniophora* may have been misidentified as *P. griffini* (Slobodian, 2017). Despite some morphological differences between the two species (*e.g.*, *Pimelodella griffini* presenting a smaller adipose fin and a shorter maxillary barbel compared to *P. taeniophora*, as well as differences in pectoral-fin spine morphology), identifying them remains an arduous process, emphasizing the importance of employing complementary methods to facilitate their delimitation. However, despite all the endeavors, overlapping characteristics persist even in geometric morphometrics. In fact, when *P. taeniophora* is omitted from the analyses, the shape patterns become clearer in the morphospace for taxonomic delimitation (Fig. 17). In the dorsal view dataset, for instance, a dichotomy in morphospace becomes more discernible, with *P. gracilis*, *P. guato*, and *P. mucosa* occupying one extreme of PC1, while *P. griffini* and *P. megalura* are situated at the opposite extreme (Fig. 17C).

In a recent taxonomic investigation using geometric morphometrics to delimitate seven species of *Pimelodella* from rio Orinoco basin, the efficacy of this method varied, successfully separating some taxa while proving ineffective for others (Cortés-Hernández, Ramírez-Gil, 2024). The same landmarks investigated by Cortés-Hernández and Ramírez-Gil (2024) were applicable for the present work, except for the pelvic-fin insertion, as several specimens exhibited a swollen ventral region in lateral view. Their Canonical Variance Analyses (CVA) evidenced an overlap between *P. figueroai*, *P. megalops*, *P. metae*, and *Pimelodella* sp., while *P. longibarbata*, *P. cristata*, and *P. cruxenti* were discernible in the morphospace (Cortés-Hernández, Ramírez-Gil, 2024). The shape changes observed in our study corroborate with those presented in Cortés-Hernández and Ramírez-Gil (2024), with the most variable landmarks corresponding to the position and extent of adipose fin along the body.

The morphology of fishes is generally highly correlated to their functional traits (Wainwright, 1991, 2002), and body shape can be associated with swimming performance and strategies to mitigate energy costs (Pettersson, Hedenström, 2000; Ohlberger *et al.*, 2006). Ohlberger *et al.* (2006) compared shape differences and energetic costs between *Rutilus rutilus* (Linnaeus, 1758) and *Cyprinus carpio* Linnaeus, 1758. The latter one comprises a slander body and typically inhabits regions further upstream with high flow, while *C. carpio* encompasses a deeper body and is found in waters with lower flow (Ohlberger *et al.*, 2006). The authors asserted that a slander body is associated with faster and effective swimming, crucial for a life history in open aquatic environments (Ohlberger *et al.*, 2006). Conversely, a deeper body improves maneuvering capability, contributing to feeding habits in regions with dense vegetation (Ohlberger *et al.*, 2006).

Overall, the evolution of body shape in fish is correlated with other morphological features, including fins (Feilich, 2016). Adipose fin, despite being considerable for so long as a vestigial structure (Garstang, 1931), has been proved to be a functional and mechanosensitive trait (*e.g.*, Reimchen, Temple, 2004; Temple, Reimchen, 2008; Buckland-Nicks *et al.*, 2011; Aiello *et al.*, 2016). Studies suggest that adipose fins serve as precaudal flow sensors, supporting the coordination of caudal fin movements in turbulent flow regime, thereby contributing to swimming efficiency (Reimchen, Temple, 2004; Buckland-Nicks *et al.*, 2011). Furthermore, Temple and Reimchen (2008) correlated the presence of adipose fin with flow regimes within Siluriformes, indicating a more regular occurrence of adipose fins in species inhabiting areas with higher flow rates, such as streams and rivers.

Despite the lack of ecological and biological data regarding *Pimelodella* species, certain inferences can be drawn about shape variation. For instance, larger body sizes, coupled with elongated body shapes of *P. gracilis*, may be related to habitat aspects, probably with these organisms inhabiting water columns. On the other hand, smaller body sizes, combined with deeper body shape of *P. mucosa and P. griffini*, may be associated with marginal or benthonic habitat for these individuals. Furthermore, longer adipose fins may cover a substantial portion of the dorsal profile, while shorter adipose fins may be positioned more anteriorly or posteriorly on the body. In the latter scenario, and considering the hypothesis of a precaudal flow sensors function of the adipose fin, it is reasonable to assume that it would be situated more posteriorly (as

detected by geometric morphometrics) and, consequently, closer to the caudal fin. Nevertheless, all these inferences are based on studies concerning other taxa. Thus, a comprehensive understanding of the relations between the morphology of *Pimelodella* species with their functional traits demands investigations specifically focusing on these species.

Conclusions

Geometric morphometrics has proven to be an efficient method to recover shape variation and delimit certain species of *Pimelodella*, such as *P. mucosa,* from all the other species, as well as *P. gracilis* from *P. griffini*. Body shape primarily varied in terms of depth, describing either deeper or slender bodies, as well as the position of the adipose fin. Differences were also observed in the head, with some species displaying a bulkier or arrow-like shape, along with variations in supraoccipital process length. While linear morphometrics and meristic data can be used to delimited species in the group (Slobodian, 2017), a significant portion of the data obtained from geometric morphometrics complemented the previous delimitation, such as the relative positions of the dorsal and adipose fins, and also helped in explain and discuss body shape changes. The results presented herein complement the linear morphometrics data investigated by Slobodian (2017), demonstrating that the anatomical characters suggested by that study translate into a general change in body shape.

In summary, delimiting *Pimelodella* species involves a combination of characteristics that may overlap, to some extent, between species. Therefore, employing diverse methods is essential to gradually elucidate these issues. It would be quite interesting to, in the future, use geometric morphometrics to investigate shape differences between *P. gracilis* and *P. avanhandavae*, with a larger sample of the latter one.

Chapter 2

A new species of *Pimelodella* (Siluriformes: Heptapteridae) from the Paraguai basin, Brazil, with a discussion regarding its distribution

Disposed in Appendix I.

Conclusões gerais

As descrições e delimitações das espécies de *Pimelodella* têm sido tradicionalmente baseadas em características de morfologia externa, morfometria linear, dados merísticos e na coloração dos espécimes. No entanto, diversas dessas características diagnósticas apresentam sobreposições consideráveis entre as espécies, dificultando no processo de identificação. Nesse contexto, o emprego da morfometria geométrica como ferramenta complementar pode auxiliar a elucidar essas questões taxonômicas. Apesar de *P. guato* ter sido descrita somente a partir dos métodos tradicionais mencionados acima, a morfometria geométrica auxiliou na compreensão da sua distinção de outras espécies, revelando diferenças de forma entre *P. guato, P. mucosa*, *P. gracilis*, e *P. griffini* na morfologia externa do corpo, assim como diferenças entre *P. guato*, *P. megalura,* e *P. taeniophora* na morfologia externa da cabeça. Considerando os problemas contemporâneos relacionados à perda de biodiversidade, assim como as elevadas pressões antrópicas que afetam o Pantanal, conhecer a diversidade de *Pimelodella* é essencial para a conservação do grupo na bacia do Alto rio Paraguai.

Referências Bibliográficas

Abiadh A, Colangelo P, Capanna E, Lamine-Cheniti T, Chetoui M. Morphometric analysis of six *Gerbillus* species (Rodentia, Gerbillinae) from Tunisia. C R Biol. 2010; 333(9)680–87. https://doi.org/10.1016/j.crvi.2010.07.003

Adams D, Collyer M, Kaliontzopoulou A, Baken E. Geomorph: software for geometric morphometric analyses, R package version 4.0.6. 2023. https://cran.r-project.org/package=geomorph

Adams DC, Rohlf FJ, Slice DE. Geometric morphometrics: Ten years of progress following the 'revolution'. Ital J Zool. 2004; 71(1):5–16. http://dx.doi.org/10.1080/11250000409356545

Aguilera, G, Azpelicueta MM. First record of *Pimelodella mucosa* Eigenmann & Ward, 1907 (Siluriformes: Heptapteridae) in Formosa, Argentina and comments on the geographical distribution of *P. howesi* Fowler, 1940. Check List. 2015; 11(5):1757. https://doi.org/10.15560/11.5.1757

Aiello BR, Stewart TA, Hale ME. Mechanosensation in an adipose fin. Proc R Soc B. 2016; 283: 20152794. http://dx.doi.org/10.1098/rspb.2015.2794

Alhajeri BH, Alaqeely R, Alhaddad H. Classifying camel breeds using geometric morphometrics: A case study in Kuwait. Livest Sci. 2019; 230:103824. https://doi.org/10.1016/j.livsci.2019.103824

Allan JD, Abell R, Hogan ZS, Revenga C, Taylor BW, Welcomme RL, Winemiller K. Overfishing of inland waters. BioScience. 2005; 55(12):1041–51. https://doi.org/10.1641/0006-3568(2005)055[1041:OOIW]2.0.CO;2

ANA, GEF, PNUMA, OEA. Programa de Ações Estratégicas para o Gerenciamento Integrado do Pantanal e Bacia do Alto Paraguai – PAE – Relatório Final. Brasília: TODA Desenho & Arte Ltda [Internet]; 2004. Available from: https://arquivos.ana.gov.br/projetos/gefpantanal/PAE_Pantanal_PT.pdf

Albert JS, Tagliacollo VA, Dagosta F. Diversification of Neotropical Freshwater Fishes. Annu Rev Ecol Evol Syst. 2020; 51:27–53. https://doi.org/10.1146/annurev-ecolsys-011620031032

Anjos MS, Bitencourt JA, Nunes LA, Sarmento-Soares LM, Carvalho DC, Armbruster JW, Affonso PRAM. Species delimitation based on integrative approach suggests reallocation of genus in *Hypostomini* catfish (Siluriformes, Loricariidae). Hydrobiologia. 2019; 847:563–578. https://doi.org/10.1007/s10750-019-04121-z

Argolo LA, López-Fernández H, Batalha-Filho H, Affonso PRAM. Unraveling the systematics and evolution of the *'Geophagus' brasiliensis* (Cichliformes: Cichlidae) species complex. Mol Phylogenet Evol. 2020; 150:106855. https://doi.org/10.1016/j.ympev.2020.106855

Arredondo NJ, Núñez MCO. A new species of *Parspina* Pearse, 1920 (Digenea: Cryptogonimidae) from *Pimelodella gracilis* (Valenciennes) (Siluriformes: Heptapteridae) in the Paraná River basin, Argentina, and a key to the genus. Syst Parasitol. 2013; 84:81–7. https://doi.org/10.1007/s11230-012-9394-3

Arroyave J, Cruz-Fernández DA. Genetic and morphological evidence cast doubt on the validity of Mexican troglobitic species of the Neotropical catfish genus *Rhamdia* (Siluriformes: Heptapteridae). Rev Mex Biodivers. 2021; 92(2021):e923718. https://doi.org/10.22201/ib.20078706e.2021.92.3718

Arroyave J, Martinez CM, Martínez-Oriol FH, Sosa E, Alter SE. Regional-scale aquifer hydrogeology as a driver of phylogeographic structure in the Neotropical catfish *Rhamdia guatemalensis* (Siluriformes: Heptapteridae) from cenotes of the Yucatán Peninsula, Mexico. Freshw Biol. 2021; 66(2):332–48. https://doi.org/10.1111/fwb.13641

Assine ML, Merino ER, Pupim FN, Warren LV, Guerreiro RL, McGlue MM. Geology and geomorphology of the Pantanal Basin. In: Bergier I, Assine ML, editors. Dynamics of the Pantanal wetland in South America. Switzerland: Springer; 2016. p.23–50.

Baken E, Collyer M, Kaliontzopoulou A, Adams D. Geomorph v4.0 and gmShiny: enhanced analytics and a new graphical interface for a comprehensive morphometric experience. Methods Ecol Evol. 2021; 12:2355–63. https://doi.org/10.1111/2041-210X.13723

Barreto SB, Silva AT, Batalha-Filho H, Affonso PRAM, Zanata AM. Integrative approach reveals a new species of *Nematocharax* (Teleostei: Characidae). J Fish Biol. 2018; 93(6):1151–62. https://doi.org/10.1111/jfb.13834

Barreto SB, Nunes LA, Silva AT, Jucá-Chagas R, Diniz D, Sampaio I, Schneider H, Affonso PRAM. Is *Nematocharax* (Actinopterygii, Characiformes) a monotypic fish genus? Genome. 2016; 59(10):1–15. https://doi.org/10.1139/gen-2015-0166

Barros NHC, Nascimento WS, Araújo AS, Gurgel LL, Chellappa S. Aspectos reprodutivos de *Pimelodella gracilis* (Valenciennes, 1835) (Osteichthyes: Pimelodidae) do açude da Ecoregião Caatinga. Biota Amazôn. 2011; 1(2):53–9.

Bichuette ME, Rantin B, Hingst-Zaher E, Trajano E. Geometric morphometrics throws light on evolution of the subterranean catfish *Rhamdiopsis krugi* (Teleostei: Siluriformes: Heptapteridae) in eastern Brazil. Biol J Linn Soc. 2014; 114:136–51. https://doi.org/10.1111/bij.12405

Birindelli JLO, Zanata AM, Lima FCT. *Hypostomus chrysostiktos*, a new species of armored catfish (Siluriformes: Loricariidae) from rio Paraguaçu, Bahia State, Brazil. Neotrop Ichthyol. 2007; 5(3):271–78. https://doi.org/10.1590/S1679-62252007000300006

Bleeker P. De visschen van den Indischen Archipel. Beschreven en toegelicht. Siluri. Acta Societatis Regiae Scientiarum Indo-Neêrlandicae. 1858; 4(art. 2):i-xii+1–370.

Bockmann FA. Análise filogenética da família Heptapteridae (Teleostei, Ostariophysi, Siluriformes) e redefinição de seus gêneros. [Unpublished PhD thesis]. São Paulo: Universidade de São Paulo; 1998.

Bockmann FA, Castro RMC. The blind catfish from the caves of Chapada Diamantina, Bahia, Brazil (Siluriformes: Heptapteridae): description, anatomy, phylogenetic relationships, natural history, and biogeography. Neotrop Ichthyol. 2010; 8(4):673–706. https://doi.org/10.1590/S1679-62252010000400001

Bockmann FA, Guazzelli GM. Family Heptapteridae (Heptapterids). In: Reis RE, Kullander SO, Ferraris Jr. CJ, editors. Checklist of the freshwater fishes of South and Central America. Porto Alegre: Edipucrs; 2003. p.406–31.

Bockmann FA, Slobodian V. Family Heptapteridae: Three-barbeled Catfishes. In: van der Sleen P, Albert JS, editors. Field Guide to the fishes of the Amazon, Orinoco & Guianas. New Jersey: Princeton University Press; 2018. p.233–52.

Bockmann FA, Slobodian V. Heptapteridae. In: Queiroz LJ, Torrente-Vilara G, Ohara WM, Pires THS, Zuanon J, Doria CRC, editors. Peixes do rio Madeira. São Paulo: Dialeto Latin America Documentary; 2013. p.14–77.

Boin MN, Martins PCS, Silva CA, Salgado AAR. The Pantanal: The Brazilian wetlands. In: Salgado AAR, Santos LJC, Paisani JC, editors. The physical geography of Brazil: environment, vegetation and landscape. Switzerland: Springer Nature Switzerland AG; 2019. p.75–91.

Bookstein FL. Morphometric tools for landmark data. Nova York: Cambridge University Press; 1991.

Borodin NA. Some new catfishes from Brazil. Am Mus Novit. 1927; 266:1–7.

Breck JE. Body composition in fishes: body size matters. Aquaculture. 2014; 433:40–9. https://doi.org/10.1016/j.aquaculture.2014.05.049

Britski HA, Silimon KZS, Lopes BS. Peixes do Pantanal: manual de identificação. Brasília: Embrapa-SPI; 1999.

Britski HA, Silimon KZS, Lopes BS. Peixes do Pantanal: manual de identificação, 2ed. Brasília: Embrapa-SPI; 2007.

Buckland-Nicks JA, Gillis M, Reimchen TE. Neural network detected in a presumed vestigial trait: ultrastructure of the salmonid adipose fin. Proc R Soc B. 2011; 279(1728):553–63. https://doi.org/10.1098/rspb.2011.1009

Carvalho NO. Hidrologia da bacia do Alto Paraguai. In: Simpósio sobre Recursos Naturais e Socioeconômicos do Pantanal. Corumbá: Anais... Brasília: Embrapa-DDT; 1986. p.43–49.

Carvalho TP, Albert JS. The Amazon-Paraguay divide. In: Albert JS, Reis RE, editors. Historical biogeography of neotropical freshwater fishes. Berkeley: University of California Press; 2011. p.193–202.

Castello HP. *Pimelodella griffini* (Pisces, Pimelodidae) nueva cita para la fauna argentina: Consideraciones acerca de la alimentación, del sistema reproductor y de una papila urogenital en tres especies del género *Pimelodella*. Physis. 1969; 28(77):407–15.

Chernoff B, Machado-Allison A, Willink P, Sarmiento J, Barrera S, Menezes N, Ortega H. Fishes of three Bolivian rivers: Diversity, distribution and conservation. Interciencia. 2000; 25(6):273–83. https://doi.org/10.13140/2.1.2308.1607

Chiozzi G, Stiassny MLJ, Marchi G, Lamboj A, Fasola M, Fruciano C. A diversified kettle of fish: phenotypic variation in the endemic cichlid genus *Danakilia* of the Danakil Depression of northeastern Africa. Biol J Linn Soc. 2018; 124(4):690–705. https://doi.org/10.1093/biolinnean/bly085

Collyer M, Adams D. RRPP: an R package for fitting linear models to high-dimensional data using residual randomization. Methods Ecol Evol. 2018; 9:1772–79. https://doi.org/10.1111/2041-210X.13029

Collyer M, Adams D. RRPP: Linear Model Evaluation with Randomized Residuals in a Permutation Procedure, R package version 1.4.0. 2023. https://cran.r-project.org/package=RRPP

Conde-Saldaña CC. História evolutiva do gênero *Pimelodella* Eigenmann & Eigenmann, 1888 na região transandina e caracterizacão citogenética de uma população no Alto Magdalena, Colômbia. Viçosa: Universidade Federal de Viçosa; 2016.

Conde-Saldaña CC, Albornoz-Garzón JG, García-Melo JE, Dergam JA, Villa-Navarro FA. A new species of *Pimelodella* Eigenmann & Eigenmann, 1888 (Siluriformes: Heptapteridae) from the Sierra Nevada de Santa Marta, Colombia. Zootaxa. 2019; 4668(4):562–74. https://doi.org/10.11646/zootaxa.4668.4.8

Cortés-Hernández MÁ, DoNascimiento C, Ramírez-Gil H. A new species of *Pimelodella* Eigenmann & Eigenmann, 1888 (Siluriformes: Heptapteridae) from the Orinoco River basin. Zootaxa. 2020; 4808(3):491–506. https://doi.org/10.11646/zootaxa.4808.3.5

Cortés-Hernández MÁ, Méndez-López A, DoNascimiento C. New records of *Pimelodella* (Siluriformes, Heptapteridae) from Colombia for the Amazon River basin, and redescription of *P. serrata*. Zootaxa. 2023; 5293(1):185–95. https://doi.org/10.11646/zootaxa.5293.1.10

Cortés-Hernández MA, Ramírez-Gil H. Morfometría geométrica de especies de peces tropicales del género *Pimelodella* (Heptapteridae) de la Orinoquía. Acta biol Colomb. 2024; 29(1):93–8. https://doi.org/10.15446/abc.v29n1.105682

Craig JM, Correa-Roldán V, Ortega H, Crampton WGR, Albert JS. Revision of *Gymnotus* (Gymnotiformes: Gymnotidae) from the Upper Madeira Basin of Bolivia and Peru, with descriptions of two new species. Zootaxa. 2018a; 4413(1):111–32. https://doi.org/10.11646/zootaxa.4413.1.3

Craig JM, Crampton WGR, Albert JS. Revision of the polytypic electric fish *Gymnotus carapo* (Gymnotiformes, Teleostei), with descriptions of seven subspecies. Zootaxa. 2017; 4318(3):401–38. https://doi.org/10.11646/zootaxa.4318.3.1

Craig JM, Malabarba LR, Crampton WGR, Albert JS. Revision of Banded Knifefishes of the *Gymnotus carapo* and *G. tigre* clades (Gymnotidae Gymnotiformes) from the Southern Neotropics. Zootaxa. 2018b; 4379(1):47–73. https://doi.org/10.11646/zootaxa.4379.1.3

Cruz-Aguero J, Vergara-Solana FJ, García-Rodríguez FJ. Geometric morphometrics support the proposed molecular taxonomy for three *Eucinostomus* species (Perciformes: Gerreidae) along the coasts of Mexico. Zoomorphology. 2015; 134:125–34. https://doi.org/10.1007/s00435-014-0237-4

Cuvier G. Le Règne Animal distribué d'après son organisation pour servir de base à l'histoire naturelle des animaux et d'introduction à l'anatomie comparée. Les reptiles, les poissons, les mollusques et les annélides. A. Belin, Paris; 1816.

Cuvier G, Valenciennes A. Histoire naturelle des poissons. Tome quinzième. Suite du livre dix-septième. Siluroïdes. v. 15; 1840

Cuvier G, Valenciennes A. Histoire naturelle des poissons. Tome vingt-deuxième. Suite du livre vingt-deuxième. Suite de la famille des Salmonoïdes; 1850.

Dagosta FC, de Pinna MC. The fishes of the Amazon: distribution and biogeographical patterns, with a comprehensive list of species. Bull Am Mus Nat Hist. 2019; 431:1–163. https://doi.org/10.1206/0003-0090.431.1.1

Dahl G. Nematognathous fishes collected during the Macarena Expedition 1959. Dedicated to the memory of the Colombian ichthyologist, Doctor Ricardo Lozano. Decd May 23rd, 1959. Part II: Pimelodidae, Callophysidae. Novedades Colombianas. 1961; 1(6):483–514.

Davies AMC, Fearn T. Back to basics: the principles of principal component analysis. Spectrosc Eur. 2004; 16(6):20–3.

Deprá GC, Slobodian V. Redescription of *'Chasmocranus' brachynema* (Heptapteridae: Heptapterini). Neotrop Ichthyol. 2024; 22(1):e230091. https://doi.org/10.1590/1982-0224-2023-0091

Dudgeon D, Arthington AH, Gessner MO, Kawabata Z-I, Knowler DJ, Lévêque C, Naiman RJ, Prieur-Richard A-H, Soto D, Stiassny MLJ, Sullivan CA.

Freshwater biodiversity: importance, threats, status and conservation challenges. Biol Rev. 2006; 81(2):163–82. https://doi.org/10.1017/S1464793105006950

Ecologia e Ação – Ecoa. Represas na Bacia do Alto Paraguai (BAP). ArcGIS [Internet]; 2024. Available from: https://www.arcgis.com/home/item.html?id=ef58538671604b838a9ed5e976b4e82f

Eigenmann CH. *Pimelodella* and *Typhlobagrus*. Mem Carnegie Mus. 1917; 7(4):229–58. https://doi.org/10.5962/bhl.title.12518

Eigenmann CH. The fishes of Lake Valencia, Caracas, and of the Rio Tuy at El Concejo, Venezuela. Indiana University Studies. 1920; 7(44):1–13. https://www.biodiversitylibrary.org/part/241557

Eigenmann CH. The freshwater fishes of British Guiana, including a study of the ecological grouping of species, and the relation of the fauna of the plateau to that of the lowlands. Mem Carnegie Mus. 1912; 5(1):1–578. https://www.biodiversitylibrary.org/page/7752475#page/35/mode/1up

Eigenmann CH, Allen WR. Fishes of Western South America. I. The intercordilleran and Amazonian lowlands of Peru. II.- The high pampas of Peru, Bolivia, and northern Chile. With a revision of the Peruvian Gymnotidae, and of the genus *Orestias*. University of Kentucky; 1942.

Eigenmann CH, Eigenmann RS. Preliminary notes on South American Nematognathi I. Proc Calif Acad Sci (Series 2). 1888; 1(2):119–72.

Eigenmann CH, McAtee WL, Ward DP. On further collections of fishes from the Paraguay. Ann Carnegie Mus. 1907; 4(2):110–57. https://doi.org/10.5962/p.264300

Eigenmann CH, Norris AA. Sobre alguns peixes de S. Paulo, Brazil. Rev Mus Paul. 1900; 4:349–62.

Evin A, Baylac M, Ruedi M, Mucedda M, Pons JM. Taxonomy, skull diversity and evolution in a species complex of *Myotis* (Chiroptera: Vespertilionidae): a geometric morphometric appraisal. Biol J Linn Soc. 2008; 95:529–538. https://doi.org/10.1111/j.1095-8312.2008.01076.x

Fadda C, Corti M. Three-dimensional geometric morphometrics of *Arvicanthis*: implications for systematics and taxonomy. J Zool Syst Evol Research. 2001; 39(2001):235–45. https://doi.org/10.1046/j.1439-0469.2001.00169.x

Faustino-Fuster DR, Meza-Vargas V, Lovejoy NR, Lujan NK. Multi-locus phylogeny with dense Guiana Shield sampling supports new suprageneric classification of the neotropical three-barbeled catfishes (Siluriformes: Heptapteridae). Mol Phylogenetics Evol. 2021; 162:107186. https://doi.org/10.1016/j.ympev.2021.107186

Feilich KL. Correlated evolution of body and fin morphology in the cichlid fishes. Evolution. 2016; 70(10): 2247–67. https://doi.org/10.1111/evo.13021

Fernandes CA, Damásio JF, Guterres ZR, Abelha MCF. Cytogenetic studies in two species of genus *Pimelodella* (Teleostei, Siluriformes, Heptapteridae) from

Iguatemi River Basin, Brazil. Cytologia. 2013; 78(1):91–5. https://doi.org/10.1508/cytologia.78.91

Fernández-Yépez, A. Algunos peces del Rio Autana. Novedades Cientificas, Contribuciones Ocasionales del Museo de Historia Natural La Salle, Serie Zoológica. 1950; 2:1–18, pls. 1–3.

Ferraris CJ. Checklist of catfishes, recent and fossil (Osteichthyes: Siluriformes), and catalogue of siluriform primary types. Zootaxa. 2007; 1418(1):1–628. https://doi.org/10.11646/zootaxa.1418.1.1

Feulner PGD, Kirschbaum F, Mamonekene V, Ketmaier V, Tiedemann R. Adaptive radiation in African weakly electric fish (Teleostei: Mormyridae: *Campylomormyrus*): a combined molecular and morphological approach. J Evol Biol. 2007; 20(1):403–14. https://doi.org/10.1111/j.1420-9101.2006.01181.x

Fowler HW. A collection of fresh-water fishes obtained in eastern Brazil by Dr. Rodolpho von Ihering. Proc Acad Nat Sci Phila. 1941; 93:123–99. https://www.jstor.org/stable/4064332

Fowler HW. Fishes from the Rupununi River, British Guiana. Proc Acad Nat Sci Phila. 1914; 66:229–84. https://www.jstor.org/stable/4063634

Fowler HW. Notes on nematognathous fishes. Proc Acad Nat Sci Phila. 1915; 67:203–43.

Fowler HW. Zoological results of the second Bolivian expedition for the Academy of Natural Sciences of Philadelphia, 1936-1937, Part I.--The fishes. Proc Acad Nat Sci Phila. 1940; 92:43–103. https://www.jstor.org/stable/4064303

Fricke R, Eschmeyer WN, Van der Laan R. Eschmeyer's catalog of fishes: genera, species, references [Internet]. San Francisco: California Academy of Sciences; 2024. Available from: http://researcharchive.calacademy.org/research/ichthyology/catalog/fishcatmain.asp

Fruciano C. Measurement error in geometric morphometrics. Dev Genes Evol. 2016; 226:139–58. https://doi.org/10.1007/s00427-016-0537-4

Galdino S, Vieira LM, Pellegrin LA. Impactos Ambientais Socioeconômicos na Bacia do rio Taquari – Pantanal. Corumbá: Embrapa Pantanal; 2006.

García-Rodríguez FJ, Chollet-Villalpando JG, Martínez-Guevara A, Cruz-Agüero J. Supporting the existence of two isolated evolutionary lineages of *Gerres* (Perciformes: Gerreidae) in America. Zool Scr. 2019; 48(4):466–81. https://doi.org/10.1111/zsc.12352

Garstang W. A phyletic classification of Teleostei. Proc Leeds Philos Lit Soc Sci Sect. 1931; 2:240–61.

Gill TN. Synopsis of the fresh water fishes of the western portion of the island of Trinidad, W. I. Ann Lyceum Nat Hist New York. 1858; 6(10–13, art.38):363–430. https://www.biodiversitylibrary.org/page/16023971#page/395/mode/1up

Gimênes-Junior H, Rech R. Guia ilustrado dos peixes do Pantanal e entorno. Campo Grande: Julien Design; 2022. Available from: https://www.imasul.ms.gov.br/wp-

content/uploads/2022/11/Montagem-livro-Peixes-VERSAO-FINALMARCO-2022-ISBN97865-81066-05-5-ONLINE_FINAL-1.pdf

Goodall C. Procrustes methods in the statistical analysis of shape. J R Statist Soc B. 1991; 53(2):285–339.

Guazzelli GM. Relações filogenéticas do gênero *Pimelodella* Eigenmann & Eigenmann 1888 (Siluriformes, Pimelodidae). [Unpublished PhD Thesis]. São Paulo: Universidade de São Paulo; 2003.

Guazzelli GM. Revisão das espécies de *Pimelodella* Eigenmann & Eigenmann 1888 (Teleostei: Siluriformes: Pimelodidae) dos sistemas costeiros do Sul e Sudeste do Brasil. [Unpublished Msc. dissertation]. Porto Alegre: Pontifícia Universidade Católica do Rio Grande do Sul; 1997.

Guerra A, Oliveira PTS, Roque FO, Rosa IMD, Ochao-Quintero JM, Guariento RD, Colman CB, Dib V, Maioli V, Strassburg B, Garcia LC. The importance of Legal Reserves for protecting the Pantanal biome and preventing agricultural losses. J Environ Manage. 2020; 260:110128. https://doi.org/10.1016/j.jenvman.2020.110128

Güntert H. Beschreibung einiger zum Teil noch unbekannter südamerikanischer Siluriden aus dem Naturhistorischen Museum in Basel. Zool Anz. 1942; 138(1/2):27–40.

Günther A. Catalogue of the Fishes in the British Museum, vol. 5: Catalogue of the Physostomi, containing the families Siluridae, Characinidae, Haplochitonidae, Sternoptychidae, Scopelidae, Stomiatidae in the collection of the British Museum, Trustees, London, xxii + 455 p. 1864.

Hakamada KYP, Penha J. Occupancy dynamics in small-stream habitats: niches define the responses to floods by two neotropical fishes. Popul Ecol. 2014; 56:139–50. https://doi.org/10.1007/s10144-013-0395-0

Harvey, B.C., Stewart, A.J. Fish size and habitat depth relationships in headwater streams. Oecologia. 1991; 87:336–42. https://doi.org/10.1007/BF00634588

Herrera-Collazos EE, Galindo-Cuervo AM, Maldonado-Ocampo JA, Rincón-Sandoval M. Three new species of the *Eigenmannia trilineata* species group (Gymnotiformes: Sternopygidae) from northwestern South America. Neotrop ichthyol. 2020; 18(1):e180085. https://doi.org/10.1590/10.1590/1982-0224-2018-0085

ICMBio. Livro Vermelho da Fauna Brasileira Ameaçada de Extinção, v. 6. Brasilia: Instituto Chico Mendes de Conservação da Biodiversidade; 2018.

Ihering R von. Diversas especies novas de peixes nemathognathas do Brazil. Notas preliminares. Rev Mus Paul. 1907; 1(fasc 1):13–39.

IUCN. The IUCN Red List of Threatened Species, Version 2023-1 [Internet]. 2024. Available from: https://www.iucnredlist.org

James FC, McCulloch CE. Multivariate analysis in ecology and systematics: panacea or Pandora's box? Annu Rev Ecol Syst. 1990; 21(1):129–66. https://doi.org/10.1146/annurev.es.21.110190.001021

Jaramillo-o N, Dujardin JP, Calle-Londoño D, Fonseca-González I. Geometric morphometrics for the taxonomy of 11 species of *Anopheles* (*Nyssorhynchus*) mosquitoes. Med Vet Entomol. 2014; 29(1):26–36. https://doi.org/10.1111/mve.12091

Jolliffe IT. Principal Component Analysis: a beginner's guide – I. Introduction and application. Weather. 1990; 45(10):375–82. https://doi.org/10.1002/j.1477-8696.1990.tb05558.x

Kaliontzopoulou A. Geometric morphometrics in herpetology: modern tools for enhancing the study of morphological variation in amphibians and reptiles. Basic Appl Herpetol. 2011; 25:5–32. https://doi.org/10.11160/bah.11016

Kendall D. Shape manifolds, procrustean metrics, and complex projective spaces. Bull London Math Soc. 1984; 16:81–121.

Kendall D. The diffusion of shape. Adv Appl Probab. 1977; 9:428–430.

Klingenberg CP. MorphoJ: an integrated software package for geometric morphometrics. Mol Ecol Resour. 2011; 11:353–57. https://doi.org/10.1111/j.1755-0998.2010.02924.x

Klingenberg CP. Size, shape, and form: concepts of allometry in geometric morphometrics. Dev Genes Evol. 2016; 226:113–37. https://doi.org/10.1007/s00427-016-0539-2

Klingenberg CP. Visualizations in geometric morphometrics: how to read and how to make graphs showing shape changes. Hystrix, It J Mamm. 2013; 24(1):15–24. https://doi.org/10.4404/hystrix-24.1-7691

Kner R. Ichthyologische Beiträge. II. Abtheilung. Sitzungsberichte der Kaiserlichen Akademie der Wissenschaften. Math-Naturwiss Kl. 1858; 26(s.373):373–448.

Koerber S, Vera-Alcaraz HS, Reis RE. Checklist of the fishes of Paraguay (CLOFPY). ICP. 2017; 53:1–99. https://pecescriollos.de/icp-journal/

Lacepède BGE. Histoire naturelle des poisons. Paris: Plassan; 1803.

Lauzanne L, Loubens G. Peces del rio Mamoré. Paris: ORSTOM; 1985.

Leaché AD, Kooa MS, Spencera CL, Papenfussa TJ, Fisherb RN, McGuirea JA. Quantifying ecological, morphological, and genetic variation to delimit species in the coast horned lizard species complex (*Phrynosoma*). PNAS. 2009; 106(30):12418–23. https://doi.org/10.1073/pnas.0906380106

Linnaeus, C. Systema Naturae, Ed. X (Systema naturae per regna tria naturae, secundum classes, ordines, genera, species, cum characteribus, differentiis, synonymis, locis. Tomus I. Editio decima, reformata). Holmiae. 1758; 1:i-ii+1-824.

López HL, Miquelarena AM, Menni RC. Lista comentada de los peces continentales de la Argentina. ProBiota. 2003; 5:1–85. https://ri.conicet.gov.ar/handle/11336/32592

López RB, Castello HP. *Eigenmannia trilineata* (Teleostomi, Sternopyginae) nueva especie hallada en el Rio de la Plata. Comunicaciones del Museo Argentino de Ciencias Naturales "Bernardino Rivadavia" e Instituto Nacional de Investigación de las Ciencias Naturales, Zoológia, Buenos Aires. 1966; 4(2):7–12.

Lundberg JG, McDade LA. On the South American catfish *Brachyrhamdia imitator* Myers (Siluriformes, Pimelodidae), with phylogenetic evidence for a large intrafamilial lineage. Not Nat. 1986; 463:1–24.

Maderbacher M, Bauer C,Herler J, Postl L, Makasa L, Sturmbauer C. Assessment of traditional versus geometric morphometrics for discriminating populations of the *Tropheus moorii* species complex (Teleostei: Cichlidae), a Lake Tanganyika model for allopatric speciation. J Zool Syst Evol Res. 2007; 46(2):153–61. https://doi.org/10.1111/j.1439-0469.2007.00447.x

Marcus LF. Traditional morphometrics. In: Rohlf FJ, Bookstein FL, editos. Proceedings of the Michigan morphometrics workshop. Ann Arbor: The University of Michigan Museum of Zoology; 1990. p.77–122.

Mees GF. The Auchenipteridae and Pimelodidae of Suriname (Pisces, Nematognathi). Zool Verh. 1974; 132:1–256, pls.1–15.

Menecozi AR. O que é o meandro de um rio? [Internet]. Campo Grande: Instituto Histórico e Geográfico de Mato Grosso do Sul; 2015. Available from: https://ihgms.org.br/vc-sabia/o-que-e-o-meandro-de-um-rio-186

Miranda Ribeiro A. Pimelodidae, Trachycorystidae, Cetopsidae, Bunocephalidae, Auchenipteridae, e Hypophthalmidae. In: Commissào de Linhas Telegraphicas Estrategicas de Matto-Grosso ao Amazonas. Annexo 5:1–13, pls.1–2; 1914.

Miranda Ribeiro A. Tres generos e dezesete especies novas de peixes Brasilieros. Rev Mus Paul. 1918; 10:631–46.

Miranda Ribeiro P. Tipos das espécies e subespécies do Prof. Alipio de Miranda Ribeiro depositados no Museu Nacional. Arq Mus Nac (Rio de J). 1953; 42:389–417. https://www.biodiversitylibrary.org/bibliography/6524

Mirande JM, Koerber S. Checklist of the freshwater fishes of Argentina (CLOFFAR). ICP. 2015; 36:1–68.

Mirande JM, Koerber S. Checklist of the freshwater fishes of Argentina (CLOFFAR-2). ICP. 2020; 72:1–81. https://pecescriollos.de/icp-journal/

Mitteroecker P, Gunz P. Advances in Geometric Morphometrics. Evol Biol. 2009; 36:235–47. https://doi.org/10.1007/s11692-009-9055-x

Mitteroecker P, Gunz P, Windhager S, Schaefer K. A brief review of shape, form, and allometry in geometric morphometrics, with applications to human facial morphology. Hystrix. 2013; 24:59–66. https://doi.org/10.4404/hystrix-24.1-6369

Mitteroecker P, Schaefer K. Thirty years of geometric morphometrics: Achievements, challenges, and the ongoing quest for biological meaningfulness. Yearbook Biol Anthropol. 2022; 178(S74):181–210. https://doi.org/10.1002/ajpa.24531

MMA - Ministério do Meio Ambiente. Portaria nº 148, de 7 de junho de 2022. Altera os Anexos da Portaria nº 443, de 17 de dezembro de 2014, da Portaria nº 444, de 17 de dezembro de 2014, e da Portaria nº 445, de 17 de dezembro de 2014, referentes à atualização da Lista Nacional de Espécies Ameaçadas de Extinção [Internet]. 2022. Available from: https://www.icmbio.gov.br/cepsul/destaques-e-eventos/704-atualizacao-da-lista-oficial-das-especies-ameacadas-de-extincao.html

Monteiro LR. Multivariate regression models and geometric morphometrics: the search for causal factors in the analysis of shape. Syst Biol. 1999; 48:192–99.

Monteiro LR, Reis SF. Princípios de morfometria geométrica. Ribeirão Preto: Holos Editora; 1999.

Mosimann JE. Size allometry: size and shape variables with characterizations of the lognormal and generalized gamma distributions. J Am Stat Assoc. 1970; 65:930–45.

Müller J, Troschel FH. Fische. In: Schomburgk R, editor. Reisen in Britisch-Guiana in den Jahren 1840-1844, Volume 3: Im Auftrag Sr. Mäjestat des Königs von Preussen. Leipzig: Verlagsbuchhandlung von JJ Weber; 1849. p.618–44. https://www.biodiversitylibrary.org/item/192473#page/9/mode/1up

Myers GS. Descriptions of new South American fresh-water fishes collected by Dr. Carl Ternetz. Bull Mus Comp Zool. 1927; 68(3):107–35. https://biostor.org/reference/20601

Nascimento WS, Araújo AS, Barros NHC, Gurgel LL, Costa EFS, Chellappa S. Length–weight relationship for seven freshwater fish species from Brazil. J Appl Ichthyol. 2012; 28:272–74.

Núñez MCO, Arredondo NJ, Doma IL, Pertierra AAG. Redescription of *Parspina argentinensis* (Szidat, 1954) (Digenea: Cryptogonimidae) from freshwater fishes (Pimelodidae) in the basins of the Paraná and La Plata Rivers, Argentina, with comments on *P. bagre* Pearse, 1920. Syst Parasitol. 2011; 78:27–40. https://doi.org/10.1007/s11230-010-9274-7

Ohlberger J, Staaks G, Hölker F. Swimming efficiency and the influence of morphology on swimming costs in fishes. J Comp Physiol B. 2006; 176:17–25. https://doi.org/10.1007/s00360-005-0024-0

Pearson NE. The fishes of the eastern slope of the Andes: the fishes of the rio Beni basin, Bolivia, collected by the Mulford expedition. Indiana Univ Sci Ser. 1924; 11(64):1–83.

Peixoto MS. Estudos sobre as relações filogenéticas e biogeográficas de espécies do gênero *Pimelodella* (Siluriformes, Heptapteridae) Eigenmann & Eigenmann, 1888 do Alto Paraná. [Unpublished PhD Thesis]. São Paulo: Universidade de São Paulo; 2011.

Penha J, Hakamada KYP, Hines JE, Nichols JD. Scale-dependent effects of isolation on seasonal patch colonisation by two Neotropical freshwater fishes. Ecol Freshw Fish. 2018; 28:274–84. https://doi.org/10.1111/eff.12452

Pettersson LB, Hedenström A. Energetics, cost reduction and functional consequences of fish morphology. Proc R Soc Lond B Biol Sci. 2000; 267:759–64. https://doi.org/10.1098/rspb.2000.1068

Pierre V, Slobodian V. A new species of *Pimelodella* (Siluriformes: Heptapteridae) from the Paraguai basin, Brazil, with a discussion regarding its distribution. Neotrop Ichthyol. Forthcoming. 2024; 22(1):e230110. https://doi.org/10.1590/1982-0224-2023-0110

R Core Team. R: a language and environment for statistical computing. R Foundation for Statistical Computing. Vienna; 2023. Available from: https://www.R-project.org

Ramallo G, Ailán-Choke LG. Observations on two *Procamallanus* (*Spirocamallanus*) species (Nematoda: Camallanidae) from freshwater fishes in Argentina, including description of *Procamallanus (Spirocamallanus) juana* sp.nov. Zootaxa. 2017; 4323(2):286–94. https://doi.org/10.11646/zootaxa.4323.2.12

Regan CT. Descriptions of new South-American fishes in the collection of the British Museum. Ann Mag Nat His. 1903; 12(72):621–30. https://www.biodiversitylibrary.org/partpdf/68444

Reimchen TE, Temple NF. Hydrodynamic and phylogenetic aspects of the adipose fin in fishes. Can J Zool. 2004; 82(6):910–16. https://doi.org/10.1139/z04-069

Reis RE, Albert JS, Di Dario F, Mincarone MM, Petry P, Rocha LA. Fish biodiversity and conservation in South America. J Fish Biol. 2016; 89(1):12–47. https://doi.org/10.1111/jfb.13016

Rohlf FJ. Morphometrics. Annu Rev Ecol Syst. 1990; 21:299–316.

Rohlf FJ, Marcus LF. A revolution in morphometrics. Trends Ecol Evol. 1993; 8(4):129–32.

Rohlf FJ, Slice DE. Extensions of the procrustes method for the optimal superimposition of landmarks. Syst Biol. 1990; 39:40–59. https://doi.org/10.2307/2992207

Roque FO, Ochoa-Quintero J, Ribeiro DB, Sugai LSM, Costa-Pereira R, Lourival R, Bino G. Upland habitat loss as a threat to Pantanal wetlands. Conserv Biol. 2016; 30(5):1131–34. https://doi.org/10.1111/cobi.12713

RStudio Team. RStudio: Integrated Development for R. Boston: PBC; 2023. Available from: http://www.rstudio.com

Ruane S. Using geometric morphometrics for integrative taxonomy: an examination of head shapes of milksnakes (genus *Lampropeltis*). Zool J Linn Soc. 2015; 174:394–413. https://doi.org/10.1111/zoj.12245

Santos SL, Viana LF, Lima-Junior SE. Fator de condição e aspectos reprodutivos de fêmeas de *Pimelodella* cf. *gracilis* (Osteichthyes, Siluriformes, Pimelodidae) no rio Amambai, Estado de Mato Grosso do Sul.

Shimabukuro-Dias CK, Silva GJC, Ashikaga FY, Foresti F, Oliveira C. Molecular identification of the fish fauna from the pantanal flood plain area in Brazil. Mitochondrial DNA Part A. 2017; 28(4):588–92. http://dx.doi.org/10.3109/24701394.2016.1149826

Sidlauskas BL, Mol JH, Vari RP. Dealing with allometry in linear and geometric morphometrics: a taxonomic case study in the *Leporinus cylindriformis* group (Characiformes: Anostomidae) with description of a new species from Suriname. Zool J Linn Soc. 2011; 162:103–130. https://doi.org/10.1111/j.1096-3642.2010.00677.x

Silva GSC, Roxo FF, Melo BF, Ochoa LE, Bockmann FA, Sabaj MH, Jerep FC, Foresti F, Benine RC, Oliveira C. Evolutionary history of Heptapteridae catfishes using ultraconserved elements (Teleostei, Siluriformes). Zool Scr. 2021; 50(5):543–54. https://doi.org/10.1111/zsc.12493

Silva JSV, Abdon MM. Delimitação do Pantanal brasileiro e suas subregiões. Pesqui Agropecu Bras. 1998; 33:17031711.

Silva MA, Perazzo GX, Kavalco KF, Pasa R. Shape diversity of the fish genus *Astyanax* Baird & Girard, 1854 (Teleostei, Characidae) in adjacent basins. Biologia. 2021; 76:213–21. https://doi.org/10.2478/s11756-020-00544-5

Slobodian V. Taxonomia, sistemática e biogeografia de *Brachyrhamdia Myers*, 1927 (Siluriformes: Heptapteridae), com uma investigação sobre seu mimetismo com outros Siluriformes. [Unpublished Msc. Dissertation]. Ribeirão Preto: Universidade de São Paulo; 2013.

Slobodian V. Taxonomic revision of *Pimelodella* Eigenmann & Eigenmann, 1888 (Siluriformes: Heptapteridae): an integrative proposal to delimit species using a multidisciplinary strategy. [Unpublished PhD Thesis]. São Paulo: Universidade de São Paulo; 2017.

Slobodian V, Abreu-Santos B, Pastana MNL. The rediscovery of *Pimelodella longipinnis* (Borodin, 1927), an enigmatic Atlantic Rainforest catfish species from Southeastern Brazil (Siluriformes: Heptapteridae). Pap Avulsos Zool. 2021; 61:e20216173. http://doi.org/10.11606/1807-0205/2021.61.73

Slobodian V, Akama A, Dutra GM. A new species of *Pimelodella* (Siluriformes: Heptapteridae) from the Guiana Shield, Brazil. Zootaxa. 2017; 4338(1):85–100. https://doi.org/10.11646/zootaxa.4338.1.4

Slobodian V, Bockmann FA. Phylogeny and classification of Heptapteridae Gill, 1861 (Siluriformes: Pimelodoidea). In: Arratia G, Reis RE, editors. Catfishes, vol 2: Catfishes, evolution and Phylogeny. Forthcoming 2024.

Slobodian V, Gimênes-Junior H, Rech R. Heptapteridae. In: Gimênes-Junior H, Rech R, editors. Guia ilustrado dos peixes do Pantanal e entorno. Campo Grande: Julien Design; 2022. p.332–45.

Slobodian V, Pastana MNL. Description of a new *Pimelodella* (Siluriformes: Heptapteridae) species with a discussion on the upper pectoral girdle homology of Siluriformes. J Fish Biol. 2018; 93(5):901–16. https://doi.org/10.1111/jfb.13795

Souza-Shibatta L, Pezenti LF, Ferreira DG, Almeida FS, Sofia SH, Shibatta OA. Cryptic species of the genus *Pimelodella* (Siluriformes: Heptapteridae) from the Miranda River, Paraguay River basin, Pantanal of Mato Grosso do Sul, Central Brazil. Neotrop Ichthyol. 2013; 11(1):101–09. https://doi.org/10.1590/S1679-62252013000100012

speciesLink. speciesLink network [Internet]. Campinas: CRIA (Centro de Referência e Informação Ambiental); 2024. Available from: https://specieslink.net/

Steindachner F. Herpetologische und ichthyologische Ergebnisse einer Reise nach Südamerika, ... mit einer Einleitung von Therese Prinzessin von Bayern. Denkschr - Österr Akad Wiss Math-Naturwiss Kl. 1902; 72:89–148.

Temple NF, Reimchen TE. Adipose fin condition and flow regime in catfish. Can J Zool. 2008; 86:1079–82. https://doi.org/10.1139/Z08-086

Trajano E, Reis RE, Bichuette ME. *Pimelodella spelaea*: a new cave catfish from central Brazil, with data on ecology and evolutionary considerations (Siluriformes: Heptapteridae). Copeia. 2004; 2:315–25.

Tucci CEM, Clarke RT. Environmental issues in the la Plata Basin. Water Resour Dev. 1998; 14(2):157–73.

Tucci CEM, Silveira A, Sanchez J, Albuquerque F. Flow regionalization in the upper Paraguay basin, Brazil. Hydrol Sci J. 1995; 40(4):485–97.

UNESCO. Biosphere Reserves – World Network of biosphere reserves [Internet]. Paris: MAB Programme, 2000.

Valenciennes A. Poissons [plates]. In: d'Orbigny A, editor. Voyage dans l'Amérique méridionale. P. Bertrand, Paris and V. Levrault, Strasbourg; 1835. pls.1–16.

Valenciennes A. Poissons [plates]. In: d'Orbigny A, editor. Voyage dans l'Amérique méridionale. P. Bertrand, Paris and V. Levrault, Strasbourg; 1837. pls.1–16.

Valenciennes A. Poissons. Catalogue des principales espèces de poissons, rapportées de l'Amérique méridionale. In: A. d'Orbigny, editor. Voyage dans l'Amérique méridionale. P. Bertrand, Paris and V. Levrault, Strasbourg; 1847. 11p.

Viana LF, Santos SL, Lima-Junior SE. Variação sazonal na alimentação de *Pimelodella* cf. *gracilis* (Osteichthyes, Siluriformes, Pimelodidae) no rio Amambai, Estado de Mato Grosso do Sul. Acta Sci Biol Sci. 2006; 28(2):123–28.

Viscosi V, Cardini A. Leaf morphology, taxonomy and geometric morphometrics: a simplified protocol for beginners. PLoS ONE. 2011; 6(10): e25630. https://doi.org/10.1371/journal.pone.0025630

von Spix JB, Agassiz L. Selecta genera et species piscium quos in itinere per Brasiliam annis MDCCCXVII-MDCCCXX jussu et auspiciis Maximiliani Josephi I.... collegit et pingendos curavit Dr J. B. de Spix.... Monachii; 1829.

Wainwright PC. Ecomorphology: experimental functional anatomy for ecological problems. Am Zool. 1991; 31:635–45. https://www.jstor.org/stable/3883566

Wainwright PC. Ecomorphology of locomotion in labrid fishes. Environ Biol Fishes. 2002; 65:47–62.

White, J. Geometric morphometric investigation of molar shape diversity in modern lemurs and lorises. Anat Rec. 2009; 292(5):701–19. https://doi.org/10.1002/ar.20900

Xenopoulos MA, Lodge DM, Alcamo J, Marker M, Schulze K, Van Vuuren DP. Scenarios of freshwater fish extinctions from climate change and water withdrawal. Glob Change Biol. 2005; 11(10):1557–64. https://doi.org/10.1111/j.1365-2486.2005.001008.x

Zelditch ML, Swiderski DL, Sheets HD, Fink WL. Geometric morphometrics for biologists: A primer. San Diego: Elsevier Academic Press; 2004.

Zumak A, Tolone W, Larcher L. Caracterização geográfica da BAP e do bioma Pantanal. In: Rabelo APC, Souza MG, editors. Bacia do Alto Paraguai: uma viagem no tempo. Brasília: Instituto Brasileiro de Informação em Ciência e Tecnologia; 2021. p.24–53.

Appendix I

Chapter 2 of the present dissertation, corresponding to the original description of *Pimelodella guato* Pierre & Slobodian (2024), in the article "A new species of *Pimelodella* (Siluriformes: Heptapteridae) from the Paraguai basin, Brazil, with a discussion regarding its distribution", published in Neotropical Ichthyology.

Neotropical Ichthyology

Original article

https://doi.org/10.1590/1982-0224-2023-0110

urn:lsid:zoobank.org:pub:153660CD-6BEA-4D7F-AB0F-5B026BDC09FB

A new species of *Pimelodella* (Siluriformes: Heptapteridae) from the Paraguai basin, Brazil, with a discussion regarding its distribution

Correspondence:
Veronica Slobodian
vslobodian@unb.br

Veida Pierre and Veronica Slobodian

A new species of *Pimelodella* is described from the rio Paraguai basin in Mato Grosso do Sul and Mato Grosso States, Brazil. The new species distinguishes from all other members of the genus based on a unique combination of characteristics, which include: dorsal profile straight from snout to dorsal-fin, maxillary barbel reaching at least the anal-fin terminus when parallel to main body axis, robust dorsal-fin spine bearing small spinules along three-fourths of its posterior margin, 41–42 total vertebrae (rarely 43 or 44), 13–23 large and retrorse blades at the posterior margin of the pectoral-fin spine, and dorsolateral region of body slightly darkened. This study also discusses the ichthyofaunal similarities between the Paraguai and Amazon basins, shedding light on their biogeographic history. Additionally, the research includes considerations about the sexual dimorphism of *Pimelodella* and provides an identification key for the *Pimelodella* species found in the Paraguai basin.

Keywords: Biogeography, Catfishes, Identification key, Sexual dimorphism, Taxonomy.

Submitted October 6, 2023
Accepted January 15, 2024
by Carlos DoNascimiento
Epub April 5, 2024

Online version ISSN 1982-0224
Print version ISSN 1679-6225

Neotrop. Ichthyol.
vol. 22, no. 1, Maringá 2024

Programa de Pós-Graduação em Zoologia – UnB, Laboratório de Ictiologia Sistemática, Instituto de Ciências Biológicas, Universidade de Brasília, Campus Universitário Darcy Ribeiro, 70910-900 Brasília, DF, Brazil. (VP) veidampierre@gmail.com, (VS) vslobodian@unb.br (corresponding author).

Uma nova espécie de *Pimelodella* é descrita da bacia do rio Paraguai, nos Estados de Mato Grosso do Sul e Mato Grosso, Brasil. A nova espécie se distingue de todas as suas congêneres por apresentar uma combinação exclusiva de características, que incluem: perfil da região anterior do corpo reto do focinho à nadadeira dorsal, barbilhão maxilar alcançando pelo menos o término da nadadeira anal quando paralelo ao eixo principal do corpo, espinho da nadadeira dorsal robusto e apresentando pequenas espínulas nos três-quartos distais da sua margem posterior, 41–42 vértebras totais (raramente 43 ou 44), espinho da nadadeira peitoral apresentando 13–23 lâminas grandes e retrorsas na sua margem posterior, e região dorsolateral do corpo ligeiramente mais escura que o restante. Este estudo também discute as similaridades entre a ictiofauna das bacias do Paraguai e Amazônica, abordando a história biogeográfica entre ambas as regiões. Adicionalmente, considerações acerca do dimorfismo sexual de *Pimelodella* são apresentadas, além de uma chave de identificação para as espécies de *Pimelodella* encontradas na bacia do Paraguai.

Palavras-chave: Bagres, Biogeografia, Chave de identificação, Dimorfismo sexual, Taxonomia.

INTRODUCTION

Pimelodella, as described by Eigenmann and Eigenmann in 1888, stands as the most diverse genus within the Heptapteridae family, currently comprising 83 valid species (Fricke *et al*., 2023). The first comprehensive taxonomic review of this genus was conducted by Eigenmann in 1917. In this review, Eigenmann provided descriptions and geographic distribution information for 34 species and one subspecies of *Pimelodella* known at the time, in addition to a diagnosis for the genus. However, this initial diagnosis had undergone numerous discussions and redefinitions (*e.g*., Mees, 1983; Bockmann, Miquelarena, 2008; Bockmann, Slobodian, 2013; Souza-Shibatta *et al*., 2013; Slobodian *et al*., 2017; Slobodian, Pastana, 2018) primarily due to the discovery of new species. As a result, *Pimelodella* is currently characterized by a distinctive combination of features: body moderately elongated, usually between 12–30 cm of standard length; supraoccipital process long, usually reaching the anterior nuchal plate; anterior and posterior fontanels open, long, separated by the epiphyseal bar; limits of eyes well defined by a free orbital rim, more conspicuous anteriorly and dorsally; pectoral fin with a single, strong and pungent unbranched ray (spine), bearing both anterior and posterior ornamentations, and 7–9 (usually 8) branched rays; branchiostegal rays usually 6; caudal fin deeply forked; median caudal-fin rays not articulated to hypural plate; hypural 5 as a single structure, and not fused to hypural plate; body generally with a dark midlateral stripe, extending from the snout or posterior to the head until the insertion of, or onto, the median caudal-fin rays (Slobodian *et al*., 2017).

The distribution of *Pimelodella* encompasses both cis- and trans- Andean Neotropical drainages from Panamá to Argentina (Bockmann, Guazzelli, 2003; Ferraris, 2007; Fricke *et al*., 2023). These fishes are typically found in the major Neotropical basins,

primarily in streams, where they form schools of up to ten individuals, often associated with sandy banks, marginal vegetation, or rock crevices (Bockmann, Guazzelli, 2003; Slobodian *et al*., 2017; Slobodian, Pastana, 2018). Several *Pimelodella* species have been reported to inhabit the Paraguai basin. These include *P. gracilis* (Valenciennes, 1835), *P. griffini* Eigenmann, 1917, *P. laticeps* Eigenmann, 1917, *P. megalura* Miranda Ribeiro, 1918, *P. mucosa* Eigenmann & Ward, 1907 in Eigenmann *et al*. (1907), *P. notomelas* Eigenmann, 1917, and *P. taeniophora* (Regan, 1903) (Britski *et al*., 1999; Koerber *et al*., 2017; Mirande, Koerber, 2020; Slobodian *et al*., 2022). *Pimelodella taenioptera* Miranda Ribeiro, 1914, was also described for the Paraguai basin in Brazil, but indicated as probably a junior synonym of *P. gracilis* in Slobodian (2017). *Pimelodella parva* Günthert, 1942, was described for the Paraguay basin in Paraguay, but is probably a juvenile of *Pimelodus* (Slobodian, 2017). The name *Pimelodus parvus* is previously occupied by *Pimelodus* (*Rhamdia*) *parvus* Boulenger (1898), and the problems related to this species are already being tackled in an ongoing work (M. Rocha and V. Slobodian, work in progress).

The Paraguai basin encompasses drainages in Brazil (in the States of Mato Grosso and Mato Grosso do Sul), Bolivia, Paraguay, and Argentina. This region is susceptible to various anthropic impacts, including hydroelectric and agricultural activities, which induce significant hydrological alterations (Tucci *et al*., 1999; Hamilton, 2002; Ely *et al*., 2020). The Paraguai basin is renowned for its high biological diversity, serving as habitat for approximately three hundred fish species, with about one-third being endemic (Carvalho, Albert, 2011). Some notable examples of these endemic species include *Curimatopsis myersi* Vari, 1982, *Hyphessobrycon rutiliflavidus* Carvalho, Langeani, Miyazawa & Troy, 2008, *Ernstichthys taquari* Dagosta & de Pinna, 2021, and *Paracanthopoma saci* Dagosta & de Pinna, 2021 (Melo *et al*., 2016; Dagosta, de Pinna, 2021; Fricke *et al*., 2023).

During the examination of a *Pimelodella* material from the Paraguai basin in Brazil for an illustrated guide to Pantanal fish species (Gimênes-Junior, Rech, 2022), we encountered specimens that exhibited similarities with *P. serrata* Eigenmann, 1917. As a result, these specimens were identified as belonging to *P. serrata* in the guide (*e.g*., Slobodian *et al*., 2022). *Pimelodella serrata* is a species originally described from San Joaquin, Bolivia, within the upper rio Guaporé basin (Bockmann, Guazzelli, 2003). It has also been observed in various locations within the rio Madeira basin, spanning Bolivia and Brazil (Lauzanne, Loubens, 1985; Chernoff *et al*., 2000; Bockmann, Slobodian, 2013). However, under a more detailed examination, specimens from the Paraguai basin revealed to be distinct from *P. serrata* and other species within the *Pimelodella* genus. In this context, we proceed with a description of this newly discovered *Pimelodella* species, with nine recorded occurrences within the Paraguai basin. Additionally, we provide an identification key for *Pimelodella* species found within the Paraguai basin and discuss the similarities between the ichthyofauna of the Paraguai and Amazon basins.

MATERIAL AND METHODS

Measurements were taken as point-to-point distances using a digital caliper with a precision of 0.01 mm, according to Slobodian *et al.* (2017). All specimens were measured, including the one cleared and stained (c&s) prior to treatment. Measurements of head parts were converted to proportions of head length (HL), except for measurements of barbels, which are shown as proportions of standard length (SL). The HL and measurements of body parts were converted to proportions of SL. Meristics and fin positions followed Bockmann, Castro (2010). Vertebral counts include the Weberian complex elements counted as five, all free vertebrae, and the compound caudal centrum (PU1+U1) counted as one, following Lundberg, Baskin (1969). The number of specimens counted for each meristic characteristic is indicated in parentheses. When a range is presented, the count for the holotype is indicated by an asterisk.

Osteological nomenclature follows Bockmann, Miquelarena (2008); nomenclature for pectoral- and dorsal-fin ornamentations follows Slobodian, Pastana (2018), with modifications of Ballen, de Pinna (2022); nomenclature for lateral-line canals and pores follows Slobodian, Pastana (2018). Osteological data was obtained with X-ray images from the Faxitron LX-60 system, Faxitron DX software, and specimens c&s following the method of Taylor, Van Dyke (1985). Gonadal morphology and development phase identification follow Mazzoni *et al.* (2020).

Illustrations were prepared digitally in Adobe Illustrator CC 2019, with the assistance of photos taken with a Leica M205 stereomicroscope and a Leica DFC295 digital camera. Photos were taken using a Canon EOS 5D Mark II camera and edited in Adobe Photoshop CC 2018. The geographic distribution map was produced using Google Earth Pro v. 7.3 and QGIS v. 3.28.3 softwares, following Calegari *et al.* (2016), with modifications.

The delimitation of the Amazonas-Paraguai lowlands follows Dagosta, de Pinna (2019). Amazon bioregion delimitation follows Dagosta, de Pinna (2017), and Paraguai ecoregion delimitation follows Abell *et al.* (2008). Specimens were preserved in 70% ethanol, except for those c&s, which were preserved in glycerol. X-rayed specimens are marked as "xr".

The specimens of *P. gracilis*, *P. griffini*, *P. howesi* Fowler, 1940, *P. laticeps*, *P. megalura*, *P. mucosa*, *P. notomelas*, *P. serrata*, and *P. taeniophora* included in the examined material were identified according to their original descriptions (*i.e.*, Valenciennes, 1835; Regan, 1903; Eigenmann, Ward, 1907; Eigenmann, 1917; Miranda Ribeiro, 1918; Fowler, 1940), in addition to comments provided by Bockmann, Slobodian (2013) and Slobodian (2017), which are based on osteological characters and external morphology. Information of *P. longibarbata* is based on original description and additional photos requested to the authors. The identification key was produced using our findings and the literature above. Institutional codes follow Sabaj (2023).

RESULTS

Pimelodella guato, new species

urn:lsid:zoobank.org:act:E9B6CDE4-ACE0-466B-B97D-A6BB29C8238F

(Figs. 1, 2A, 3A; Tab. 1)

Pimelodella serrata non Eigenmann, 1917. —Slobodian *et al*., 2022:340 (rio Taquari, rio Paraguai basin; geographic distribution).

FIGURE 1 | *Pimelodella guato*, holotype, ZUFMS-PIS 8515, 78.5 mm SL, Brazil, Mato Grosso do Sul, Corumbá municipality, rio Paraguai basin, rio Miranda, sandy beaches at Passo do Lontra region, 19°34'37"S 57°00'42"W. **A.** Dorsal; **B.** Left lateral; and **C.** Ventral views. Scale bar = 1 cm.

Holotype. ZUFMS-PIS 8515, xr, 78.5 mm SL, Brazil, Mato Grosso do Sul, Corumbá municipality, rio Paraguai basin, rio Miranda, sandy beaches at Passo do Lontra region, 19°34'37"S 57°00'42"W, 31 Oct 1991, J. C. Louzan & V. M. F. Jesus.

Paratypes. All from Brazil, rio Paraguai basin. CIUnB 1772, 7, 3 xr, 79.1–99.9 mm SL, 1 c&s, 91.2 mm SL, Mato Grosso do Sul, Corumbá municipality, rio Miranda, sandy beaches at Passo do Lontra region, 19°34'37"S 57°00'42"W, 17 Sep 1993, O. Froehlich. MZUEL 11088, 1, 103.7 mm SL, Mato Grosso do Sul, Corumbá municipality, corixo, fifth bridge after the entrance to Passo do Lontra, Estrada Parque, 19°38'S 57°02'W, 3 Sep 2002, O. A. Shibatta *et al*. MZUEL 16829, 1, 79.6 mm SL, Mato Grosso do Sul, Corumbá municipality, rio Miranda, BEP/UFMS (Base de Estudos do Pantanal), 19°34'36"S 57°1'5"W, 22 Aug 2016, O. A. Shibatta *et al*. NUP 14295, 1, 72.3 mm SL, Mato Grosso, Cáceres municipality, baía de Cáceres, tributary of rio Paraguai, 16°04'02"S 57°41'38"W, 28 Mar 2012, Nupelia. NUP 19919, 3, 64.8–83.2 mm SL, Mato Grosso do Sul, Coxim municipality, rio Coxim, tributary of rio Taquari, 18°33'32"S 54°44'37"W, 8 Oct 2017, Nupelia. ZUFMS-PIS 647, 5, xr, 37.1–94.3 mm SL, Mato Grosso do Sul, Corumbá municipality, rio Miranda, Passo do Lontra, across from the BEP, 19°34'37"S 57°00'42"W, 6 Sep 1990, O. Froehlich. ZUFMS-PIS 676, 15, 62.3–107.4 mm SL, Mato Grosso do Sul, Corumbá municipality, rio Miranda, sandy beaches at Passo do Lontra region, 19°34'37"S 57°00'42"W, 17 Sep 1993, O. Froehlich. ZUFMS-PIS 4843, 2, xr, 64.6–65.4 mm SL, Mato Grosso do Sul, Corumbá municipality, rio Miranda, across from the BEP, 19°34'37"S 57°00'42"W, 5 Sep 2008, O. Froehlich. ZUFMS-PIS 6370, 2, xr, 98.6–127.9 mm SL, Mato Grosso do Sul, Coxim municipality, rio Taquari, 18°31'32"S 54°44'30"W, 16 Dec 2019, H. Gimenes-Jr, M. B. Mendonça, P. Camelier, M. Kaluza, F. Severo-Neto, R. Rech, F. Vasconcelos & R. Mochi. ZUFMS-PIS 8516, 4, xr, 49.7–109.0 mm SL, same data as holotype.

Diagnosis. *Pimelodella guato* differs from all *Pimelodella* species except *P. boliviana*, *P. chaparae*, *P. cristata*, *P. cruxenti*, *P. dorseyi*, *P. geryi*, *P. gracilis*, *P. howesi*, *P. humeralis*, *P. laurenti*, *P. longibarbata*, *P. longipinnis*, *P. martinezi*, *P. megalops*, *P. mucosa*, *P. notomelas*, *P. odynea*, *P. ophthalmica*, *P. parnahybae*, *P. serrata*, *P. steindachneri*, *P. taeniophora*, *P. tapatapae*, *P. wesselii*, and *P. witmeri* by the long maxillary barbel, reaching at least the anal-fin terminus when parallel to main body axis (*vs*. reaching at best posterior limit of anal-fin base). It differs from *P. longipinnis* and *P. tapatapae* by having the supraoccipital process reaching the anterior nuchal plate (*vs.* not reaching, gap between distal terminus of supraoccipital process and anterior nuchal plate *ca*. 20–25% of supraoccipital process length). It differs from *P. boliviana*, *P. cruxenti*, *P. geryi*, *P. laurenti*, *P. martinezi*, *P. megalops*, *P. notomelas*, *P. odynea*, and *P. taeniophora* by having a robust dorsal-fin spine, bearing small, straight spinules along three-fourths of its posterior margin (*vs.* dorsal-fin spine not particularly robust, with posterior margin spinules inconspicuous or absent). It differs from *P. cristata*, *P. dorseyi*, *P. gracilis*, *P. howesi*, *P. humeralis*, *P. ophthalmica*, *P. parnahybae*, *P. steindachneri*, *P. wesselii*, and *P. witmeri* by usually having 41–42 (rarely 43 or 44) total vertebrae (*vs.* always 43–44 in *P. howesi;* 46 or more in the remaining species). It further differs from *P. howesi* by having the dorsolateral region of body slightly darkened (*vs.* not darkened), dorsal fin with light brown stripe near its origin, followed by a hyaline stripe, and distal half dark (*vs.* basal half of dorsal fin hyaline, and distal half dark), and by the dorsal lamina of the

Weberian apparatus reaching the ventral margin of the supraoccipital process only at its first third (*vs.* dorsal lamina reaching the supraoccipital process along all its extension). It differs from *P. mucosa* and *P. longibarbata* by the preoperculomandibular laterosensory canal openings at dentary not particularly large (*vs*. large openings). It differs from *P. chaparae*, *P. longibarbata*, and *P. serrata* by the wide midlateral stripe (*vs*. narrow) and by the dorsal lamina of the Weberian apparatus reaching the ventral margin of the supraoccipital process only at its first third (*vs.* first half in *P. longibarbata*; and almost its entire extension in *P. chaparae* and *P. serrata*) (Figs. 2A, D).

Furthermore, *P. guato* can be diagnosed from all congeners by the following exclusive character combination: dorsal profile straight from snout to dorsal fin; maxillary barbel reaching at least the anal-fin terminus when parallel to main body axis; supraoccipital process reaching anterior nuchal plate; dorsal-fin spine robust, bearing small, straight spinules along three-fourths of its posterior margin; posterior margin of pectoral-fin spine bearing 13–23 large, retrorse blades along basal two-thirds (Fig. 3A); adipose fin 2.5 to 3.0 times in SL; usually 41–42 (rarely 43 or 44) total vertebrae; epiphyseal branch of supraorbital canal on the head (S6) emerging as a single pore; brown midlateral stripe wide, not well delimited, extending from snout to caudal-fin origin.

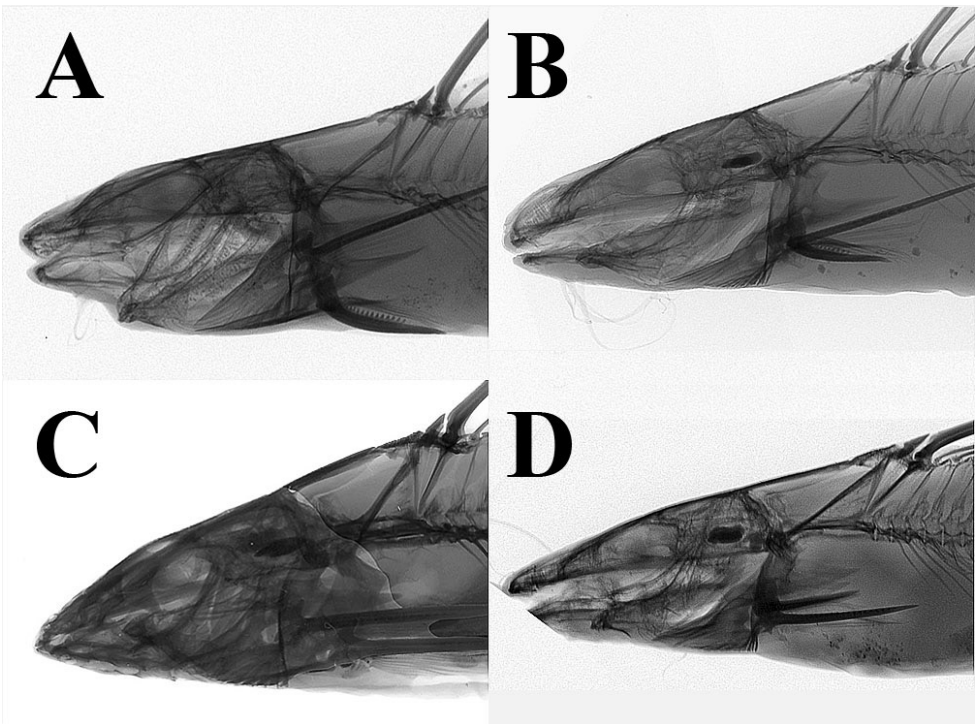

FIGURE 2 | Left lateral view of radiographs of *Pimelodella* species, illustrating the dorsal lamina of Weberian complex vertebrae of **A.** *Pimelodella guato*, paratype, ZUFMS-PIS 647, 90.1 mm SL; **B.** *P. taeniophora*, ZUFMS-PIS 6320, 68.9 mm SL; **C.** *P. mucosa*, holotype, CAS 63720, 97.4 mm SL; and **D.** *P. serrata*, LIRP 10022, 83.6 mm SL.

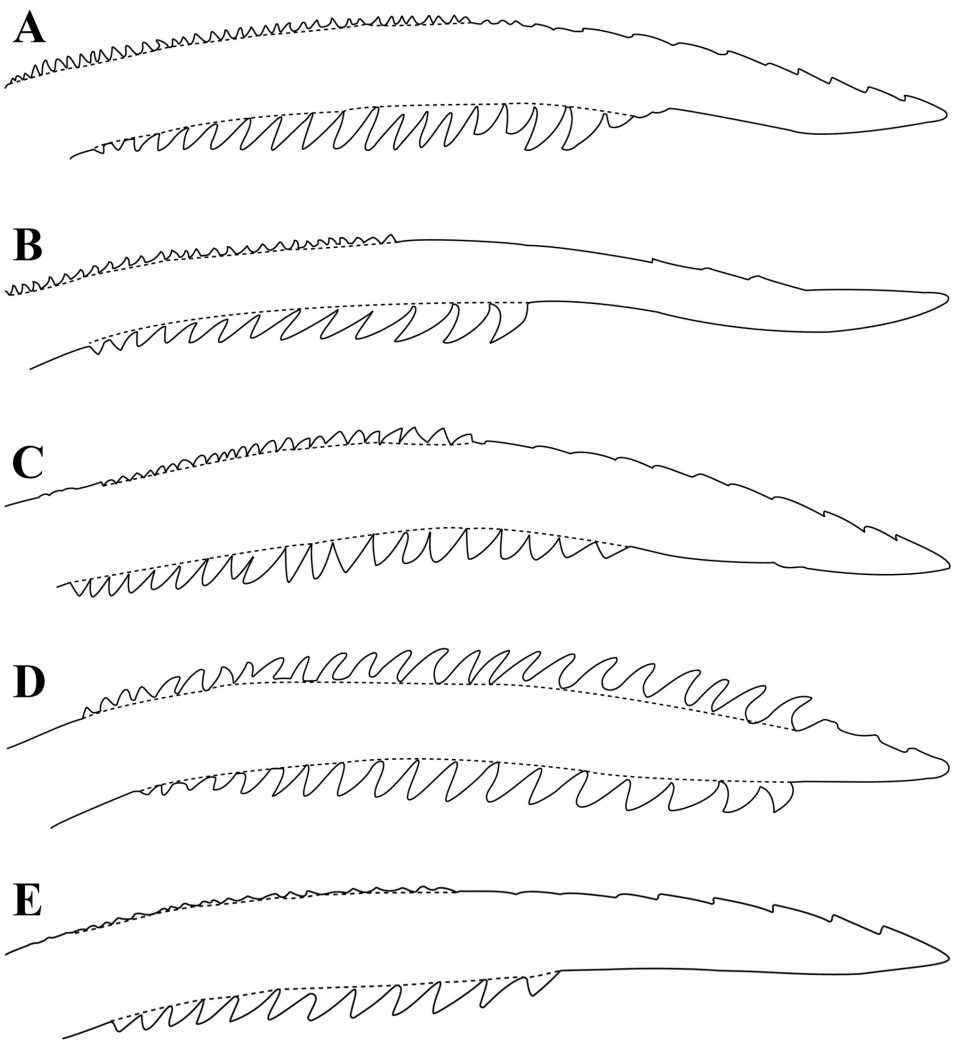

FIGURE 3 | Pectoral-fin spine of **A.** *Pimelodella guato*, paratype, CIUnB 1772, 91.2 mm SL, length of spine 16.7 mm; **B.** *P. taeniophora*, ZUFMS-PIS 6320, 68.9 mm SL, length of spine 11.4 mm; **C.** *P. mucosa*, holotype, CAS 63720, 97.4 mm SL, length of spine 22.8 mm; **D.** *P. serrata*, holotype, FMNH 57979, 55.7 mm SL, length of spine 18.3 mm; and **E.** *P. howesi*, holotype, ANSP 69036, 79.3 mm SL, length of spine 17.8 mm.

Description. Morphometric data are summarized in Tab. 1. Body moderately depressed, depth at dorsal-fin origin 5.0 to 6.5 times in SL; and moderately compressed; body width at dorsal-fin origin 7.0 to 9.0 times in SL (Fig. 1). Greatest body depth at dorsal-fin origin. Dorsal profile straight from snout to dorsal-fin origin, concave from dorsal fin to adipose fin, slightly convex along adipose fin, and concave along caudal peduncle. Ventral profile of body slightly convex from snout to branchiostegal membrane, convex between pectoral and pelvic fins, slightly convex from pelvic fin to anal-fin origin, and concave from this point along the caudal peduncle.

Pseudotympanum externally visible, large, oval, dorsal to posterior process of cleithrum and reaching vertical line of sixth (16) vertebrae. Posterior process of cleithrum triangular, long, its dorsal border slightly concave. Anus and urogenital papilla adjacent. Urogenital papilla tubular, triangular, short. Anus between verticals through half and last third of adpressed pelvic fin; urogenital papilla between verticals through second third and terminus of adpressed pelvic fin. Some specimens might present enlarged urogenital papillae (see Discussion).

TABLE 1 | Morphometric data for the holotype and 42 paratypes of *Pimelodella guato*. N = number of specimens; SD = Standard deviation.

	Holotype	Range	N	Mean	SD
Total length (mm)	97.1	47.5–161.2	42	99.9	
Standard length (mm)	78.5	37.1–127.9	43	82.5	
Percents of standard length					
Body depth (dorsal)	17.6	15.0–20.8	43	17.9	1.3
Body width (dorsal)	12.0	11.1–14.1	43	12.9	0.8
Cleithral width	16.0	15.2–18.2	43	16.7	0.6
Head length	29.2	27.2–31.3	43	29.0	1.0
Maxillary-barbel length (left side)	87.1	81.0–113.6	42	94.6	7.4
Outer mental-barbel length (left side)	36.7	28.7–49.7	43	37.3	3.9
Inner mental-barbel length (left side)	21.2	16.8–32.3	43	22.0	3.0
Predorsal length	32.3	28.5–34.1	43	32.3	1.2
Distance between snout tip and terminus of dorsal-fin base	45.4	42.3–48.9	43	46.2	1.2
Distance between snout tip and dorsal-fin distal end	62.1	54.4–75.2	38	58.3	3.4
Dorsal fin to adipose fin	5.0	3.8–22.2	43	7.3	2.9
Dorsal-fin base	15.2	12.7–18.3	43	14.9	1.0
Length of first dorsal-fin ray (unbranched)	30.5	20.1–42.5	29	24.8	4.3
Length of rigid part of first dorsal-fin ray	20.4	14.3–20.7	38	18.5	1.4
Length of second dorsal-fin ray (first branched)	24.0	18.6–24.0	42	21.3	1.2
Length of third dorsal-fin ray (second branched)	19.3	16.4–23.3	42	19.4	1.6
Prepectoral length	23.2	20.0–27.5	43	24.0	2.0
Distance between snout tip and terminus of pectoral-fin base	24.7	22.5–29.0	43	25.9	1.7
Distance between snout tip and pectoral-fin distal end	43.0	38.8–46.0	42	42.4	1.7
Length of first left pectoral-fin ray (unbranched)	21.2	17.3–21.2	39	19.4	1.1
Length of rigid part of first left pectoral-fin ray	18.7	15.5–18.8	43	17.4	0.9
Length of second left pectoral-fin ray (first branched)	19.2	14.7–19.9	42	17.6	1.2
Length of third left pectoral-fin ray (second branched)	17.9	12.4–17.9	41	15.4	1.2
Prepelvic length	42.1	42.1–49.2	43	45.5	1.5
Distance between snout tip and terminus of pelvic-fin base	43.6	43.6–50.8	43	47.1	1.4
Distance between snout tip and pelvic-fin distal end	61.3	58.6–65.5	43	61.4	1.7
Distance between pelvic fins	3.7	2.7–6.4	43	4.3	0.8
Length of first left pelvic-fin ray (unbranched)	18.1	11.5–18.1	43	14.8	1.4
Length of second left pelvic-fin ray (first branched)	18.2	14.3–18.2	43	16.1	1.0

TABLE 1 | (Continued)

	Holotype	Range	N	Mean	SD
Length of third left pelvic-fin ray (second branched)	17.4	14.0–17.9	42	15.8	1.0
Anal-fin base	10.3	8.6–12.9	43	10.5	0.9
Preanal length	65.7	65.1–71.4	43	67.8	1.4
Distance between snout tip and terminus of anal-fin base	76.7	74.8–82.5	43	77.4	1.5
Distance between snout tip and anal-fin distal end	84.3	82.0–90.3	42	85.2	1.7
Adipose-fin length	39.1	32.5–39.4	43	36.4	1.5
Preadipose length	51.6	51.1–56.4	43	53.2	1.2
Distance between snout tip and adipose-fin base end	86.9	86.3–91.1	43	88.2	1.0
Adipose-fin depth	4.4	3.6–5.2	42	4.4	0.4
Caudal-peduncle length posterior to adipose-fin	10.9	8.1–12.9	43	10.5	0.9
Caudal-peduncle depth at adipose-fin terminus	8.2	6.5–9.2	43	8.0	0.5
Snout-anus distance	48.6	48.2–54.4	42	51.0	1.3
Snout-urogenital papilla distance	55.4	53.2–60.0	40	56.3	1.5
Anus-urogenital papilla distance	6.8	3.9–9.4	40	5.4	1.3
Dorsal lobe of caudal fin length	23.6	21.2–29.2	39	25.8	2.2
Ventral lobe of caudal fin length	26.7	20.8–29.8	42	25.1	1.9
Percents of head length					
Head depth	48.4	42.3–63.5	43	51.4	4.0
Head width	48.9	46.1–57.7	43	51.8	3.1
Eye diameter (left)	19.3	17.6–25.3	43	20.3	1.6
Fleshy interorbital	28.2	22.1–28.4	43	24.9	1.7
Bony interorbital	18.0	12.0–20.5	43	17.2	1.5
Mouth gape	32.0	27.3–37.2	42	32.2	2.4
Snout length (left)	35.8	31.2–38.2	43	35.0	1.5
Distance between snout tip and posterior nare (left side)	18.6	15.6–21.5	43	18.5	1.3
Anterior internarial width	12.1	9.1–15.3	43	12.0	1.1
Posterior internarial width	12.1	11.3–15.5	43	13.7	1.0
Intranarial length (left side)	11.9	10.9–15.4	43	12.8	0.9

Head moderately depressed, depth at supraoccipital-process base 1.5 to 2.5 times in HL. Mouth sub-terminal. Eyes elliptical, 4.0 to more than 5.5 times in HL. Bony interorbital distance roughly equal to eye diameter. Barbels thin, slightly depressed, elliptical in cross-section. Maxillary barbel reaching at least the anal-fin terminus when parallel to main body axis. Outer mental barbel, when parallel to main body axis, reaching between second third of adpressed pectoral fin and first third of adpressed pelvic fin. Inner mental barbel, when parallel to main body axis, reaching between pectoral-fin origin and second third of adpressed pectoral-fin. Supraoccipital process subrectangular to triangular, wide. Dorsal lamina of Weberian complex vertebrae moderately deep, usually reaching the ventral margin of the supraoccipital process along its first third (Fig. 2A). Branchiostegal 6(17).

Dorsal fin triangular, distal margin convex, moderate in length (second branched dorsal-fin ray almost 4.5 to 6.0 times in SL), depressed tip reaching between vertical line through half and terminus of adpressed pelvic fin. Dorsal fin with II,6(24), being the anteriormost the spinelet. Distance between terminus of dorsal-fin base and adipose-fin origin at least a third shorter than dorsal-fin base. Anteriormost dorsal-fin pterygiophore posterior to neural spine of vertebra 4(17); posteriormost dorsal-fin pterygiophore anterior to neural (or pseudoneural) spine of vertebra 10*(7)–12(2). Second unbranched dorsal-fin ray mostly ossified as a spine, long (spine three-fourths of first dorsal-fin ray total length). Dorsal-fin spine robust, bearing small, straight spinules along distal three-fourths of its posterior margin. Second unbranched dorsal-fin ray may present a non-spinuous filamentous portion (see Discussion).

Pectoral-fin rays I,7(4)–I,9(5) (holotype I,8), pectoral-fin triangular with convex or slightly straight distal margin. First pectoral-fin ray curved, with proximal part rigid, forming a spine, and short distal tip, flexible and distinctly segmented. Pectoral-fin spine long, 5.5 to 6.5 times in SL. Anterior margin of pectoral-fin spine with small, straight spinules along its basal two-thirds and flat spinules along its distal third (Fig. 3A). Posterior margin of pectoral-fin spine bearing 13–23 (holotype 17) retrorse blades along basal two-thirds (Fig. 3A). Blades larger and more inclined, hook-like, near distal tip, meanwhile smaller, less inclined, near pectoral-fin base.

Pelvic-fin rays i,5(23), pelvic fin triangular with convex distal margin when expanded. Pelvic-fin origin at vertical through penultimate branched dorsal-fin ray. Tip of adpressed pelvic fin between verticals through second eighth and second fifth of adipose fin. First unbranched ray distinctly shorter than subequal branched second and third rays; remaining rays progressively shorter.

Anal-fin rays iv,7(6); v,7*(4); iv,8(3); or v,8(2); distal border of expanded anal fin convex. One or two anteriormost anal-fin rays vestigial, unsegmented, embedded in thick skin fold. Anal-fin origin between verticals through second third and half adipose-fin base; adpressed anal-fin terminus between verticals through last eighth and terminus of adipose fin. Anteriormost anal-fin pterygiophore posterior to hemal spine of vertebrae 20(1), 21*(5), 22(7) or 23(4); posteriormost anal-fin pterygiophore anterior to hemal spine of vertebrae 27(2), 28*(9), 29(5) or 30(1).

Adipose fin 2.5 to 3.0 times in SL, forming ascending elevated curve in lateral profile, with deepest point approximately midlength. Adipose fin emerging gradually, its posterior limit as a rounded, free lobe. Adipose-fin origin usually at vertical through vertebral centra 16*(6)–18(4), rarely 15(1) or 19(1); adipose-fin terminus usually at vertical through vertebral centra 35(2)–37(7) (holotype 36), rarely 34(1) or 38(1).

Caudal fin deeply forked, lobes subequal, or ventral lobe slightly longer than dorsal. Caudal peduncle length posterior to adipose fin roughly equal to or slightly larger than its depth. Dorsal lobe with 7(18) branched, 1(18) unbranched principal, and 13(2)–23(1) (holotype 17) procurrent fin-rays. Ventral lobe with 7(2)–8*(14) branched, 1(18) unbranched principal, and 14(2)–22(1) (16*) procurrent fin-rays. Hypural 5 completely free, not fused to hypural 3+4. Median caudal-fin rays not articulated directly to caudal plate. Seven* (13) or 8(3) rays articulated to dorsal caudal-fin plate (5 or 6 on hypurals 3+4, and 2 on hypural 5) and 7*(14) or 8(2) rays articulated to ventral caudal-fin plate (5 or 6 on hypurals 1+2, and 2 on parahypural). Total vertebrae usually 41(7)–42*(7), rarely 43(2) or 44(2). Ribs 7*(6)–9(1).

Epiphyseal branch of supraorbital canal on the head (S6) with contralateral canals connecting at midline, proceeding posteriorly as a single canal and opening in a single pore (diaulic S6+S6 pore).

Coloration in alcohol. Background body coloration pale yellow, dorsal and lateral regions of body with sparsely distributed dark brown chromatophores, more concentrated dorsal to midlateral stripe. Ventral region of body and head lacking pigmentation. Brown midlateral stripe wide, faint, not well-delimited, extending from snout to eye and posterior to eye onto the caudal-fin origin. Dorsal region of body with slightly more concentrated brown chromatophores from dorsal-fin origin to half adipose-fin base, fading posteriorly. Pseudotympanum area darker than surrounding areas. Dorsal region of head with scattered dark brown chromatophores. Cephalic brown pigment at posterior fontanel region. Paired dorsal dark-brown stripes, weakly delimited, extending along supraoccipital process. Maxillary barbel dorsal surface brown; mental barbels weakly pigmented along their dorsal surfaces. Dorsal fin with scattered brown chromatophores, more heavily pigmented at the dorsal-fin spine. Dorsal fin with light brown stripe near its base, followed by a hyaline stripe, and distal half darkened. Pectoral-fin spine and branched rays with scattered chromatophores along their extension. Pelvic, anal and caudal fins almost hyaline, with sparse brown chromatophores along rays. Adipose fin hyaline.

Geographical distribution. *Pimelodella guato* is known from the rio Paraguai basin, which includes all rivers where the new species was sampled, *i.e.* the rio Miranda, rio Coxim, rio Taquari, and rio Paraguai itself (Fig. 4). The rio Miranda drains from Mato Grosso do Sul State, ultimately joining the rio Paraguai on its left bank within the municipality of Corumbá. Moreover, the rio Miranda basin interconnects with the northwest region of the rio Taquari basin (Mendes *et al*., 2004). The rio Taquari originates in the highlands of Mato Grosso State and courses into Mato Grosso do Sul, in Brazil (Galdino *et al*., 2003). In the latter State, the rio Taquari flows east-to-west, with the rio Coxim serving as its primary tributary before its confluence with rio Paraguai on its left bank (Galdino *et al*., 2003).

Ecological notes. Within the rio Taquari, *Pimelodella guato* was sampled at the Palmeiras waterfall, in an area characterized by shallow waters, moderate water flow, and a sandy substrate (Slobodian *et al*., 2022). This species exhibits abundance during the rainy season and is notably easy to capture, particularly during the nighttime (Slobodian *et al*., 2022).

Etymology. The species name *guato* is in honor of the indigenous Guató people, who are affectionately known as "people of the Pantanal waters" due to their primary mode of transportation, canoes. Historically, the Guató people inhabited an extensive area along the rio Paraguai (Schmidt, 1942). However, in the 1940s, they began to lose their territory due to cattle ranching, and many relocated to cities such as Cáceres and Corumbá. This dispersal led to a reduction in the Guató population, and since then, they have been fighting for recognition of their ethnicity and the demarcation of their lands (Costa, 2015). The choice of *guato* is a homage to the resilience and cultural

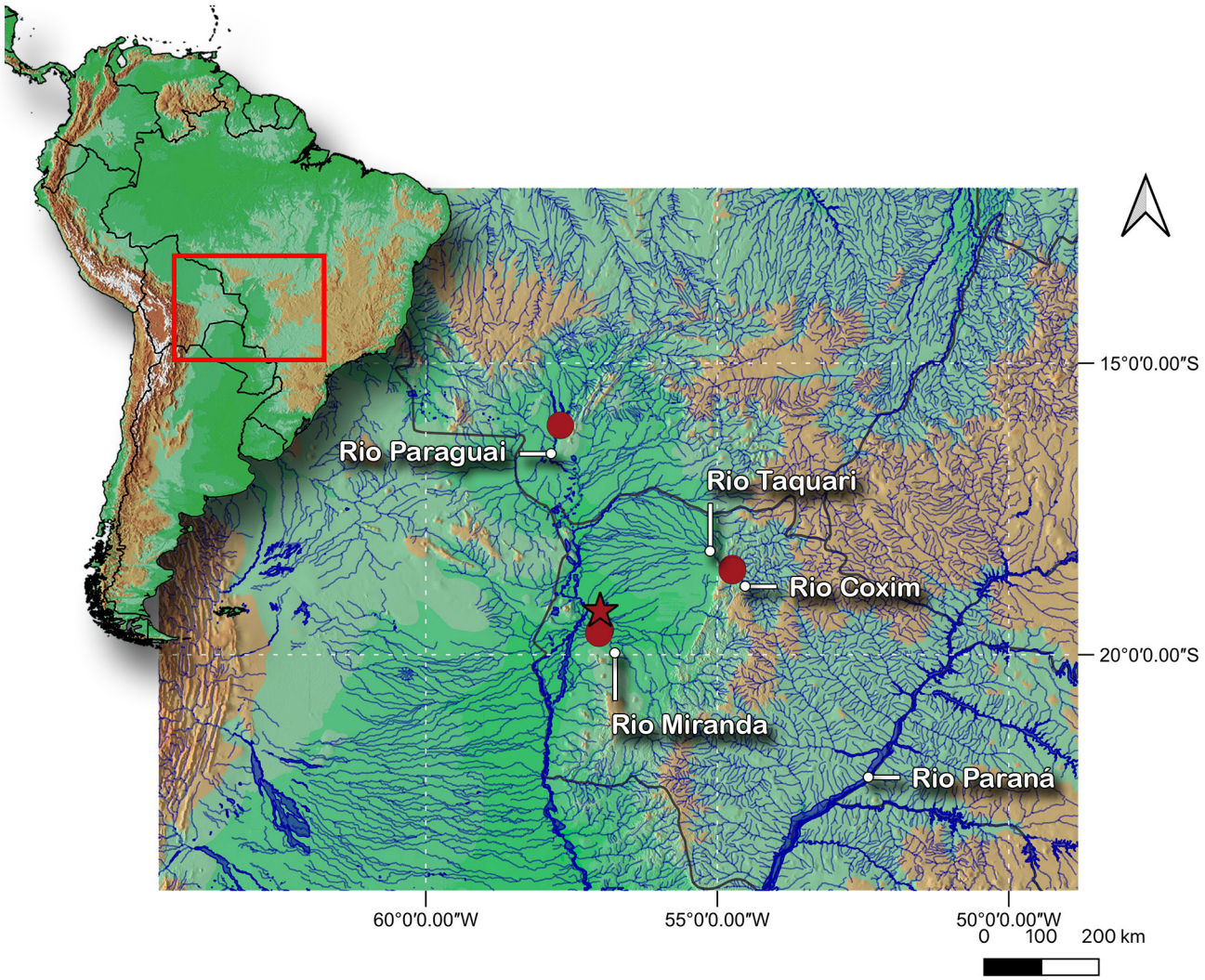

FIGURE 4 | Geographic distribution of *Pimelodella guato* in the rio Paraguai basin (red star, type-locality; red dots, paratype localities). The symbols might represent more than one voucher specimen each.

significance of these people who inhabit the same region where the new species is found. It also recognizes the ongoing struggles with land delimitation that indigenous communities continue to face, particularly in Brazil. A noun in apposition.

Conservation status. *Pimelodella guato* has predominantly been documented within the rio Miranda in the rio Paraguai basin. Despite several anthropic activities in this region, such as ecotourism and land use, which adversely affect water quality, comprehensive conservation plans and projects are notably lacking (Boin *et al*., 2019; Leite *et al*., 2022). Moreover, both the rio Taquari and rio Coxim confront significant challenges related to erosion and river siltation (Galdino *et al*., 2003, 2006; Rabelo, Souza, 2021), also correlated to road paving in the Coxim municipality region (H. Gimênes-Júnior, 2023, pers. comm.). While geological factors in the region render it more susceptible to these issues, deforestation and livestock activities exacerbate

erosion and siltation to alarming levels (Galdino *et al*., 2003, 2006; Rabelo, Souza, 2021). Biological and ecological information on *P. guato* remains unavailable, posing a challenge to accurately categorizing its conservation status. Nevertheless, despite the restrictive known distribution of the species, we suggest that *P. guato* be classified as Least Concern (LC), according to the International Union for Conservation of Nature (IUCN) categories and criteria (IUCN Standards and Petitions Subcommittee, 2022).

Key to the species of *Pimelodella* from the Paraguai basin

1a. Total vertebrae 46 (rarely 45); anal-fin adpressed terminus always anterior to adipose-fin terminus, reaching at least the vertical through three-fourths of adipose fin; adipose fin very long, slightly more than 2.0 to 2.5 times in SL ..... *P. gracilis*

1b. Total vertebrae 39–44; anal-fin adpressed terminus between verticals through adipose-fin terminus and slightly posterior to adipose-fin terminus; adipose fin 2.5 or more times in SL 2

2a. Openings of preoperculomandibular laterosensory canal at dentary large and conspicuous; posterior margin of pectoral-fin spine bearing 14–20 small, retrorse blades along basal two-thirds (Fig. 3C); head roof heavily ornamented ..... *P. mucosa*

2b. Openings of preoperculomandibular laterosensory canal at dentary not large or particularly conspicuous; posterior margin of pectoral-fin spine not as above; head roof ornamentation inconspicuous 3

3a. Supraoccipital process not reaching the anterior prenuchal plate; dorsal-fin spine small, approximately half or slightly more of second dorsal-fin ray total length; dorsal lobe of caudal fin notably longer than ventral caudal-lobe; hypural 5 variably fused to hypural 3+4 ..... *P. megalura*

3b. Supraoccipital process reaching the anterior prenuchal plate; dorsal-fin spine at least a third of second dorsal-fin total ray length (excepting the filamentuous portion, if present); caudal-fin lobes subequal or ventral lobe slightly longer than dorsal; hypural 5 completely free 4

4a. Maxillary barbels always surpassing caudal-fin origin; posterior margin of pectoral-fin spine bearing 4–6 notably triangular, short and straight blades along basal two-thirds; dorsal fin distal third notably dark brown to black ..... *P. notomelas*

4b. Maxillary barbels reaching between pelvic-fin origin and may extend beyond caudal-fin origin; posterior margin of the pectoral-fin spine not as above; dorsal fin not presenting a notably dark brown to black coloration 5

5a. Dorsal profile straight from snout to dorsal fin; dorsal-fin spine robust, large, bearing small, straight spinules along three-fourths of its distal posterior margin; posterior margin of pectoral-fin spine bearing 13–23 retrorse blades along basal two-thirds (Fig. 3A) ..... *P. guato*

5b. Dorsal profile convex from snout to dorsal fin; dorsal-fin spine not particularly robust, nor bearing spinules at its posterior margin; posterior margin of pectoral-fin spine bearing 9–13 retrorse blades along basal two-thirds 6

6a. Maxillary barbels reaching at least anal-fin terminus when parallel to main body axis; adipose fin 2.5 to almost 3.0 times in SL ..... *P. taeniophora*

6b. Maxillary barbels reaching between pelvic-fin origin and anal-fin terminus; adipose fin short, more than 3.5 times in SL..... 7

7a. Epiphyseal branch of supraorbital canal on the head (S6) with contralateral canals connecting at midline, proceeding posteriorly as a single canal and opening in a single pore (S6+S6 diaulic pore); total vertebrae 41–42; dorsal region of body usually presenting a well-delimited darker stripe from supraoccipital process to first third of adipose-fin base .....*P. griffini*

7b. Epiphyseal branch of supraorbital canal on the head (S6) emerging as two separated pores; total vertebrae 39–40; dorsal region of head and body slightly darkened, with a dark brown mark extending just between dorsal and adipose fins.....*P. laticeps*

DISCUSSION

The genus *Pimelodella* presents several unsettled taxonomic problems despite being an important component of Neotropical ichthyofauna found in all major cis- and trans-Andean basins. Most of them are due to the highly conservative morphology of its species, allied with their putatively broad distributions (Slobodian *et al*., 2017). Many species of *Pimelodella* lack rigorous published taxonomic study, contributing to a high number of specimens undetermined at the species level or wrongly identified in scientific collections (Slobodian *et al*., 2017; pers. obs.). Nevertheless, recent studies are contributing to the taxonomy of *Pimelodella* species (*e.g*., Souza-Shibatta *et al*., 2013; Slobodian *et al*., 2017, 2021; Slobodian, Pastana, 2018; Conde-Saldaña *et al*., 2019; Cortés-Hernández *et al*., 2020, 2023), and a complete revision is underway (V. Slobodian and M. de Pinna, work in progress).

Despite the morphological similarities found among *Pimelodella* species in general, *P. guato* is relatively easy to identify (especially among those species that occur in the rio Paraguai basin) due to its diagnostic features, such as the presence of large blades at the posterior margin of the pectoral-fin spine. Within the *Pimelodella* species of the upper Paraguai basin, only *Pimelodella mucosa* and *P. taeniophora* have pectoral-fin spines that might present large blades at their posterior margin (Figs. 3B, C). In *P. taeniophora*, the pectoral-fin spine is narrower, and smaller specimens (less than 45 mm SL) also have smaller spinules besides proportionally longer adipose fins and maxillary barbels. On the other hand, *P. mucosa* can be promptly distinguished from *P. guato* by its enlarged preopercular and mandibular cephalic lateral-line canals. Such conspicuous cephalic lateral-line canals are also found in *P. longibarbata* from the western rio Orinoco basin.

Pimelodella guato superficially resembles *P. chaparae* Fowler, 1940*, P. howesi*, and *P. serrata*, three species distributed in the Amazon basin. *Pimelodella chaparae* and *P. howesi* were described from Boca Chapare, Bolivia, upper rio Madeira basin (Fowler, 1940), and *P. chaparae* was recently indicated as a senior synonym of *P. pallida* Dahl, 1961, from Río Guayabero, Colombia (Cortés-Hernández *et al*., 2020). *Pimelodella serrata* was described from San Joaquin, Bolivia, probably from upper Guaporé basin (Bockmann, Guazzelli, 2003), and previously reported for the rio Madeira basin, in Bolivia and Brazil (Lauzanne, Loubens, 1985; Chernoff *et al*., 2000; Bockmann, Slobodian, 2013), and from streams draining into the Amazon River channel in Colombia (Cortés-Hernandez *et al*., 2023).

Despite the absence of published phylogenetic relationships among *Pimelodella* species, *P. guato*, *P. chaparae*, *P. howesi*, and *P. serrata* share several morphological characteristics that promptly distinguish them from all other *Pimelodella* species. These characteristics are restricted to a few *Pimelodella* species. They can be interpreted as putatively apomorphic, indicating a possible close phylogenetic relationship between the three species, *e.g.*, head lateral profile straight and robust dorsal-fin spine with large posterior blades (Eigenmann, 1917; Bockmann, Slobodian, 2013; Slobodian, 2017). The long barbels, usually surpassing the caudal-fin insertion, are shared between *P. guato*, *P. howesi*, and *P. serrata,* but could not be ascertained in *P. chaparae* type material due to their damaged condition. In addition, the vertebral count of *P. chaparae* (41 in the holotype), *P. howesi* (44 in the holotype), and *P. serrata* (43 in the holotype) fall into the interval of P. *guato* (41–44). Among these four species, *P. guato* is particularly similar to *P. howesi* since both species exhibit a pectoral-fin spine with a moderately wide shaft and small flat spinules at its anterior margin (Figs. 3A, E); meanwhile, *P. chaparae* and *P. serrata* share an extensive pectoral-fin spine, with conspicuous, antrorse flat spinules at its anterior margin (Fig. 3D). Nevertheless, *P. guato* can be promptly distinguished from *P. howesi*, among other features (see Diagnosis), by having the dorsolateral region of body slightly darkened (*vs.* not darkened), dorsal fin with light brown stripe near its origin, followed by a hyaline stripe (*vs.* basal half of dorsal fin hyaline), and by the dorsal lamina of the Weberian apparatus reaching the ventral margin of the supraoccipital process only at its first third (*vs.* dorsal lamina reaching the supraoccipital process along all its extension).

The taxonomic similarities between the ichthyofauna of the Amazon and Paraguai basins have been discussed for decades (*e.g.*, Eigenmann, Eigenmann, 1891; Jordan, 1896; Eigenmann *et al*., 1907; Pearson, 1937; Hubert, Renno, 2006; Carvalho, Albert, 2011; Ribeiro *et al*., 2013; Ota *et al*., 2014; Dagosta, de Pinna, 2017, 2018, 2019, 2021). Several events might have allowed the sharing of fish fauna between the southern tributary headwaters of the Amazon basins and the Paraguai basin, such as upper Paraguai captures of proto-Amazonas-Orinoco headwaters, the Amazon capture of upper Paraguai headwaters, or other events related to megafans and river captures, involving especially the upper Mamoré and upper Guaporé tributaries along with upper Paraguai tributaries (Pearson, 1937; Lundberg *et al*., 1998; Wilkinson *et al*., 2006, 2010; Carvalho, Albert, 2011; Ota *et al*., 2014; Dagosta, de Pinna, 2019). Therefore, the presence of shared or closely related species on both sides of the Amazon-Paraguai is attributed to the diffusion of species arising from one side to the other by headwater capture events (Carvalho, Albert, 2011), or species being present in a paleo area encompassing both basins before the occurrence of a vicariant event that originated present-day hydrographic configuration (Ribeiro *et al*., 2013). Among the Amazonian headwaters that integrate this route (*i.e*., Mamoré-Guaporé, Tocantins, Xingu, and Tapajós basins), the Mamoré-Guaporé presents the largest divide extension with the Paraguai basin and largest number of shared species (Carvalho, Albert, 2011; Dagosta, de Pinna, 2019).

The Mamoré and Guaporé rivers are tributaries of the upper rio Madeira basin, one of the major Amazonian drainages. The Mamoré sub basin presents headwaters in the Andes region, in Bolivia, and connects with the Paraguai basin, mainly in the Bolivian Chaco, but also in the Bolivian Sub-Andean region (Pearson, 1937; Carvalho, Albert, 2011). The Guaporé sub basin, on the other hand, originates in Brazil, with headwaters in the Chapada dos Parecis (Pearson, 1937), and its connections with the Paraguai basin

probably occur in the rio Jauru (Paraguai basin) and its affluents (Reclus, 1895; Pearson, 1937; Carvalho, Albert, 2011). The Aguapeí and Alegre rivers (from Paraguai and Guaporé basins, respectively), for instance, are eventually separated by a narrow isthmus (Reclus, 1895; Carvalho, Albert, 2011), and species migration or shared supra specific taxa between these rivers has already been suggested (Schaefer, 1990). Thus, Carvalho, Albert (2011) indicates that lowland areas separating the headwaters of Paraguai and Mamoré-Guaporé basins allow the diffusion of the ichthyofauna between them.

Ribeiro *et al.* (2013), on the other hand, suggest that the shared ichthyofauna between the Paraguai and Amazon basins could also be possible due to a major central-Brazilian Amazonian paleoplateau rearrangement caused by a subsidence in the upper Paraguai basin. In this way, the lowland areas in the Amazon-Paraguai divide would be more ephemeral than highland areas due to tectonic movements, resulting in lowland fish species more broadly distributed in both basins, in a time when the divide did not exist (Lima, Ribeiro, 2011; Ribeiro *et al*., 2013). Meanwhile, upland species would have been shared between the basins due to headwaters captures and only present nowadays in the headwaters since such species would not be adapted to the ecological conditions of lowland regions (Lima, Ribeiro, 2011; Ribeiro *et al*., 2013).

Thus, there are several indications in the literature that the shared taxa between Madeira (especially Guaporé and Mamoré sub basins) and Paraguai basins might be due to several biogeographic events that emerged on different ages, since congruent distributions are partly temporally decoupled, being pseudocongruences (Dagosta, de Pinna, 2019). In that sense, discussions on the common biogeographic history between both regions should highlight which of such events better explain the taxa distribution, depending on them being lowland or highland taxa.

Given the putatively apomorphic characteristics shared between *P. guato* (from the Paraguai basin) and *P. chaparae*, *P. howesi*, and *P. serrata* (from rio Madeira drainage), the occurrence of *P. guato* in the Paraguai basin may be related to the geological and hydrological features of the Amazon-Paraguai divide, that might have allowed the cladogenesis of this group of *Pimelodella*. Since *P. guato* was collected in lowland areas, in sites up to 200 m asl, we infer it is a lowland species, with two main biogeographical events that might explain its distribution: (1) the river avulsion in megafans that lead to taxa shared between upper Mamoré and tributaries to upper Paraguay in Bolivia (following Wilkinson *et al*., 2006, 2010); and (2) river captures from upper Paraguai tributaries to upper Guaporé, at mid-elevations (following Carvalho, Albert, 2011; Ota *et al*., 2014). The first mentioned event dates from the Late Miocene (late Tertiary) or later, and this divide is occupied by the modern rio Parapetí megafan nowadays, which leads water into both basins today, despite being well above 200 m a.s.l. (Wilkinson *et al*., 2006, 2010). The second event is also considerably recent, dating from the late Tertiary or Quaternary (Ota *et al*., 2014). However, in the absence of a published *Pimelodella* phylogeny, we can scarcely discuss the biogeographic events that led to the presence of *P. guato* in the Paraguai basin.

Anyway, much remains to be understood about the shared ichthyofauna between the Amazon and Paraguai basins. Among the species of *Pimelodella* that are found in the Paraguai basin, *P. gracilis* was described from rio Paraná in Argentina and is known to occur in the Paraguai, upper and lower Paraná basins, in Argentina, Brazil and Paraguay (Bockmann, Guazzelli, 2003; Carvalho, Albert, 2011; Slobodian, 2017,

unpublished data), but a few specimens were also reported for the rio Madeira basin (*e.g.*, Pearson, 1924; Bockmann, Slobodian, 2013 [their *Pimelodella* sp. n.]; Slobodian, 2017, unpublished data). Although *P. guato* shares resemblances with *P. gracilis* in certain aspects, such as the length of the maxillary barbel and the morphology of the pectoral-fin spine, there are several characteristics that distinguish both species. *Pimelodella guato* presents 41–42 (rarely 43 or 44) total vertebrae; anal-fin adpressed terminus aligned with the verticals through adipose-fin terminus; and adipose fin 2.5 to 3.0 times in SL. In contrast, *P. gracilis* contains 46 total vertebrae; anal-fin adpressed terminus consistently anterior to the adipose-fin terminus, reaching the vertical through three-fourths of the adipose fin; adipose fin longer, slightly more than 2.0 to 2.5 times in SL; the presence of darker midlateral and dorsolateral stripes; and a notably more elongated body shape. *Pimelodella gracilis* is known to occur syntopically with *P. guato* in the Paraguai basin (pers. obs., ZUFMS-PIS 6678, ZUFMS-PIS 838), being another indication for closely related taxa shared between both Amazon and Paraguai basins.

Lastly, another noteworthy aspect is the reaffirmation of the presence of filaments on the non-spinous portion of the second (unbranched) and the first (unbranched) rays in the dorsal and pectoral fins, respectively, of *P. guato* as a sexually dimorphic trait (Fig. 5A). While this characteristic has been used as a diagnostic feature in the description of several species in the past, such as *Pimelodella boschmai* van der Stigchel, 1964, *P. insignis* (Schubart, 1964), *P. figueroai* Dahl, 1961, *P. griffini*, *P. linami* Schultz, 1944, *P. megalura,* and *P. taenioptera*, the hypothesis of this filament as a secondary sexual character was first introduced by Dahl (1961). Dahl conducted dissections on immature, mature male, and mature female *P. linami* specimens to verify their sex and developmental stage, and the filamentous prolongations were exclusively found in adult males (Dahl, 1961:498). Subsequently, Souza-Shibatta *et al.* (2013) reached the same conclusion based on examinations of *P. griffini* and *P. taenioptera* specimens.

In the specimens we examined for this work, the presence of filamentous prolongation was observed in individuals also displaying an enlarged urogenital papilla (2.4 times the average size of the papilla found in other specimens) (Fig. 5B), which also appears to be a secondary sexual characteristic. An enlarged urogenital papilla and filamentous prolongation were exclusively found in specimens measuring over 73.7 mm SL, suggesting a potential correlation with the size of sexual maturity in males. This finding aligns with observations in other species, such as *P. avanhandavae* Eigenmann, 1917, and *P. meeki* Eigenmann, 1910, whose males reach sexual maturity at sizes of 74 mm SL and 54 mm SL, respectively (Orsi, 2017). Conversely, in *P. lateristriga* (Lichtenstein, 1823) and *P. pappenheimi* Ahl, 1925, no discernible difference was observed in size between males and females at first maturity. Both sexes in these species attain maturity at 44.5 mm SL in *P. lateristriga* (Moraes *et al*., 2013) and 63 mm SL in *P. pappenheimi* (Amaral *et al*., 1998).

In this work, five specimens were dissected to ascertain the correlation between the presence of filamentous prolongation and enlarged urogenital papilla and the sex. Two dissected specimens without the filamentous prolongation were confirmed as females, probably at the spawning-capable phase (CIUnB 1772, 79.1 and 91.0 mm SL). Three dissected specimens were confirmed as males, two of these presenting both a filamentous prolongation (of at least a fourth of the total length of the ray) and an enlarged papilla (CIUnB 1772, 86.0 and 93.8 mm SL), and one presenting only a small filamentous

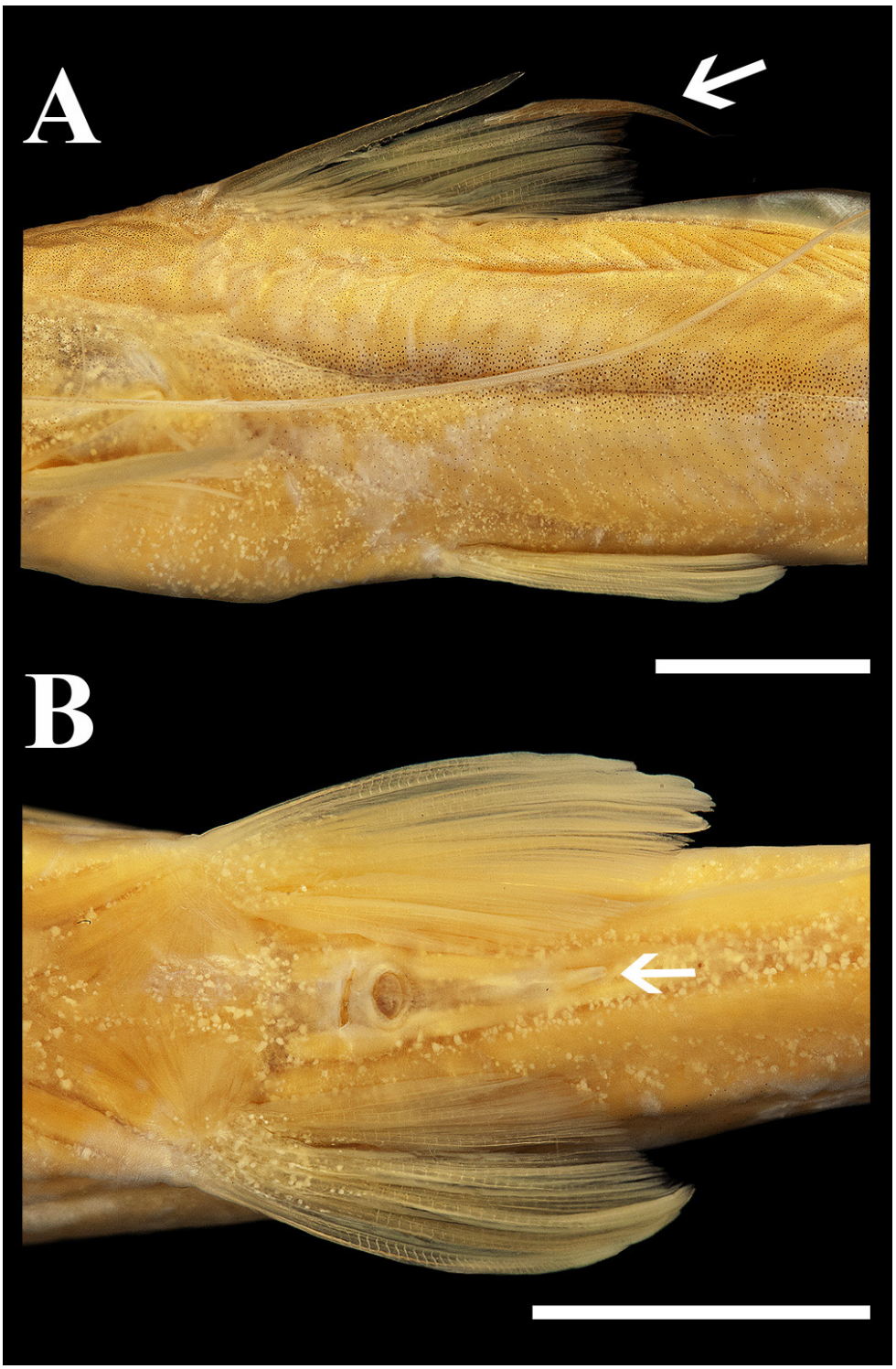

FIGURE 5 | Sexually dimorphic traits in an adult male specimen of *Pimelodella guato* (paratype, CIUnB 1772, 93.8 mm SL). **A.** Filament on the non-spinous portion of dorsal-fin second (unbranched) ray, indicated by a white arrow; and **B.** Enlarged urogenital papilla, indicated by a white arrow. Scale bars = 1 cm.

prolongation (of one sixth of the total length of the ray) and not the enlarged papilla (CIUnB 1772, 89.4 mm SL). However, the testis gross morphology of the three specimens was not different. Therefore, we conclude the presence of the filamentous prolongation is a good indicator for sex determination for males. However, histological studies are needed to ascertain the gonadal development phase of filamentous males. Nevertheless, we highlight the importance of conducting further studies on the biology and systematics of *P. guato* and other species of *Pimelodella* that comprise the Paraguayan basin ichthyofauna, as they are key taxa in advancing our understanding of South American biogeography.

Comparative material examined. Besides the material indicated in Slobodian *et al.* (2017), the following comparative materials were examined: *Pimelodella gracilis*: **Argentina:** MZUSP 337, 2, 100.4–113.3 mm SL. **Brazil:** CPUFMT 679, 3, 106.8–133.5 mm SL; CPUFMT 850, 4, 100.2–135.2 mm SL; CPUFMT 1546, 1, 162.6 mm SL; CPUFMT 2306, 3, 107.0–107.3 mm SL; LIRP 9531, 1, 88.4 mm SL; MCP 26120, 2, 96.9–97.6 mm SL; MZUEL 6457, 1, 90.0 mm SL; MZUEL 11185, 5, 136.5–185.8 mm SL; MZUEL 11190, 6, 72.3–119.7 mm SL; MZUEL 14001, 6, 56.9–93.7 mm SL; MZUSP 23195, 1, 189.3 mm SL; MZUSP 24856, 1, 107.8 mm SL; MZUSP 27728, 2, 137.4–205.8 mm SL; MZUSP 38033, 3, 65.0–71.6 mm SL; MZUSP 82381, 1, 114.7 mm SL; MZUSP 87788, 1, 147.1 mm SL; NUP 2231, 4, 94.4–158.5 mm SL; NUP 3408, 10, 98.1–118.4 mm SL; NUP 3473, 15, 87.8–103.1 mm SL; NUP 3505, 9, 90.3–114.0 mm SL; NUP 14300, 10, 56.7–71.7 mm SL; ZUFMS-PIS 620, 1, 144.1 mm SL; ZUFMS-PIS 838, 2, 101.8–127.5 mm SL; ZUFMS-PIS 6488, 12, 49.4–166.4 mm SL; ZUFMS-PIS 6678, 4, 135.2–156.6 mm SL. *Pimelodella griffini*: **Brazil:** CPUFMT 5352, 6, 46.4–58.9 mm SL; LIRP 11407, 2, 44.7–51.6 mm SL; MCP 36117, 10, 46.9–56.6 mm SL; MCP 36127, 15, 39.2–53.7 mm SL; MZUEL 3830, 9, 43.2–56.3 mm SL; MZUEL 6460, 2, 71.4–74.6 mm SL; MZUEL 7748, 3, 40.4–56.1 mm SL; MZUEL 9034, 2, 47.6–60.7 mm SL; MZUEL 9035, 3, 51.1–63.6 mm SL; MZUSP 44487, 10, 41.7–54.2 mm SL; MZUSP 90671, 10, 40.1–50.1 mm SL; MZUSP 100564, 2, 67.7–81.1 mm SL; NUP 11627, 10, 52.4–62.9 mm SL; NUP 21728, 3, 47.9–51.7 mm SL; ZUFMS-PIS 876, 20, 45.9–60.0 mm SL; ZUFMS-PIS 1417, 4, 37.3–53.8 mm SL; ZUFMS-PIS 1428, 6, 46.8–67.8 mm SL; ZUFMS-PIS 1433, 1, 55.3 mm SL; ZUFMS-PIS 1465, 10, 43.9–70.6 mm SL; ZUFMS-PIS 1607, 20, 55.4–86.1 mm SL; ; ZUFMS-PIS 3696, 1, 94.8 mm SL; ZUFMS-PIS 3900, 2, 69.0–73.3 mm SL. *Pimelodella longibarbata*: **Colombia:** IAvH 17879, paratype, 1, c&s, 48.8 mm SL (photo). *Pimelodella megalura*: **Brazil:** MCP 15620, 6, 45.1–72.6 mm SL; MCP 15708, 1, 74.3 mm SL; MZUEL 3829, 2, 69.9–79 mm SL; NUP 14702, 15, 42.6–63.9 mm SL; ZUFMS-PIS 1417, 14, 52.9–81.9 mm SL; ZUFMS-PIS 1428, 3, 58.6–67.8 mm SL; ZUFMS-PIS 1477, 1, 66.6 mm SL; ZUFMS-PIS 3900, 3, 71.5–79.7 mm SL; ZUFMS-PIS 4703, 1, 80.8 mm SL. *Pimelodella mucosa*: **Brazil:** CPUFMT 3081, 1, 66.7 mm SL; CPUFMT 3569,1, 70.3 mm SL; CPUFMT 3714, 2, 87.6–97.1 mm SL; CPUFMT 3870, 1, 92.8 mm SL; LIRP 9528, 7, 46.3–66.8 mm SL; MZUEL 11088, 1, 77.5 mm SL; MZUEL 13217, 3, 55.1–78.0 mm SL; MZUEL 14055, 2, 45.5–57.2 mm SL; MZUSP 25091, 1, 86.1 mm SL; NUP 1067, 12, 58.8–101.7 mm SL; NUP 13590, 3, 50.3–59.7 mm SL; NUP 14201, 10, 56.5–82.4 mm SL; NUP 14355, 15, 66.5–91.9 mm SL; ZUFMS-PIS 1613, 1, 44.8 mm SL; ZUFMS-PIS 3256, 2, 75.3–75.4 mm SL; ZUFMS-PIS 3269, 1, 56.5 mm SL; ZUFMS-PIS 3478, 1, 31.0 mm SL; ZUFMS-PIS 4194, 1, 81.6 mm SL. *Pimelodella notomelas*: **Brazil:** MZUEL 7743, 3, 43.9–52.6 mm SL; MZUEL 9032, 1, 39.7 mm SL; MZUEL 9694, 1, 33.0 mm SL. Brazil: ZUFMS-PIS 5438, 2, 34.3–34.4 mm SL. *Pimelodella serrata*: **Brazil:** LIRP 10022, 4, 71.3–83.6 mm SL; LIRP 10029, 12, 66.7–83.9 mm SL. *Pimelodella taeniophora*: **Brazil:** CPUFMT 870, 3, 36.8–68.3 mm SL; CPUFMT 4003, 8, 60.4–75.7 mm SL; LIRP 9528, 2, 47.9–61.2 mm SL; LIRP 9533, 2, 51.3–55.8 mm SL; LIRP 9534, 7, 53.2–71.4 mm SL; LIRP 9535, 6, 50.4–63.3 mm SL; LIRP 10024, 4, 45.1–52.1 mm SL; MCP 10924, 2, 91.2–91.6 mm SL; MCP 15708, 4, 64.8–86.1 mm SL; MCP 15775, 30, 50.1–79.9 mm SL; MCP 36138, 9, 33.7–54.1 mm SL; MZUSP 44289, 1, 61.1 mm SL;

NUP 3390, 16, 56.6–107.0 mm SL; NUP 11390, 5, 70.0–80.0 mm SL; NUP 12222, 2, 38.5–50.2 mm SL; NUP 14189, 15, 55.1–66.9 mm SL; NUP 21860, 2, 79.5–83.5 mm SL; ZUFMS-PIS 648, 1, 51.6 mm SL; ZUFMS-PIS 5549, 3, 45.6–50.0 mm SL; ZUFMS-PIS 6320, 9, 66.8–82.3 mm SL; ZUFMS-PIS 6327, 1, 51.0 mm SL; ZUFMS-PIS 6442, 1, 69.8 mm SL; ZUFMS-PIS 6488, 6, 16.1–64.7 mm SL. *Pimelodella yaharo* (only photos): **Colombia:** CZUT-IC 10922, holotype, 74.7 mm SL; CZUT-IC 10942, paratype, 1, 69.9 mm SL; CZUT-IC 12602, paratypes, 2, 72.4–82.0 mm SL; CZUT-IC 15262, paratypes, 2, 1 c&s, 66.9–76.9 mm SL; IAvH-P 22004, paratypes, 2, 1 c&s, 68.7–72.7 mm SL.

ACKNOWLEDGMENTS

We thank F. Severo, R. Rech and Y. Suárez from the ZUFMS-PIS and H. Gimênes-Júnior from Bioparque Pantanal for providing the specimens of the Paraguai basin, that brought to our attention the new records reported herein. We thank J. Klaczko and A. Martins from the Laboratório de Anatomia Comparativa dos Vertebrados (LACV-UnB) for providing space and equipment to obtain the photos. We thank F. Bockmann for allowing us to use the digital radiography equipment hosted at the LIRP, belonging to the Center for Biodiversity Documentation, Department of Biology, FFCLRP/University of São Paulo, Brazil. We thank M. Cortés-Hernandez for providing photos of *P. longibarbata* type material. We are grateful to M. Arce, J. Birindelli, F. Bockmann, R. Castro, J. Clayton, A. Datovo, G. Deprá, C. Doria, A. Esguícero, M. Gianneti, J. Lundberg, C. McMahan, S. Mochel, O. Oyakawa, C. Pavanelli, K. Swagel for providing assistance during visits at their institutions, loaning and providing information, photos and x-rays of types and comparative materials of *Pimelodella*. The second author thanks M. de Pinna for his orientation, insights, and suggestions in her doctorate. The second author is also grateful to C. Vilela for advice and guidance. We want to express our gratitude to CHAT GPT, a language model developed by OpenAI, for assistance in proofreading and refining the English language of this article. The Research funding for VP was provided by Coordenação de Aperfeiçoamento de Pessoal de Nível Superior (Capes, Master's scholarship) and Programa de Apoio à Pós-Graduação (PROAP-Capes, PPGZOO 04/2021). The Research funding for VS was provided by Fundação de Amparo à Pesquisa do Estado de São Paulo (FAPESP, projects #2013/18623–4, 2015/26804–4 and 2017/01073–0), Universidade de Brasília (Edital DPI 02/2023), and Fundação de Amparo à Pesquisa do Distrito Federal (FAPDF, #00193–00000229/2021–21).

REFERENCES

- **Abell R, Thieme ML, Revenga C, Bryer M, Kottelat M, Bogutskaya N *et al*.** Freshwater ecoregions of the world: a new map of biogeographic units for freshwater biodiversity conservation. Bioscience. 2008; 58(5):403–14. https://doi.org/10.1641/B580507
- **Amaral MF, Aranha JMR, Menezes MS.** Reproduction of the freshwater catfish *Pimelodella pappenheimi* in Southern Brazil. Stud Neotrop Fauna Environ. 1998; 33(2):106–10.
- **Ballen GA, de Pinna MCC.** A standardized terminology of spines in the order Siluriformes (Actinopterygii: Ostariophysi). Zool J Linn Soc. 2022; 194(2):601–25. https://doi.org/10.1093/zoolinnean/zlab008

- **Bockmann FA, Castro RMC.** The blind catfish from the caves of Chapada Diamantina, Bahia, Brazil (Siluriformes: Heptapteridae): description, anatomy, phylogenetic relationships, natural history, and biogeography. Neotrop Ichthyol. 2010; 8(4):673–706. https://doi.org/10.1590/S1679-62252010000400001
- **Bockmann FA, Guazzelli GM.** Family Heptapteridae (Heptapterids). In: Reis RE, Kullander SO, Ferraris Jr. CJ, editors. Check list of the freshwater fishes of South and Central America. Porto Alegre: Edipucrs; 2003. p.406–31.
- **Bockmann FA, Miquelarena AM.** Anatomy and phylogenetic relationships of a new catfish species from northeastern Argentina with comments on the phylogenetic relationships of the genus *Rhamdella* Eigenmann and Eigenmann 1888 (Siluriformes, Heptapteridae). Zootaxa. 2008; 1780(1):1–54. https://doi.org/10.11646/zootaxa.1780.1.1
- **Bockmann FA, Slobodian V.** Heptapteridae. In: Queiroz LJ, Torrente-Vilara G, Ohara WM, Pires THS, Zuanon J, Doria CRC, editors. Peixes do rio Madeira. São Paulo: Dialeto Latin America Documentary; 2013. p.14–77.
- **Boin MN, Martins PCS, Silva CA, Salgado AAR.** The Pantanal: The Brazilian wetlands. In: Salgado AAR, Santos LJC, Paisani JC, editors. The physical geography of Brazil: environment, vegetation and landscape. Cham: Springer; 2019. p.75–91.
- **Britski HA, Silimon KZS, Lopes BS.** Peixes do Pantanal: manual de identificação. Brasília: Embrapa-SPI; 1999.
- **Calegari BB, Delapieve MLS, Souza LM.** Tutorial para preparação de mapas de distribuição geográfica. Bol Soc Bras Ictiol. 2016; 118:15–30. https://www.sbi.bio.br/pt/boletim-sbi
- **Carvalho TP, Albert JS.** The Amazon-Paraguay divide. In: Albert JS, Reis RE, editors. Historical biogeography of neotropical freshwater fishes. Berkeley: University of California Press; 2011. p.193–202.
- **Chernoff B, Machado-Allison A, Willink P, Sarmiento J, Barrera S, Menezes N *et al*.** Fishes of three Bolivian rivers: diversity, distribution and conservation. Interciencia. 2000; 25(6):273–83.
- **Conde-Saldaña CC, Albornoz-Garzón JG, García-Melo JE, Dergam JA, Villa-Navarro FA.** A new species of *Pimelodella* Eigenmann & Eigenmann, 1888 (Siluriformes: Heptapteridae) from the Sierra Nevada de Santa Marta, Colombia. Zootaxa. 2019; 4668(4):562–74. https://doi.org/10.11646/zootaxa.4668.4.8
- **Cortés-Hernández MÁ, DoNascimiento C, Ramírez-Gil H.** A new species of *Pimelodella* Eigenmann & Eigenmann, 1888 (Siluriformes: Heptapteridae) from the Orinoco River basin. Zootaxa. 2020; 4808(3):491–506. https://doi.org/10.11646/zootaxa.4808.3.5
- **Cortés-Hernández MÁ, Méndez-López A, DoNascimiento C.** New records of *Pimelodella* (Siluriformes, Heptapteridae) from Colombia for the Amazon River basin, and redescription of *P. serrata*. Zootaxa. 2023; 5293(1):185–95. https://doi.org/10.11646/zootaxa.5293.1.10
- **Costa AMRFM**. Guató: povo das águas. In: Chamorro G, Combès I, editors. Povos indígenas em Mato Grosso do Sul: história, cultura e transformações sociais. Dourados: Universidade Federal da Grande Dourados; 2015. p.199–215.
- **Dagosta FCP, de Pinna M.** Biogeography of Amazonian fishes: deconstructing river basins as biogeographic units. Neotrop Ichthyol. 2017; 15(3):e170034. https://doi.org/10.1590/1982-0224-20170034
- **Dagosta FCP, de Pinna M.** A history of the biogeography of Amazonian fishes. Neotrop Ichthyol. 2018; 16(3):e180023. https://doi.org/10.1590/1982-0224-20180023
- **Dagosta FCP, de Pinna M.** The fishes of the Amazon: distribution and biogeographical patterns, with a comprehensive list of species. Bull Am Mus Nat Hist. 2019; 2019(431):1–163. https://doi.org/10.1206/0003-0090.431.1.1
- **Dagosta FCP, de Pinna M.** Two new catfish species of typically Amazonian lineages in the upper rio Paraguay (Aspredinidae: Hoplomyzontinae and Trichomycteridae: Vandelliinae), with a biogeographic discussion. Pap Avulsos Zool. 2021; 61:e20216147. https://doi.org/10.11606/1807-0205/2021.61.47
- **Dahl G.** Nematognathous fishes collected during the Macarena Expedition 1959. Dedicated to the memory of the Colombian ichthyologist, Doctor Ricardo Lozano. Decd May 23rd, 1959. Part II: Pimelodidae, Callophysidae. Noved Colomb. 1961; 1(6):483–514.
- **Eigenmann CH.** *Pimelodella* and *Typhlobagrus*. Mem Carnegie Mus. 1917; 7(4):229–58. https://doi.org/10.5962/bhl.title.12518
- **Eigenmann CH, Eigenmann RS.** A catalogue of the freshwater fishes of South America. Proc U S Natl Mus. 1891; 14(842):1–81. https://doi.org/10.5479/si.00963801.842
- **Eigenmann CH, McAtee WL, Ward DP.** On further collections of fishes from the Paraguay. Ann Carnegie Mus. 1907; 4(2):110–57. https://doi.org/10.5962/p.264300

- **Ely P, Fantin-Cruz I, Tritico HM, Girard P, Kaplan D.** Dam-induced hydrologic alterations in the rivers feeding the Pantanal. Front Environ Sci. 2020; 8:579031. https://doi.org/10.3389/fenvs.2020.579031
- **Ferraris CJ.** Checklist of catfishes, recent and fossil (Osteichthyes: Siluriformes), and catalogue of siluriform primary types. Zootaxa. 2007; 1418(1):1–628. https://doi.org/10.11646/zootaxa.1418.1.1
- **Fowler HW.** Zoological results of the second Bolivian expedition for the Academy of Natural Sciences of Philadelphia, 1936-1937, Part I.--The fishes. Proc Acad Nat Sci Philadelphia. 1940; 92:43–103.
- **Fricke R, Eschmeyer WN, Van der Laan R.** Eschmeyer's catalog of fishes: genera, species, references [Internet]. San Francisco: California Academy of Sciences; 2023. Available from: http://researcharchive.calacademy.org/research/ichthyology/catalog/fishcatmain.asp
- **Galdino S, Risso A, Soriano BMA, Vieira LM, Padovani CR, Pott A *et al*.** Perdas de solo na bacia do Alto Taquari. Corumbá: Embrapa Pantanal [Internet]; 2003. Available from: https://www.infoteca.cnptia.embrapa.br/bitstream/doc/811022/1/BP44.pdf
- **Galdino S, Vieira LM, Pellegrin LA.** Impactos Ambientais Socioeconômicos na Bacia do rio Taquari – Pantanal. Corumbá: Embrapa Pantanal [Internet]; 2006. Available from: https://www.embrapa.br/busca-de-publicacoes/-/publicacao/811632/impactos-ambientais-e-socioeconomicos-na-bacia-do-rio-taquari---pantanal
- **Gimênes-Junior H, Rech R, editors.** Guia ilustrado dos peixes do Pantanal e entorno. Campo Grande: Julien Design; 2022. Available from: https://www.imasul.ms.gov.br/wp-content/uploads/2022/11/Montagem-livro-Peixes-VERSAO-FINAL-MARCO-2022-ISBN97865-81066-05-5-ONLINE_FINAL-1.pdf
- **Hamilton SK.** Human impacts on hydrology in the Pantanal wetland of South America. Water Sci Technol. 2002; 45(11):35–44. https://doi.org/10.2166/wst.2002.0377
- **Hubert N, Renno J-F.** Historical biogeography of South American freshwater fishes. J Biogeogr. 2006; 33(8):1414–36. https://doi.org/10.1111/j.1365-2699.2006.01518.x
- **International Union for Conservation of Nature (IUCN). Standards and petitions subcommittee.** Guidelines for using the IUCN Red List categories and criteria. Version 15.1 [Internet]. Gland; 2022. Available from: https://www.iucnredlist.org/resources/redlistguidelines
- **Jordan DS.** The dispersion of fresh-water fishes. In: Jordan DS, editor. Science Sketches. Chicago: AC McClurg and Company; 1896. p.83–132.
- **Koerber S, Vera-Alcaraz HS, Reis RE.** Checklist of the fishes of Paraguay (CLOFPY). ICP. 2017; 53:1–99. https://pecescriollos.de/icp-journal/
- **Lauzanne L, Loubens G.** Peces del rio Mamoré. Paris: ORSTOM; 1985.
- **Leite EF, Berezuk AG, Silva CA.** A vulnerabilidade ambiental da bacia hidrográfica do rio Miranda, Mato Grosso do Sul. Rev Bras Geogr Fís. 2022; 15(5):2613–39. https://doi.org/10.26848/rbgf.v15.5.p2613-2639
- **Lichtenstein MHC.** Verzeichniss der Doubletten des zoologischen Museums der Königl. Universität zu Berlin, nebst Beschreibung vieler bisher unbekannter Arten von Säugethieren, Vögeln, Amphibian und Fishen. Berlin: T. Trautwein; 1823.
- **Lima FCT, Ribeiro AC.** Continental-scale tectonic controls of biogeography and ecology. In: Albert JS, Reis RE, editors. Historical biogeography of Neotropical freshwater fishes. Berkeley: University of California Press; 2001. p.145–64.
- **Lundberg JG, Baskin JN.** The caudal skeleton of the catfishes, order Siluriformes. Am Mus Novit. 1969; 2398:1–49. http://hdl.handle.net/2246/2608
- **Lundberg JG, Marshall LG, Guerrero J, Horton B, Malabarbarba MC, Wesselingh F.** The stage for neotropical fish diversification: a history of tropical South American rivers. In: Malabarba LR, Reis RE, Vari RP, Lucena CAS, Lucena ZMS, editors. Phylogeny and classification of Neotropical fishes. Porto Alegre: Edipucrs; 1998. p.13–48.
- **Mazzoni TS, Bombardelli RA, Quagio-Grassiotto I.** Reproductive biology of Neotropical fishes: a guide to identification to the gonadal morphology during the reproductive cycle of catfish *Rhamdia quelen* (Siluriformes: Heptapteridae). Aquat Sci Tech. 2020; 8(2):15–35. https://doi.org/10.5296/ast.v8i2.17102
- **Mees GF.** Naked catfishes from French Guiana (Pisces, Nematognathi). Zool Meded. 1983; 57(5):43–58. https://repository.naturalis.nl/pub/318898
- **Melo BF, Vari RP, Oliveira C.** *Curimatopsis maculosa*, a new species from the rio Tapajós, Amazon basin, Brazil (Teleostei: Curimatidae). Ichthyol Explor Freshw. 2016; 27(4):303–08. http://hdl.handle.net/11449/228284
- **Mendes CAB, Grehs SA, Pereira MCB, Barreto SR, Becker M, Lange MBR *et al*.** Bacia hidrográfica do rio Miranda: estado da arte. Campo Grande: UCDB; 2004.

- **Miranda Ribeiro A.** Tres generos e dezesete especies novas de peixes Brasilieros. Rev Mus Paul. 1918; 10:631–46.
- **Mirande JM, Koerber S.** Checklist of the freshwater fishes of Argentina (CLOFFAR-2). ICP. 2020; 72:1–81. https://pecescriollos.de/icp-journal/
- **Moraes M, Silva Filho JJ, Costa R, Miranda JC, Rezende CF, Mazzoni R.** Life history and ontogenetic diet shifts of *Pimelodella lateristriga* (Lichtenstein 1823) (Osteichthyes, Siluriformes) from a coastal stream of Southeastern Brazil. North West J Zool. 2013; 9(2):300–09. Available from: https://biozoojournals.ro/nwjz/content/v9n2/nwjz.131403.Mazzoni.pdf
- **Orsi ML.** Estratégias reprodutivas de peixes: estratégias reprodutivas de peixes da região média-baixa do rio Paranapanema, reservatório de Capivara, 2 ed. São Paulo: Blucher; 2017.
- **Ota RP, Lima FCT, Pavanelli CS.** A new species of *Hemigrammus* Gill, 1858 (Characiformes: Characidae) from the rio Madeira and rio Paraguai basins, with a redescription of *H. lunatus*. Neotrop Ichthyol. 2014; 12(2):265–79. https://doi.org/10.1590/1982-0224-20130176
- **Pearson NE.** The fishes of the eastern slope of the Andes: the fishes of the rio Beni basin, Bolivia, collected by the Mulford expedition. Indiana Univ Sci Ser. 1924; 11(64):1–83.
- **Pearson NE.** The fishes of the Beni-Mamoré and Paraguay basins, and a discussion of the origin of the Paraguayan fauna. Proc Calif Acad Sci. 1937; 23(8):99–114. https://www.biodiversitylibrary.org/part/21375
- **Rabelo APC, Souza MG.** Bacia do Alto Paraguai: uma viagem no tempo. Brasília: Instituto Brasileiro de Informação em Ciência e Tecnologia [Internet]; 2021. Available from: https://ridi.ibict.br/handle/123456789/1199
- **Reclus E.** The Earth and its inhabitants: South America; Amazonia and La Plata. New York: D. Appleton and Company; 1895.
- **Regan CT.** Descriptions of new South-American fishes in the collection of the British Museum. Ann Mag Nat His. 1903; 12(72):621–30. https://www.biodiversitylibrary.org/partpdf/68444
- **Ribeiro AC, Jacob RM, Silva RRSR, Lima FCT, Ferreira DC, Ferreira KM *et al*.** Distributions and phylogeographic data of rheophilic freshwater fishes provide evidences on the geographic extension of a central-brazilian Amazonian palaeoplateau in the area of the present day Pantanal Wetland. Neotrop Ichthyol. 2013; 11(2):319–26. https://doi.org/10.1590/S1679-62252013000200010
- **Sabaj MH.** Codes for Natural History Collections in Ichthyology and Herpetology (online supplement), version 9.5 [Internet]. Washington, DC: American Society of Ichthyologists and Herpetologists; 2023. Available from: https://asih.org
- **Schaefer SA.** Anatomy and relationships of the scoloplacid catfishes. Proc Acad Nat Sci Phila. 1990; 142:167–210. https://www.jstor.org/stable/4064976
- **Schmidt M.** Estudos de etnologia brasileira: peripécias de uma viagem entre 1900 e 1901, seus resultados etnológicos. São Paulo: Companhia Editora Nacional; 1942.
- **Slobodian V.** Taxonomic revision of *Pimelodella* Eigenmann & Eigenmann, 1888 (Siluriformes: Heptapteridae): an integrative proposal to delimit species using a multidisciplinary strategy. [PhD Thesis]. São Paulo: Universidade de São Paulo; 2017.
- **Slobodian V, Abreu-Santos B, Pastana MNL.** The rediscovery of *Pimelodella longipinnis* (Borodin, 1927), an enigmatic Atlantic Rainforest catfish species from Southeastern Brazil (Siluriformes: Heptapteridae). Pap Avulsos Zool. 2021; 61:e20216173. https://doi.org/10.11606/1807-0205/2021.61.73
- **Slobodian V, Akama A, Dutra GM.** A new species of *Pimelodella* (Siluriformes: Heptapteridae) from the Guiana Shield, Brazil. Zootaxa. 2017; 4338(1):85–100. https://doi.org/10.11646/zootaxa.4338.1.4
- **Slobodian V, Gimênes-Junior H, Rech R.** Heptapteridae. In: Gimênes-Junior H, Rech R, editors. Guia ilustrado dos peixes do Pantanal e entorno. Campo Grande: Julien Design; 2022. p.332–45.
- **Slobodian V, Pastana MNL.** Description of a new *Pimelodella* (Siluriformes: Heptapteridae) species with a discussion on the upper pectoral girdle homology of Siluriformes. J Fish Biol. 2018; 93(5):901–16. https://doi.org/10.1111/jfb.13795
- **Souza-Shibatta L, Pezenti LF, Ferreira DG, Almeida FS, Sofia SH, Shibatta OA.** Cryptic species of the genus *Pimelodella* (Siluriformes: Heptapteridae) from the Miranda River, Paraguay River basin, Pantanal of Mato Grosso do Sul, Central Brazil. Neotrop Ichthyol. 2013; 11(1):101–09. https://doi.org/10.1590/S1679-62252013000100012
- **Van der Stigchel JWB.** A new species of pimelodid catfish from eastern Brazil, *Pimelodella boschmai* nov spec. Zool Meded. 1964; 39(34):327–30. https://repository.naturalis.nl/pub/317947

- **Taylor WR, Van Dyke GC.** Revised procedures for staining and clearing small fishes and other vertebrates for bone and cartilage study. Cybium. 1985; 9(2):107–19. Available from: https://sfi-cybium.fr/en/node/2423
- **Tucci CEM, Genz F, Clarke RT.** The hydrology of the upper Paraguay basin. In: Biswas AK, Cordeiro NV, Braga BPF, Tortajada C, editors. Management of Latin American river basins: Amazon, Plata, and São Francisco. Tokyo: United Nations University Press; 1999. p.103–22.
- **Valenciennes A.** Poissons [plates]. In: d'Orbigny A, editor. Voyage dans l'Amérique méridionale. Paris: Chez Pitois-Levrault et ce; 1835. pls.1–16.
- **Wilkinson MJ, Marshall LG, Lundberg JG.** River behavior on megafans and potential influences on diversification and distribution of aquatic organisms. J South Am Earth Sci. 2006; 21:151–72. https://doi.org/10.1016/j.jsames.2005.08.002
- **Wilkinson MJ, Marshall LG, Lundberg JG, Kreslavsky MH.** Megafan environments in northern South America and their impact on Amazon Neogene aquatic ecosystems. In: Hoorn C, Wesselingh FP, editors. Amazonia, landscape and species evolution: a look into the past. Oxford: Wiley-Blackwell; 2010. p.162–84.

AUTHORS' CONTRIBUTION

Veida Pierre: Conceptualization, Data curation, Formal analysis, Funding acquisition, Investigation, Methodology, Project administration, Resources, Visualization, Writing-original draft, Writing-review and editing.

Veronica Slobodian: Conceptualization, Data curation, Formal analysis, Funding acquisition, Investigation, Methodology, Project administration, Resources, Supervision, Visualization, Writing-original draft, Writing-review and editing.

ETHICAL STATEMENT

Since we only utilized specimens from scientific collections, no collection permits were required.

COMPETING INTERESTS

The author declares no competing interests.

HOW TO CITE THIS ARTICLE

- **Pierre V, Slobodian V.** A new species of *Pimelodella* (Siluriformes: Heptapteridae) from the Paraguai basin, Brazil, with a discussion regarding its distribution. Neotrop Ichthyol. 2024; 22(1):e230110. https://doi.org/10.1590/1982-0224-2023-0110

Neotropical Ichthyology

OPEN ACCESS

Official Journal of the
Sociedade Brasileira de Ictiologia
SBI